Field Testing of Hand-Held Infrared Thermography, Phase II TPF-5(247) Final Report

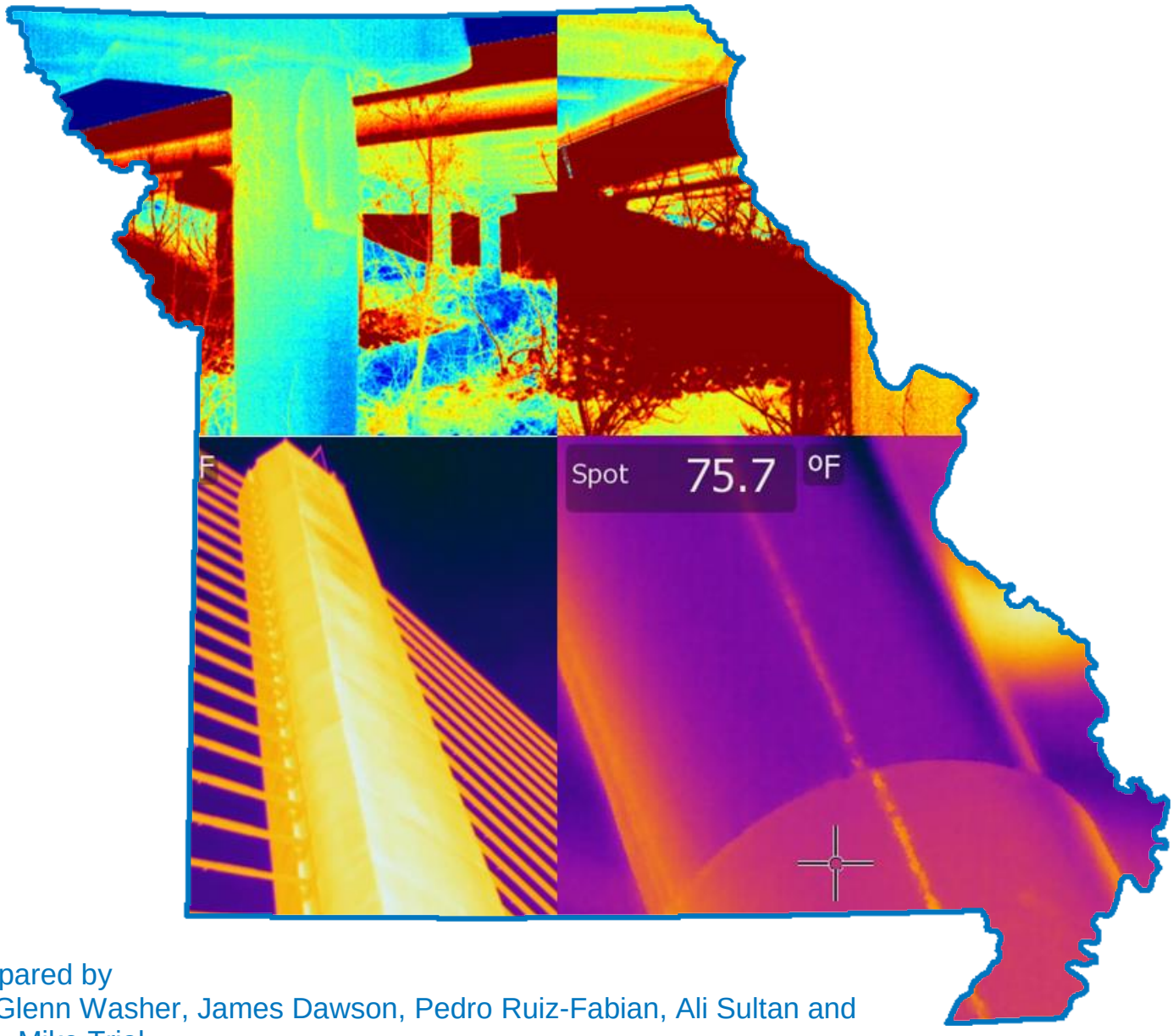

Prepared by
Glenn Washer, James Dawson, Pedro Ruiz-Fabian, Ali Sultan and Mike Trial
University of Missouri-Columbia Department of Civil & Environmental Engineering

Paul Fuchs, Ph.D.
FCI/Thermalstare

Final Report Prepared for Missouri Department of Transportation
May 2016 Project TRyy1144 Report cmr16-007

TECHNICAL REPORT DOCUMENTATION PAGE

1. Report No. cmr 16-007	**2. Government Accession No.**	**3. Recipient's Catalog No.**
4. Title and Subtitle Field Testing of Hand-Held Infrared Thermography, Phase II		**5. Report Date** April 2016 Published: May 2016 **6. Performing Organization Code**
7. Author(s) Glenn Washer, James Dawson, Pedro Ruiz-Fabian, Ali Sultan http://orcid.org/0000-0002-9717-5231, and Mike Trial (Univ of Mo-Columbia); Paul Fuchs, Ph.D. (FCI)		**8. Performing Organization Report No.**
9. Performing Organization Name and Address Department of Civil and Environmental Engineering, University of Missouri-Columbia E2509 Lafferre Hall, Columbia, MO 65201 FCI/Thermalstare 75 Lawson Rd, SE, Suite 204 Leesburg, VA 20175		**10. Work Unit No.** **11. Contract or Grant No.** MoDOT project #TRyy1144 FHWA TPF-5(147)
12. Sponsoring Agency Name and Address Missouri Department of Transportation (SPR) http://dx.doi.org/10.13039/100007251 Construction and Materials Division P.O. Box 270 Jefferson City, MO 65102		**13. Type of Report and Period Covered** TPF-5(147) Final Report (November 2011-May 2016) **14. Sponsoring Agency Code**

15. Supplementary Notes

Conducted in cooperation with the U.S. Department of Transportation, Federal Highway Administration. MoDOT research reports are available in the Innovation Library at http://www.modot.org/services/or/byDate.htm. This report and appendices are available at http:// http://library.modot.mo.gov/RDT/reports/TRyy1144/ and http://www.pooledfund.org/Details/Study/475.

16. Abstract

This report is the second of two volumes that document results from the pooled fund study TPF-5 (247), Development of Handheld Infrared Thermography, Phase II. The interim report (volume I) studied the implementation of handheld thermography by participating state Departments of Transportation (DOTs). This final report (volume II) provides a summary of field testing conducted to evaluate the capabilities of two different IR imaging technologies for detecting subsurface damage in concrete. The IR-UTD technology collects thermal images over a period of time; these data are processed to measure thermal inertia of a material. The IR-UTD technology is an entirely new approach for imaging damage in concrete structures. The IR-DSS technology automatically captures thermal images while the system is moved from one position to another. The IR-DSS technology produces images based on the radiant thermal energy from a material in the same manner as other typical thermal imaging systems. However, the IR-DSS has a unique design that allows the system to be implemented from different mobile platforms and uses a precision encoder to trigger data collection.

In general, it was found that the IR-UTD technologies had capabilities that exceeded the capabilities of conventional IR imaging. The technology provided highly accurate data that documented the size and shape of delaminations in bridge decks and other structures. The IR-UTD technology also provided data on the depth of damage and could image the structural features of a bridge. Traffic control was not required to implement the IR-UTD technology.

The IR-DSS capability was demonstrated to include the ability to produce spatially-referenced images that provided accurate depictions of subsurface damage, and these data were presented to-scale in a plan-view image of an entire deck. Traffic control was required to implement this technology, because the travel speed of the system is limited to < 10 mph.

17. Key Words Concrete bridges; Field tests; Nondestructive tests; Rehabilitation (Maintenance); Infrared thermography	**18. Distribution Statement** No restrictions. This document is available through the National Technical Information Service, Springfield, VA 22161.

19. Security Classif. (of this report) Unclassified.	**20. Security Classif. (of this page)** Unclassified.	**21. No. of Pages** 100	**22. Price**

Project No. TPF-5(247)

Field Testing of Hand-Held Infrared Thermography, Phase II

Final Report
Volume II: New Technologies

Prepared By:
Glenn Washer, James Dawson, Pedro Ruiz-Fabian, Ali Sultan, Mike Trial
University of Missouri
Columbia, MO

and

Paul Fuchs, Ph.D.
FCI/Thermalstare

April, 2016

ACKNOWLEDGEMENT OF SPONSORSHIP

This research was funded by the Missouri (MO) Department of Transportation under pooled fund TPF – 5 (247). Twelve additional states participated in the pooled fund, as indicated below. The authors gratefully acknowledge their support.

Texas, Minnesota, Oregon, Iowa, Pennsylvania, New York, Michigan, Georgia, Wisconsin, Ohio, Kentucky, and Florida

TABLE OF CONTENTS

LIST OF FIGURES

LIST OF TABLES

1 INTRODUCTION

This report is the second of two volumes that document results from the pooled fund study TPF – 5 (247), Development of Handheld Infrared Thermography, Phase II. This project included a study of the implementation of handheld thermography by participating state Departments of Transportation (DOTs), which is documented in Volume I of this report. During the course of the study, innovative Infrared (IR) technologies were developed outside the project that offered new and potentially more effective approaches to detecting subsurface damage in concrete. These technologies were procured and tested to evaluate their capabilities.

This report provides a summary of field testing conducted to evaluate the capabilities of two different IR imaging technologies. One of these technologies captures thermal images over time and processes those data to characterize delaminations and to image structural features of a bridge. Chapter 2 of this report describes testing completed to evaluate the capabilities of this technology. A second technology is comprised of a vehicle-mounted IR imaging technology that creates plan-view thermal images of a deck (or other structure). The plan-view images show thermal contrasts created by delaminations or debonding in the concrete. Testing conducted to demonstrate the capabilities of this technology are described in Chapter 3 of the report.

1.1 Background

Highway bridges form an important component of the transportation infrastructure in the United States. There are more than 600,000 bridges in the US with an average age of 42 years. Exposure to the environment, loading from traffic, and natural hazards affect the condition of bridges, leading to deterioration and damage that reduces the service life. Damage in highway bridges can present hazards to the traveling public and reduces the serviceability of bridges. For bridge decks in particular, damage that evolves due to corrosion leads to spalling in the bridge deck that requires repair to maintain the serviceability of the bridge. Repairs can range from simple patching operations to full-scale deck replacement.

A periodic inspection program, in place since the early 1970s, requires visual condition assessments of bridges, typically on a 24 month inspection interval [1]. The visual assessments of bridge condition are unable to detect deterioration early in the damage process, when damage may be subsurface and therefore not visible. If damage could be detected during this early stage then cost-effective mitigation strategies could be employed to extend the service life of a bridge and ensure safety. Additionally, the geometry and construction of bridges makes access for inspection very challenging. Man-lifts and specialized under-bridge inspection

trucks are required to gain hands-on access to the entire bridge; resource constraints within state DOTs are such that for the majority of bridges these types of equipment cannot be used. For the inspection of bridge decks, traffic control is required to gain access to the deck. Inspections are typically conducted without traffic control due to cost, and therefore, assessment of the deck must be done from the roadside.

Infrared thermography (IR) offers a potential solution to these inspection challenges. IR cameras produce images of the surface temperature distribution over a large area and can produce these images from distances of 100 ft. or more from the surface being imaged. For example, thermal images of a bridge deck can be produced from a position along the roadside without the use of traffic control. For the soffit (i.e., underside) portion of the bridge, IR images can be produced from positions on the ground below the bridge. The IR images reveal subsurface damage in the concrete, which is manifested as temperature variation at the surface of the concrete. The subsurface damage is typical in reinforced concrete structures and is commonly known as delamination. The delamination is produced by the expansion of the reinforcing steel in the concrete as a result of corrosion processes. The reinforcing bars are placed in a manner such that when multiple bars are corroding, cracking in the concrete joins between the bars. This results in a horizontal crack parallel to the surface of the concrete that is subsurface (i.e., a delamination). Figure 1 shows an image captured by an infrared camera that shows an example of the detection of subsurface delamination in a concrete bridge deck. Figure 1A shows a photograph (visual image) of the area of the deck imaged using an infrared camera (Figure 1B). As shown in the visual image, the deck appears to be intact and in good condition. Figure 1B shows the IR image of a bridge deck that reveals an area of deck that is hotter than the surrounding areas. This area is a subsurface delamination; other delaminations are also shown farther away in the image. The image is captured from a standing position on the shoulder of the roadway while the roadway remained open to traffic. The subsurface delamination shown in Figure 1B was verified by sounding the area.

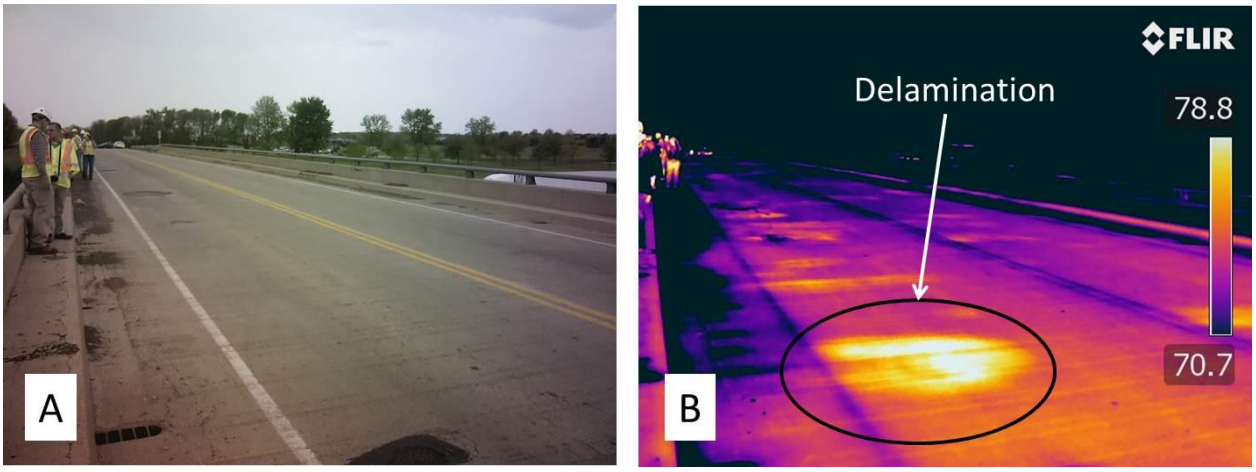

Figure 1. Photograph of a bridge deck (A) and an IR image of the same deck area showing a subsurface delamination (B).

Previous work has demonstrated that under the appropriate weather conditions, subsurface delaminations produce measureable surface temperature variations [2-6]. A study was completed during phase I of this project that examined the weather conditions under which delaminations could be imaged by an IR camera based on experimental observation of a large concrete block [7]. Styrofoam targets embedded at depths of 1, 2, 3 and 5 inches were used as models of delaminations in order to assess the thermal response under different weather conditions. A guideline was developed which describes the ambient weather conditions needed to image subsurface damage in concrete [5, 7, 8]. This guideline covered both solar-exposed surfaces of concrete, such as a bridge deck exposed to the sun, and shaded conditions, such as the underside of a bridge deck (soffit). The detailed results of this previous study are available in the referenced literature.

Figure 2 shows a selected result from the study for a single day for a surface exposed to solar loading. This image shows the thermal contrast for the Styrofoam targets at different depths in the concrete block. The thermal contrast is the temperature difference between the surface above an embedded Styrofoam sheet and a surface area above intact concrete. The horizontal axis of the figure shows a single 24 hour period from midnight (0:00) to midnight the next day. The left vertical axis shows the thermal contrast developed at the target and the right vertical axis shows the solar exposure in watts/m^2. This figure illustrates how the thermal contrast for a subsurface target develops over the course of the day. In the overnight period, the thermal contrast is negative, meaning the target area appears as a cold spot on the concrete surface. During the daytime, the sun rises, increasing the solar loading on the deck.

During this period, the thermal contrast at the targets changes from a negative value to a positive value, i.e., the surface above the target appears as a hot spot. Several notable features in this figure illustrate key characteristics of thermal imaging of subsurface damage in concrete:

1. The magnitude of thermal contrast depends on the depth of the target, with more shallow targets developing a greater maximum thermal contrast than deeper targets.
2. The time at which the maximum thermal contrast develops depends on the depth of the target, with deeper targets reaching their maximum much later in the day than shallow targets.
3. There is a point in time (marked A in the figure) when the contrast magnitude is essentially the same, regardless of the depth of the target.
4. There are two time periods during the day (marked B and C in the figure) during which there is no thermal contrast between the target areas and the sound concrete.
5. The rate at which thermal contrast develops between the target areas and the sound areas of the block is a function of the target depth, with shallow targets displaying a higher rate than deeper targets.

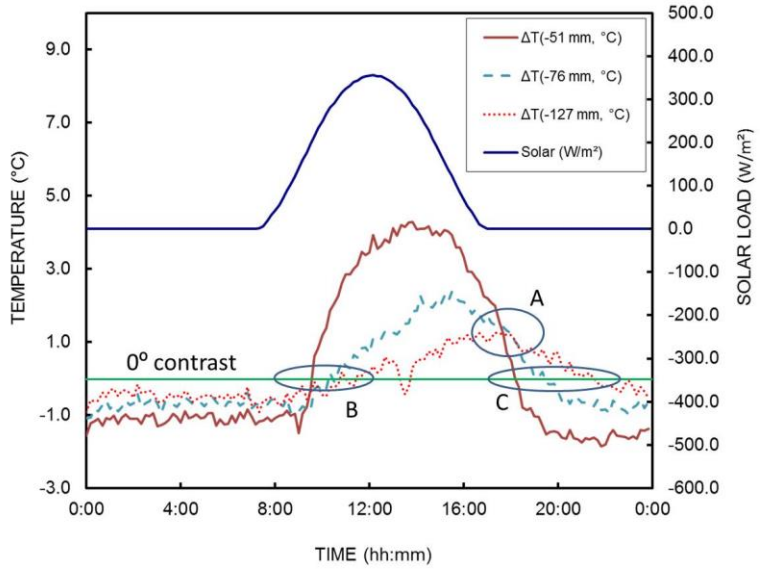

Figure 2. Graph showing thermal contrast for subsurface targets in concrete, and the solar loading during a 24 hour time interval.

It should be noted that solar loading is not required to detect subsurface delaminations in concrete. Typical ambient temperature variations are sufficient to create the necessary thermal contrast for detection of delaminations. However, the thermal contrast is reduced relative to solar-exposed surfaces [5, 7].

These data illustrate the challenge of imaging subsurface damage in concrete using ambient environmental conditions as the driving force for thermal gradients in the concrete. The time of the inspection is a key parameter, and this obviously depends on the surrounding

weather conditions. There is a peak time during the day when thermal contrast is greatest, and this time depends on the depth of the damage. At other times, the thermal contrast may be reduced or there may be no thermal contrast, as shown in the figure. There are times when the thermal contrast is the same for each of the targets, regardless of the depth. Given that the thermal contrast magnitude depends on the ambient environmental conditions as well as the depth and thickness of the subsurface delamination, it is not possible to assess the depth of a delamination from a single IR image.

An additional complication is that inspection results are difficult to reproduce because the thermal contrast produced by a subsurface defect is changing over time, and is dependent on several surrounding environmental conditions, such as solar loading, wind speed, weather conditions leading up the testing, rainfall, etc. As a result, it can be very difficult to reproduce testing results on a different day, or even a different time of the same day.

An additional limitation of the hand-held IR technologies used during the course of the research is that the thermal images produced typically show only portions of a bridge in areas where damages are detected. These images are captured by individual inspectors from a standing position on, adjacent to, or below the structure. A vehicle-mounted system that could capture the entire bridge deck or soffit would be advantageous for more thoroughly documenting a bridge's condition and make data collection more consistent than hand-held thermography. Such vehicle-mounted systems have existed for some time and typically include a video camera and a video capture of IR data while a vehicle moves across the bridge deck [9-12].

New technologies that could address the limitations of the technology used during this phase of the research were sought out. These technologies are described in Section 1.2.

1.1.1 Implementation Study

The implementation of this technology was studied during the pooled fund and the results of this study are documented in Volume I of this report. A brief summary of the results of that study are presented here for readers that have not reviewed the Volume I report.

Thirteen state DOTs participated in the study, which consisted of developing tools to assist in the implementation of the technology, training individuals to use the cameras in the field, and field testing the technology. The project focused on providing state DOTs the opportunity to use and test IR thermography within their existing programs for the inspection and maintenance of their bridge inventory. To achieve this objective, an FLIR 620 hand-held infrared camera was purchased for each participating state. A training course was developed

to instruct bridge inspection and maintenance personnel on the use and application of the technology. This training course featured ½ day of training in the classroom, followed by ½ day of field testing.

Simple guidelines were developed for field inspection that address these variables in the performance of IR imaging. These guidelines provide information on the necessary ambient weather conditions at the time of the inspection (and prior to the inspection), as well as suitable time intervals for conducting the inspection. These guidelines were used to develop and implement a web-based application that can be used in the field by inspectors to analyze current weather conditions and determine if appropriate conditions exist for successful thermographic inspection. The web-based application, known as the IR Bridge Inspection Planner (IR-BIP), utilizes location technology to identify the location of the user, and queries nearby weather stations (from a network of existing weather stations located all over the US) to obtain recorded temperature variations at that location. Weather predictions are obtained to provide a forecast of weather conditions at that location over the next 24 hours for the purpose of planning an inspection for the following day. The web site also allows the user to obtain data from any location through the use of an interactive map, GPS location, or a zip code (*http://thermalstare.com/FCIWeatherChecker1.aspx*).

A study of the implementation challenges faced by DOTs in using these cameras was completed after approximately 12 months of use by the state DOTs. In this implementation study, it was found that the primary barrier to implementing this technology was limited resources. State DOTs reported that a lack of equipment and personnel constrained their application of the technology. It was also reported that there was a high level of confidence that damage detected using the thermal cameras was in fact damage, and could be confirmed using sounding. The complete results of this phase of the research are included in Volume I of this report.

An increasing number of states in the US are implementing thermal imaging as part of their inspection and project planning regimes. Generally, the technology is being used to determine the scope of repairs needed to maintain a bridge. The ability of the thermal imaging technology to detect damage in portions of the bridge that are difficult to access without ancillary equipment (such as under bridge inspection trucks or man-lifts) make it a suitable tool for field engineers. The technology can be used by these engineers to make assessments of where further hands-on inspection is required and to determine the quantity of repairs when scoping a project. Infrared thermography is not being used typically for routine, biannual bridge inspections.

1.2 New IR Technology

To address the identified limitations for thermal imaging, two new technologies were explored that could improve the reliability of IR imaging. A transient imaging technology that captures IR data over time was explored to address the variable nature of IR results that stem from the interaction between environmental conditions and the thermal contrast that developed at delaminations. This technology has been name “Ultra Time Domain Infrared” (IR-UTD) because it examines the thermal behavior of the concrete over the course of a long time period (hours, days, or weeks). This is in contrast to a hand-held camera that collects a single image at a single point in time. The second technology is known as a Deck and Soffit Scanner (IR-DSS), which is a vehicle-mounted IR system that is intended to scan an entire bridge deck or soffit. The IR-DSS collects a single image of each location at a particular point in time, and these individual images can be stitched together to display, for example, an entire bridge deck. These technologies will be described in this section.

1.2.1 IR-UTD

Generally this new technology collects IR data at several different points in time over the course of the day rather than capturing images at a single point in time, when the observed thermal image may or may not represent the optimum time for inspection. The transient thermal behavior of the concrete is then analyzed to identify anomalies in the thermal behavior caused by subsurface damage in the concrete.

Previous efforts to introduce transient thermography applications for civil infrastructure have focused largely on the use of active heating for detecting delamination of composite overlays or subsurface damage in concrete structures [13-18]. Generally, these approaches use an external heat source, such as radiant heaters, to impart transient heat flow in the concrete. Transient heat flow is analyzed to reveal subsurface damage in the concrete based on thermal contrast at the surface of the concrete, in much the same manner as traditional thermal imaging. Under this approach, specimens are heated for some time interval, and then observed during the cooling process after the heating has been turned off. Phase analysis has also been explored to improve the data resulting from active heating [14]

In the case of a bridge in the ambient environment, the sun provides a powerful radiant heating source that can be used to generate transient heat flow in the concrete. In addition, diurnal ambient temperature variations provide transient heat flow through convective heating (and cooling), even in areas not exposed to solar loading. For example, the soffit (underside) area of a bridge is not exposed to direct solar loading, yet subsurface delaminations still result in

temperature variations on the surface that can be detected with a thermal camera [5]. Results such as those shown in Figure 2 suggest that an optimized thermographic imaging system for bridges would collect images at different times such that maximum contrast from defects at different depths would be captured. Alternatively, data collected over heating and/or cooling cycles could reveal variations in the rate of change (ROC) associated with intact concrete as compared to damaged concrete. Additionally, the thermal cycles of heating and cooling over a 24 hour period are repeated daily, which offers the opportunity to monitor several heating and cooling cycles to analyze data for the purpose of detecting subsurface damage.

The IR-UTD technology is capable of capturing transient images of a concrete surface under the heating and cooling conditions cause by diurnal temperature variations. Thermal images are captured periodically over a time interval that ranges from a few hours to a few days. This allows for thermal images to be captured at times when the thermal contrast is maximized for subsurface delamination in the concrete. In addition, data is processed to identify rate of temperature change to image the thermal inertia rather than surface temperature. Since subsurface damage results in surface temperature changes whose rates are depth-dependent (see Figure 2), information related to the depth of the damage can be ascertained, which is not possible using a single, static IR image.

This new technology allows for significantly more information to be captured than is possible with traditional IRT. For example, the structural configuration of a bridge, such as the location of beams, webs, and diaphragms, can be illustrated in addition to subsurface defects such as delaminations. This technology was originally developed for the application of coating for bridges. The following section will briefly describe the development of the technology.

1.2.1.1 Background on UTD-IR

The IR-UTD instrumentation was developed for the condition assessment of bridges. The technology was developed by Fuchs Consulting, Inc. (FCI) of Leesburg, VA. This technology was developed under a Small Business Innovative Research (SBIR) project funded by the Federal Highway Administration (FHWA) [19]. During the course of the SBIR project, a modular IR system was developed focused on the application of the technology for damage detection for bridge coatings. This technology is known as the IR Coating Inspection System (IR-CIS).

The principles of the IR-CIS technology are illustrated in Figure 3. A camera head affixed with an illumination source was developed by FCI that captures IR data and visual images of the surface under inspection. The illumination source is used to heat the surface of

the material under inspection for a very short time interval (several seconds). Images are capture at a high rate, such as 30 or 60 samples per second, to observe the distribution of heat on the surface during the heating and cooling cycles. These data are then analyzed to image areas on the surface where the dissipation of heat varies; these variations result from either degradation of the coating, or a defect at the bond area of the coating and the substrate. These variations are displayed as an image of the surface, with indications on the surface being imaged in a similar manner as with a conventional IR technology. However, the data displayed in the image are not temperature, but rather a measurement of the thermal inertia on the surface under inspection. Algorithms were developed that quantify the ROC during the heating and cooling cycles and differential changes in the surface emission between different specific points in time during data collection.

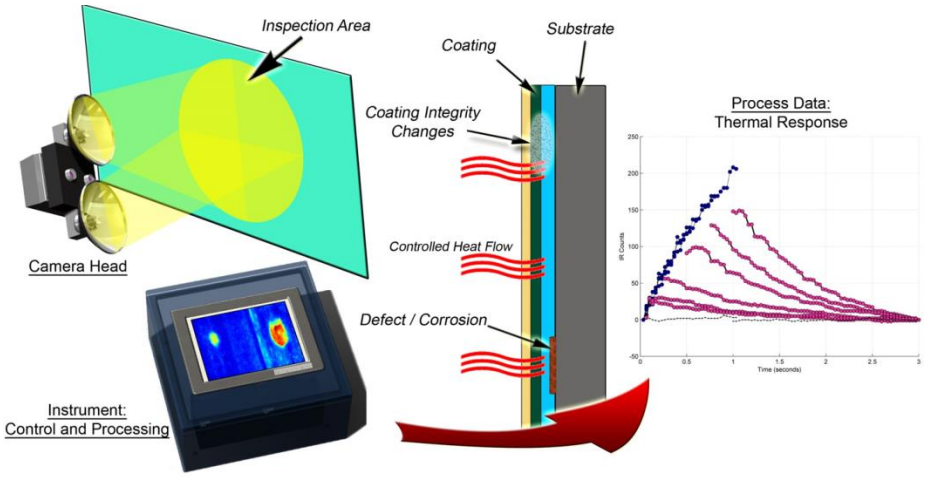

Figure 3. Schematic diagram of active thermography for detecting damage in bridge coatings.

This technology is applied to detect defects, such as corrosion, that are under coatings so they are not visually observable. Figure 4 provides an example of the application of the IR-CIS technology for detection of corrosion on a steel bridge. Figure 4A shows the hand-held prototype instrument being used to image an area of the surface of a steel bridge. Figure 4B shows the IR-CIS results from an area of intact coating that has corrosion beneath the coating. Figure 4C shows the defect following extraction, i.e., the intact coating was removed to verify the results shown in the image [19].

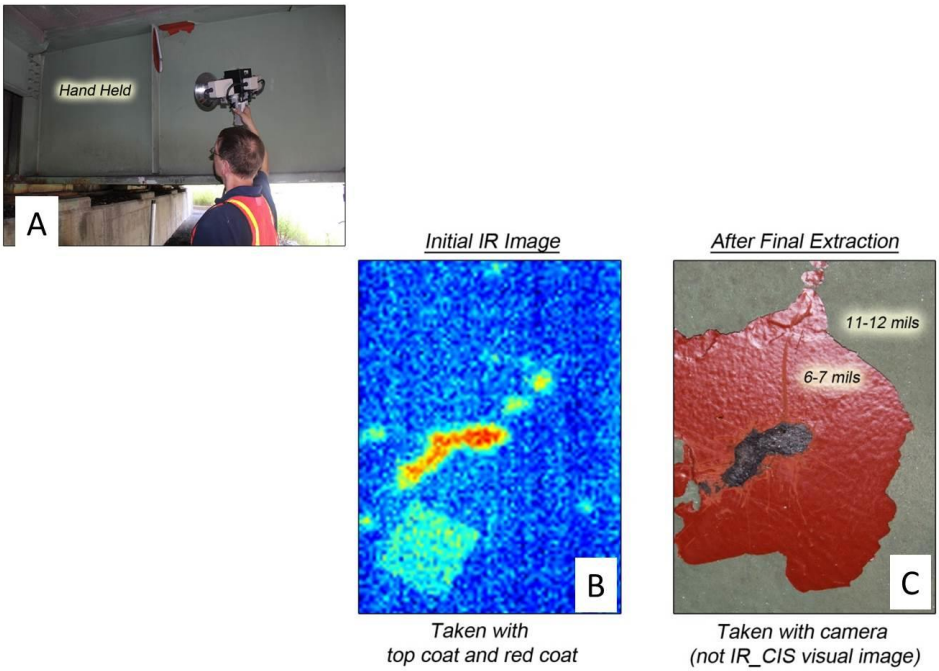

Figure 4. Figure showing the application of active IR system for detecting corrosion under coatings on a steel bridge. Photograph of the instrument being used in the field (A), image of a defect in the intact coating system (B), and the defect after extraction of the coating (C).

Based on this approach for imaging subsurface defects in coatings on steel bridges, it was conceived that this technology could be applied to subsurface defects in concrete bridges. The primary change necessary to apply the technology was to simply change the time basis over which the testing was conducted. To image a large area of a bridge deck, the IR system could be mounted above the structure on a mast, light pole, or other support as shown in Figure 5. Data could be collected over a longer time interval, such as several hours or several days, and processed using the FCI algorithms originally developed for coating assessment.

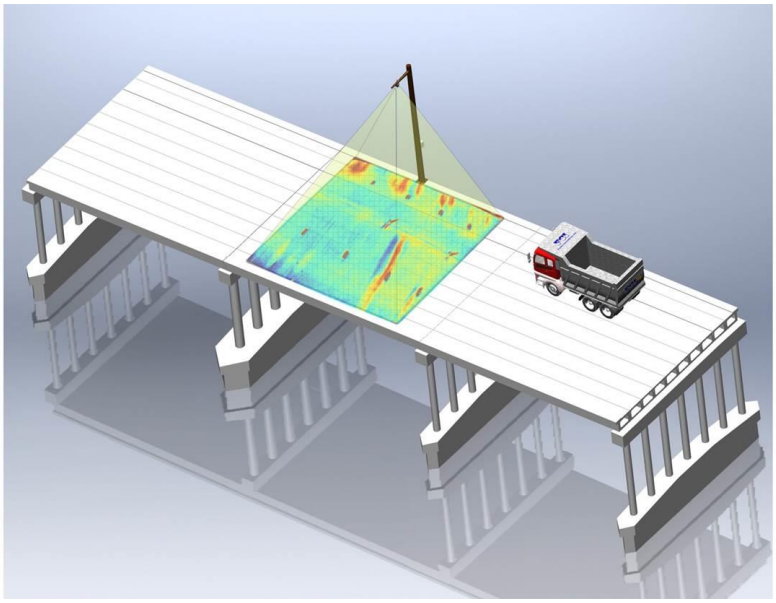

Figure 5. Schematic diagram of imaging a large area of bridge deck from a light pole or mast.

Figure 6 illustrates the application of this new technology. The imager is placed on a mast above the surface of the deck such that a large area is captured in a single image, as shown in Figure 5. Data is collected over the course of temperature cycles of the bridge deck caused by varying environmental conditions, such that many images of exactly the same area are captured. The time interval over which data are collected can range from several hours to several days. Time intervals in-between images typically range from 1 to 10 minutes. These individual images are then processed to create an image of the thermal inertia of the deck as shown in Figure 6. This figure shows the IR-UTD image of the bridge deck that reveals internal features of the bridge, such as webs and diaphragms, as well as delaminations in the bridge deck. The bridge deck imaged is the 7 in. nominal thickness deck of a cast-in-place box girder with three webs and intermediate diaphragms located mid-span, with additional diaphragms located above the supporting pier. The webs and diaphragms can be seen in the IR-UTD image as well as the delaminations in the bridge deck.

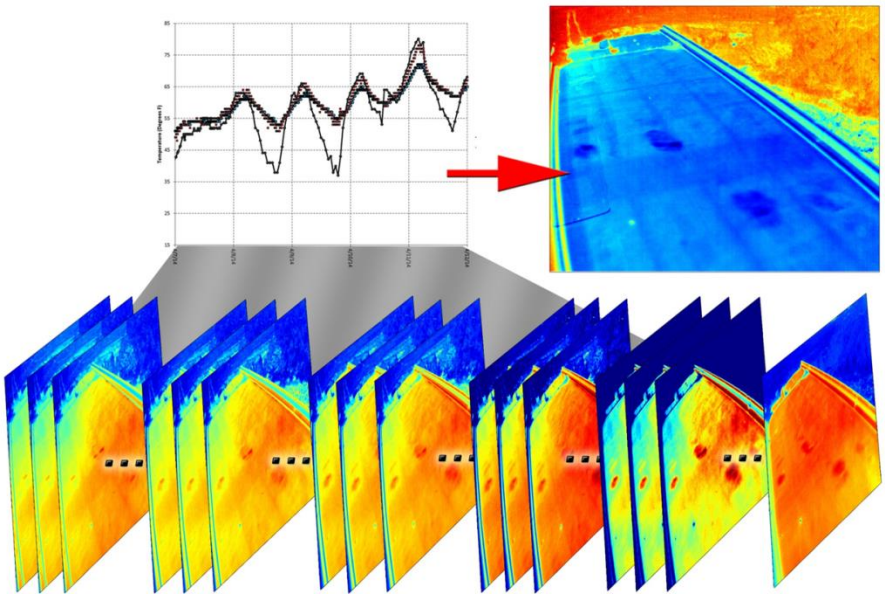

Figure 6. Illustration of the IR-UTD process for collecting data during temperature cycles to produce an image of damage in a bridge deck.

The resulting image can be compared to an image captured using the traditional approach of analyzing the radiant flux of IR energy emitted by the concrete. For example, Figure 7 compares a traditional IR image, taken at a time of maximum thermal contrast for the subsurface delamination in the bridge deck, with the image using the IR-UTD technology. Note that Figure 7A, which shows a typical thermal image of surface temperature on the deck, has significant variations across the surface due to uneven heating of the deck and changes in surface material properties. Additionally, the data displayed in Figure 7A were captured at the optimum time showing the greatest thermal contrast between the delaminated and sound areas of bridge deck. This result would only be obtained by an inspector using a hand-held camera if the inspection were done at the optimum time, which is difficult to determine particularly if the depth of the damage in the concrete is not known. Figure 7B, showing the IR-UTD data obtained from processing the transient thermal data over a longer time interval, provides much better signal-to-noise ratio, more clearly defined extent of the delaminations, and also shows the internal diaphragms and webs of the bridge. Color variations within the individual delaminations correspond to depth variations of the damage, as the initially subsurface delamination extends toward the surface of the deck which is the typical progress of a delamination from subsurface damage to a spall in the concrete deck.

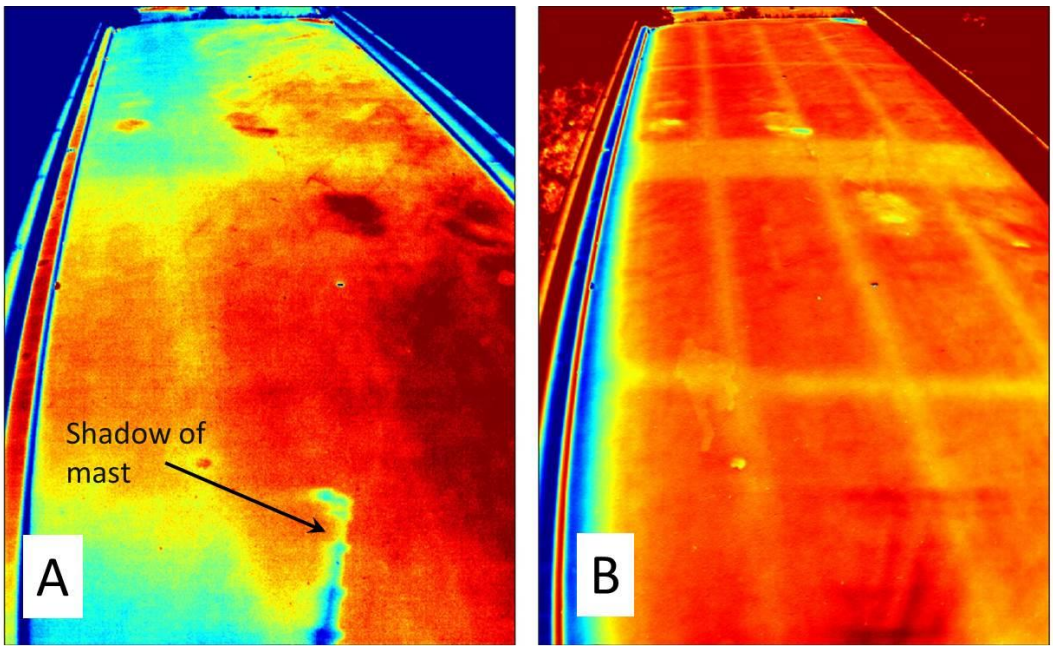

Figure 7. Image of a concrete deck showing A) traditional thermal image and B) IR-UTD image showing the delaminations in the bridge deck.

These data illustrate the potential of the IR-UTD technology. However, the IR-UTD is an entirely new technology for bridge deck inspection that has not previously existed. Therefore, the anticipated performance and capabilities of the system needed verification to demonstrate that the concept could be implemented effectively. As such, a number of field tests were completed to evaluate the capabilities and performance of this new technology. The results of these tests are described in Chapter 2 of this report.

1.2.1.2 IR – UTD System Overview

The IR-UTD system consists of three components as shown in Figure 8: a camera head, data acquisition module, and interactive display. The camera head includes both an IR imaging camera and a visual imaging camera. These two cameras are aligned to image approximately the same area of the bridge deck. The camera head is attached to a data acquisition (DAQ) module by a 32 ft. cable for powering the cameras and transferring data to the data acquisition module. The data acquisition module includes a battery pack for powering the system for about 7 hours or more, a computer interface for controlling the IR cameras, and data storage. A touch screen interactive display that is connected to the data acquisition module is used to observe the visual and IR images produced; it also interacts with the system software to control data acquisition. A wireless key board and an external display can also be used to interact with the system (not pictured).

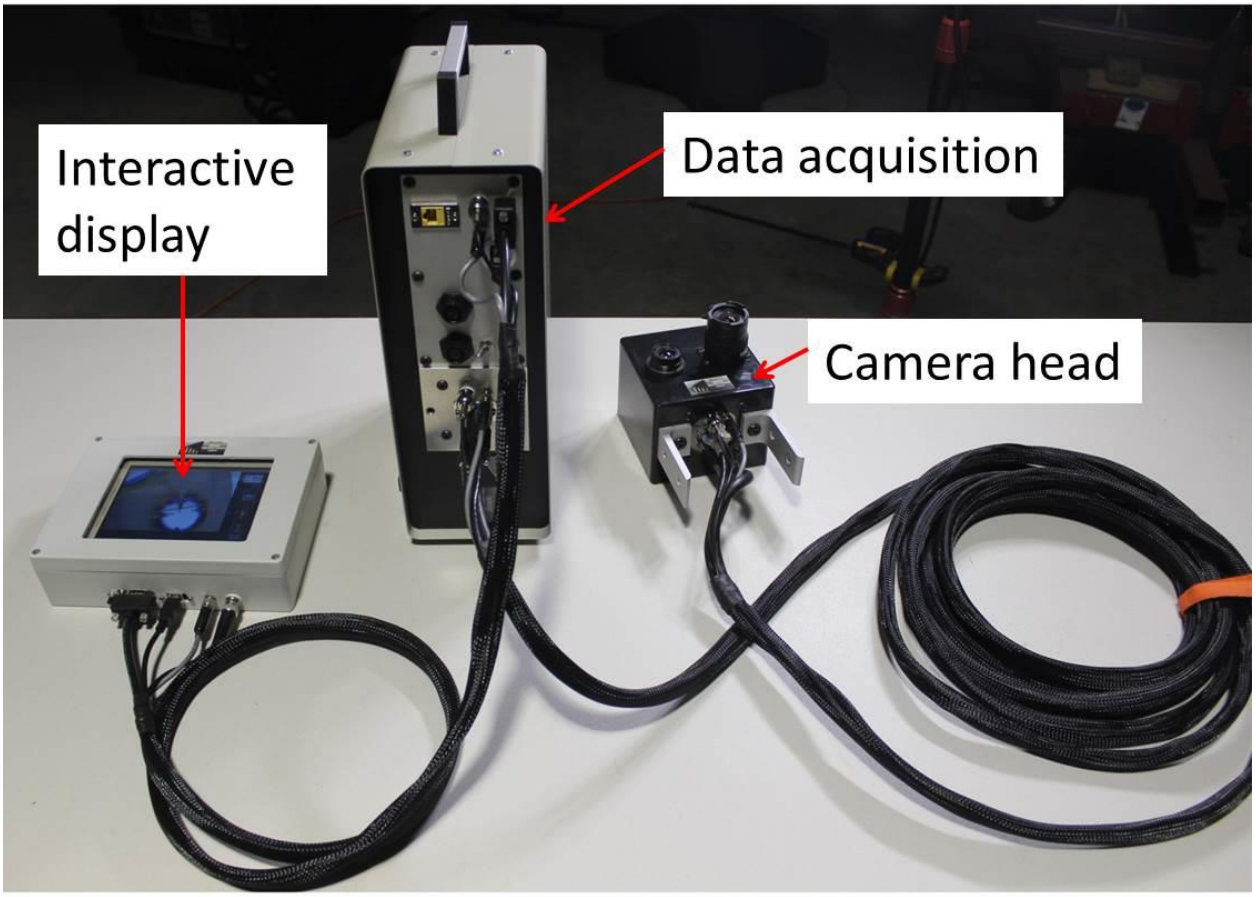

Figure 8. Photograph of the IR-UTD system components showing the camera head, the data acquisition module, and the touch-screen display.

1.2.1.3 Pan and Tilt Technology

The camera head for the IR-UTD was mounted on a manual pan and tilt stage during the early portions of the research as shown in Figure 9A and B. This manual pan and tilt allowed for the angle of the camera head to be adjusted manually to provide different field-of-view from the position on a mast. During the course of the research, an automated pan and tilt capability was added to the IR-UTD system to extend its capabilities. This automated pan and tilt stage is shown in Figure 9C. The addition of the automated pan and tilt technology allowed the IR-UTD camera head to be repositioned automatically during the course of testing to image a larger area of a structure. This pan and tilt technology was integrated into the control system software such that images could be collected from multiple camera head positions.

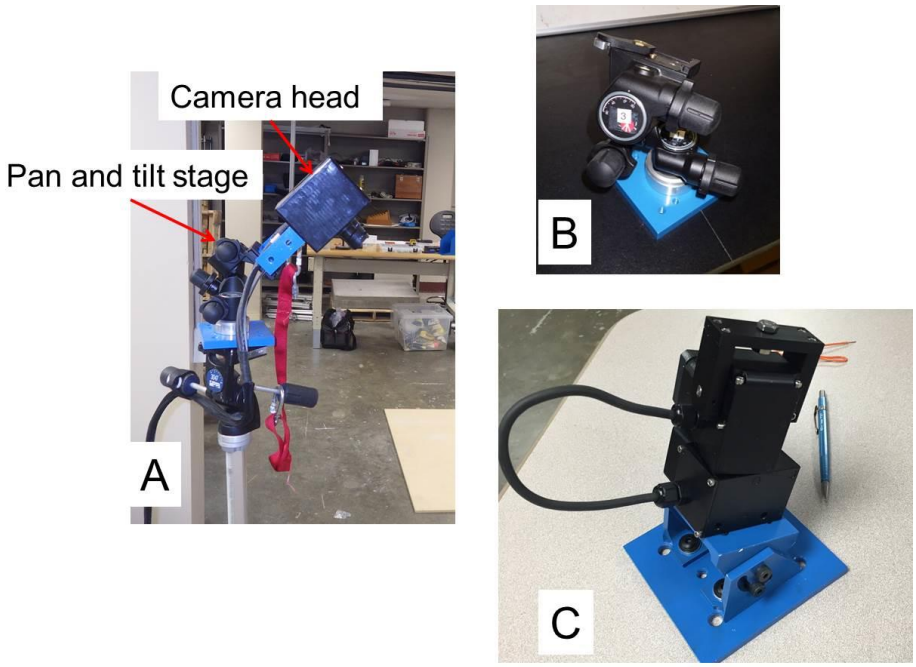

Figure 9. Photographs showing the IR-UTD camera on a manual pan and tilt stage (A), the manual pan and tilt stage (B), and the automated pan and tilt stage.

1.2.1.4 Data Processing

Data processing consists of using specialized algorithms to process sequential thermal images collected by the IR-UTD. A typical dataset consist of approximately 1000 images and processing time is ~ 2-3 minutes. Data is typically processed following the testing interval, for example, after data is collected for 24 hours. Data can also be downloaded and processed during the testing interval to obtain initial results or to assess if additional data collection is warranted.

1.2.2 IR-DSS

The IR-DSS system is intended to provide a vehicle-mounted system for capturing IR data. The components of the IR-DSS system are essentially the same as the components for the IR-UTD system shown in Figure 8. The IR-DSS is intended to capture individual images as the system is moving from one position to another position, e.g., being driven over a bridge deck. This is in contrast with the IR-UTD system that captures many images of the same area and subsequently processes data for the purpose of detecting subsurface damage. The IR-DSS captures only a single image of each area; this means that transient thermal behavior is not analyzed by the IR-DSS. As such, the images produced by the IR-DSS are similar to thermal image captured by a hand-held thermal camera.

The primary difference between the components of the IR-UTD and the components of the IR-DSS is a precision linear encoding device used in the IR-DSS for monitoring the position of the camera during data acquisition. The linear encoding device is a fifth wheel that attaches to the vehicle and tracks the position of the system. This encoder is used to trigger data collection, such that images are spatially-referenced, i.e., the exact position of the image on the surface of the bridge deck is measured and recorded. Both visual and IR images are captured and these images are spatially correlated via the alignment of the cameras and the precision encoding wheel that triggers data collection for each camera simultaneously. The system is designed to travel at speeds of less than 10 mph to ensure quality IR images will be produced.

A photograph of the system is shown in Figure 10. The figure shows the camera mounted on a mast connected via the tow hitch to a truck. The camera head is positioned approximately 10 feet above the surface of the deck. The encoder wheel is attached to the frame that is constructed to hold the camera. A cable connects the camera head and the encoder wheel to the data acquisition module and the interactive display, both of which are located in the cab of the vehicle. In this way, the IR-DSS system can be controlled by the driver or by an assistant in the passenger's seat.

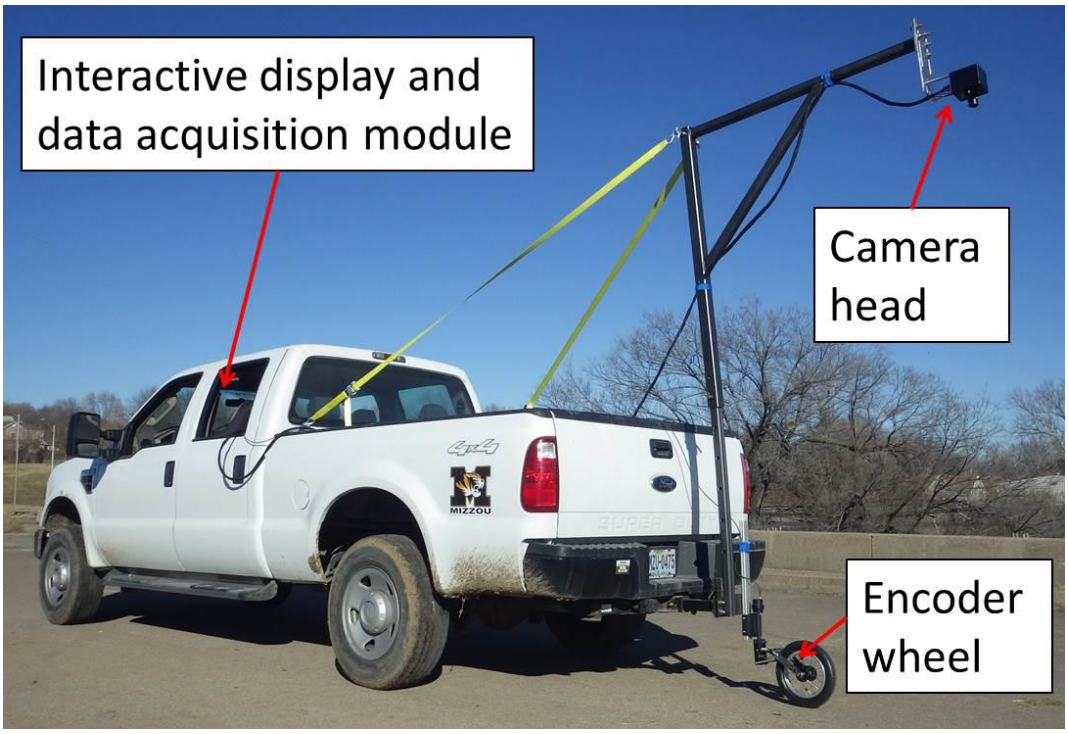

Figure 10. Photograph showing the IR-DSS system mounted on a vehicle.

An advantage of the modular configuration of the IR-DSS system is that the system can be mounted on any vehicle with a suitable tow mount. The system can also be mounted on a

rolling cart or other transportation device. This allows flexibility in the system for collecting data on ancillary structures such as culverts where vehicular access is not possible. Soffit areas of bridges can be scanned by inverting the camera to an upward viewing angle and driving beneath the bridge.

Data presented by the IR-DSS consist of thermal images and visual images from adjacent positions along the direction that the system is scanned. These images can then be stitched together to form, for example, a plan view diagram of a bridge deck. Because the images are spatially referenced, the plan view image provided is to scale.

1.2.2.1 Data processing

Thermal images captured by the IR-DSS are available in real-time while scanning over the bridge deck, or reviewed following the scanning process. These images can be reviewed individually or as a video formed from each individual image across the surface of the deck. Individual images include an 8 ft x 10 ft area of the bridge deck. Post-processing of the data is required to stitch together images to create a plan-view of the bridge deck. The stitching process typically takes ~1hr to align images and generate a single image from the images collected during each scan across the bridge deck.

2 IR-UTD TESTING

This portion of the report describes nine different field tests conducted to evaluate the capabilities of the IR-UTD system. Table 1 provides a summary of the date, location, and general purpose of each of these tests. These tests included using the IR-UTD technology to image four different bridge decks, a test block with embedded Styrofoam targets of a known depth, the soffit area of a voided slab bridge, and vertical columns. Each test is described in this chapter. Table 1 also lists the field testing conducted to evaluate the capabilities of the IR-DSS system. The results of these tests are documented in Chapter 3 of this report.

Table 1. Summary of testing conducted to evaluate new imaging technologies.

System	Dates of Testing	Location	Object Imaged	Purpose
IR-UTD	9/16/2014 – 9/19/2014	Midway MO	Test Block	Test the depth measurement effects
	5/6/2014	Columbia MO	Providence Road Bridge	Initial field testing of the technology; evaluate the IR-UTD system capabilities
	9/8/2014 – 9/11/2014	Lamoni IA	Bridge Deck during epoxy injection	Demonstrate a field application of the technology; determine if epoxy injection affected results
	6/5/2014, 8/20/2014, 9/3/2015	Kansas City, MO	Closed Highway Bridge A0295	Evaluate the repeatability of the technology Accuracy compared with chain drag
	12/12/2014, 12/17/2014	Columbia MO	Columns at MU	Demonstrate the noncontact imaging of a vertical surface
	6/30/2015 – 7/1/2015	Columbia MO	Grindstone Bridge	Evaluate the capabilities of the system; pan and tilt, imaging a bridge open to traffic, imaging a bridge with an asphalt overlay
	1/16/2015	Columbia MO	West Blvd Bridge	Demonstrate the ability of the system to image the soffit area of a bridge
IR-DSS	11/20/2015	Fulton MO	Bridge A2111	Initial testing of the technology. Comparison with GPR
	1/29/2016	Kansas City, MO	Decommissioned Highway Bridge	Comparison of results to a known condition

This chapter provides a summary of each of the tests completed under the study. Each section includes a general summary of the test situation and key findings from the test. Key findings are generally in the form of images generated by the IR-UTD or IR-DSS system.

2.1 Providence Road Bridge

The first field test of the IR-UTD system was conducted on a local roadway bridge carrying Route 163 in Columbia, MO. The concrete bridge deck had a thin polymer modified asphalt overlay. Several areas on the bridge had existing spalls. The area imaged by the IR-UTD system is shown in Figure 11. The test was completed on May 6, 2014 between the hours of 6:30 AM and 9:00 pm. Traffic control for the test consisted of diverter cones to indicate an obstacle on the shoulder of the roadway. The bridge remained open to traffic throughout the IR-UTD test. The purpose of this test was to perform an initial evaluation of the technology to learn its operating characteristics and capabilities.

The IR-UTD system was deployed using the portable light plant that was modified to support the camera head at the top of the mast, where lights would typically be placed. The DAQ was stored in the generator compartment of the light plant as shown in Figure 12. Using this mast positioned the IR-UTD camera at a height of 25 ft.

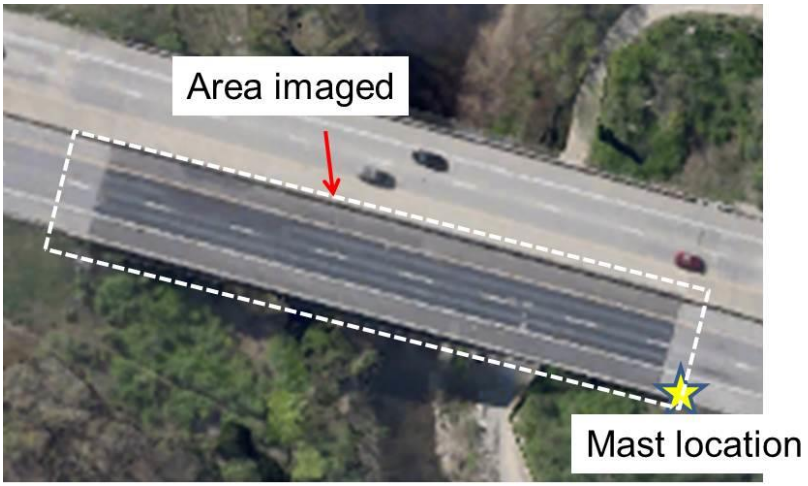

Figure 11. Aerial view of the Providence Road Bridge.

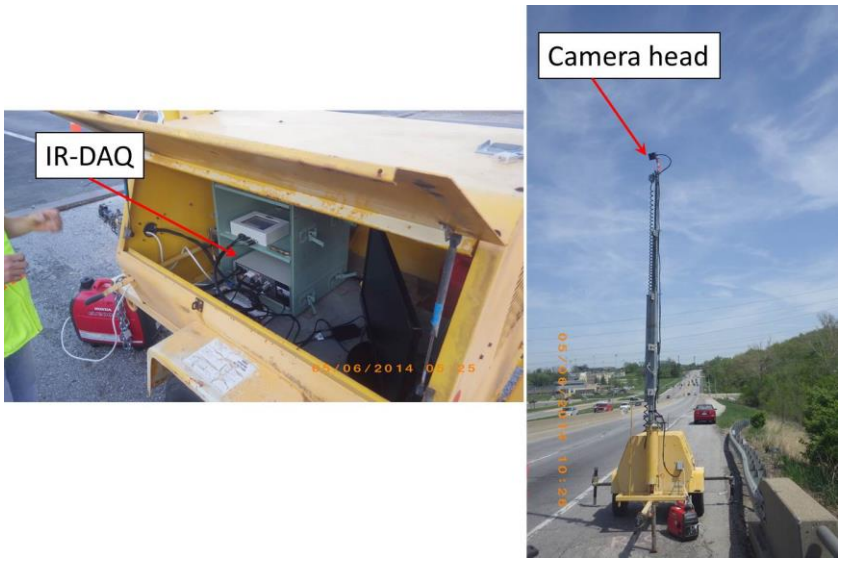

Figure 12. Mounting of the IR-UTD system for the testing the Providence Road Bridge.

Figure 13 shows both the processed IR-UTD data and the visual camera image captured by the IR-UTD camera positioned on top of the mast. In the IR-UTD image, the spalled areas of the bridge deck are shown as dark red areas. Delaminations in the deck are shown as dark

blue areas. These data indicated delamination adjacent to the joint and adjacent to spalling in the bridge deck. The spalling of the bridge deck is apparent in the visual image.

A notable feature of the IR-UTD data in Figure 13 is that no vehicles are shown in the image. The bridge remained open to traffic throughout the testing; however, the processed IR-UTD data does not show any vehicles. The transient thermal signatures resulting from vehicles passing over the bridge are removed through the processing of the data. The visual image (right) also shows no vehicles; this image was selected from a particular point in time when there were no vehicles on the bridge.

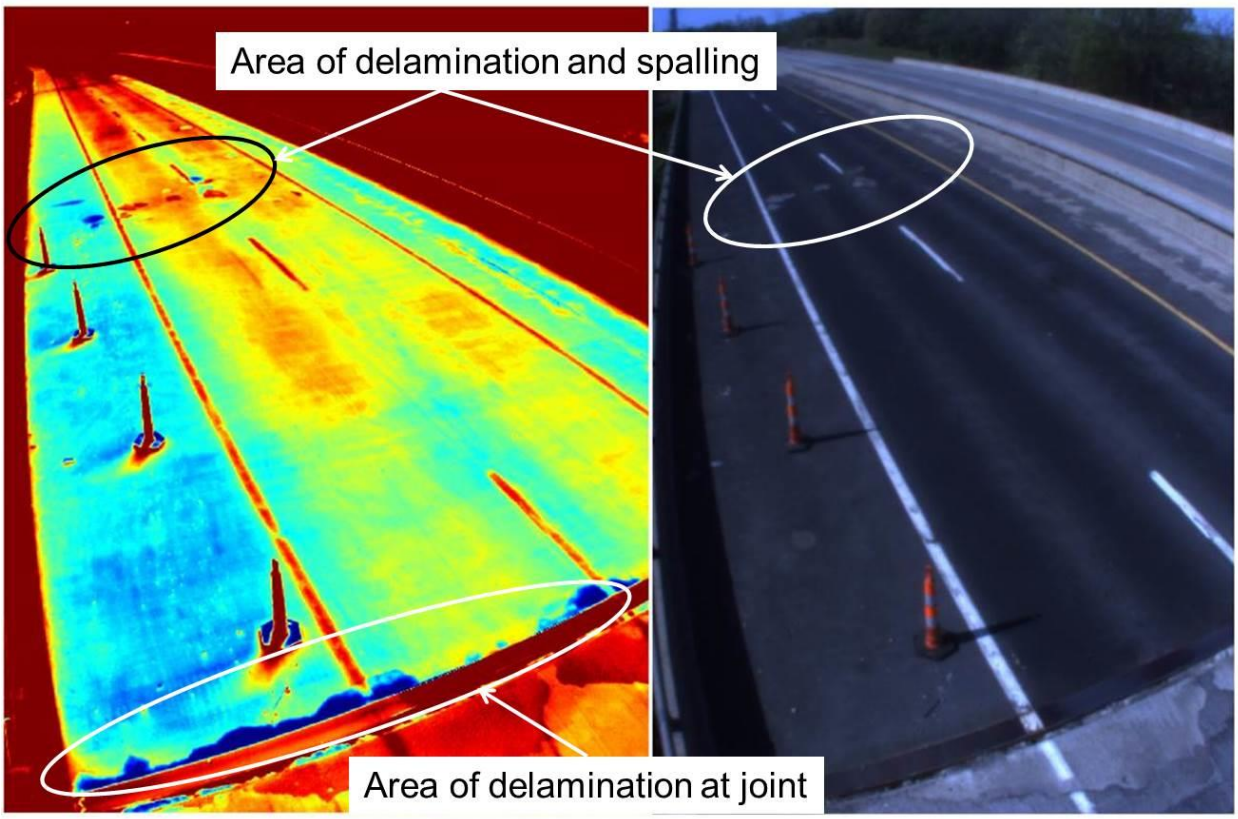

Figure 13. Side by side image of the infrared image (left) next to the visual image (right) of the Providence Road Bridge.

The data shown in Figure 13 also indicate that surface areas of the deck greater than ~ 130 ft from the IR-UTD system were not imaged effectively when the IR-UTD was mounted on the 25 ft. mast. This is due to low angle of incidence between the camera head and the surface of the deck. These data were used to establish basic test set-up parameters for future tests.

2.2 Midway Test Block

To evaluate the performance of the IR-UTD in comparison to conventional hand-held IR imaging, the test block that had been studied during the first phase of the research was evaluated. This test block is a 3 x 3 x 8 ft concrete block with embedded Styrofoam targets as shown in Figure 14, which shows a photograph of the concrete block during construction. Full details of the construction of this block are available in the Phase I research report [7]. The 12 x 12 in. targets in the test block are positioned at depths of 1, 2, 3, and 5 in. These depths correspond, respectively, to the roman numerals "I," "II," "III," and "IV" in Figure 14.

Figure 14. Preparation for concrete pouring of the Midway test block with the Styrofoam targets labeled "I," "II," "III," and "IV" corresponding to the depth of the target.

Data was collected over a period of three days from September 16, 2014 thru September 19, 2014. Ambient temperature conditions during data collection are shown in Figure 15. A box placed on the figure indicates the period of data collection. The IR-UTD

camera was positioned to observe the north side of the block, which is not exposed to radiant heating from the sun.

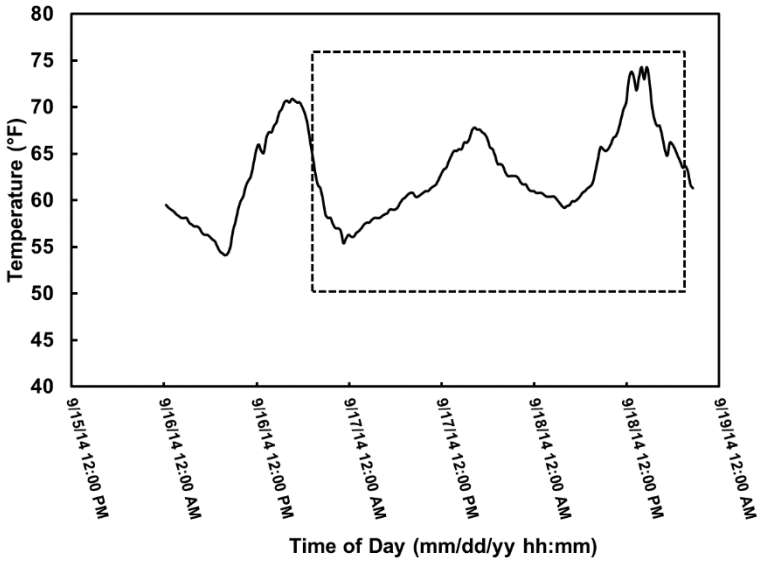

Figure 15. Ambient weather data for the Midway test block from September 16 thru September 19, 2014.

The IR-UTD data was analyzed during cooling and heating cycles throughout the testing interval. Figure 16 shows the results of data processing during the heating cycle (Figure 16A), cooling cycle (Figure 16B), and the difference between the heating and the cooling cycle (Figure 16C). A 2 in. thick concrete paver and a 6 in concrete cylinder placed on the block's footing are also shown in the image. These objects were placed on the block's footing to investigate how the objects would appear in the processed IR-UTD image as compared with test block. The most notable feature of these images is that the Styrofoam target at a depth of 5 in. in the concrete could be observed in the images, although the edges of the target are less defined than the targets located at depths of 1, 2, or 3 inches. Generally, the definition of the edges of the targets is diminished with increasing depth of the targets, such that the 1 in. deep target is more clearly defined than the 2 in. deep target, etc. It is also notable that the color representations of the images correspond to the depth of the target and the temperature cycle analyzed. For example, for the heating cycle (I), the 1 in. deep target is a more intense red than the 2 in. deep target, and the 5 in. deep target is mostly blue, indicated a low thermal inertia relative to the more shallow targets. In the image created from the cooling cycle, the targets appear blue, indicating a negative ROC. In the differential image, which shows the difference

between the inertia in the heating and cooling cycle, the 5 in. deep target is better defined than in either the heating or the cooling cycle.

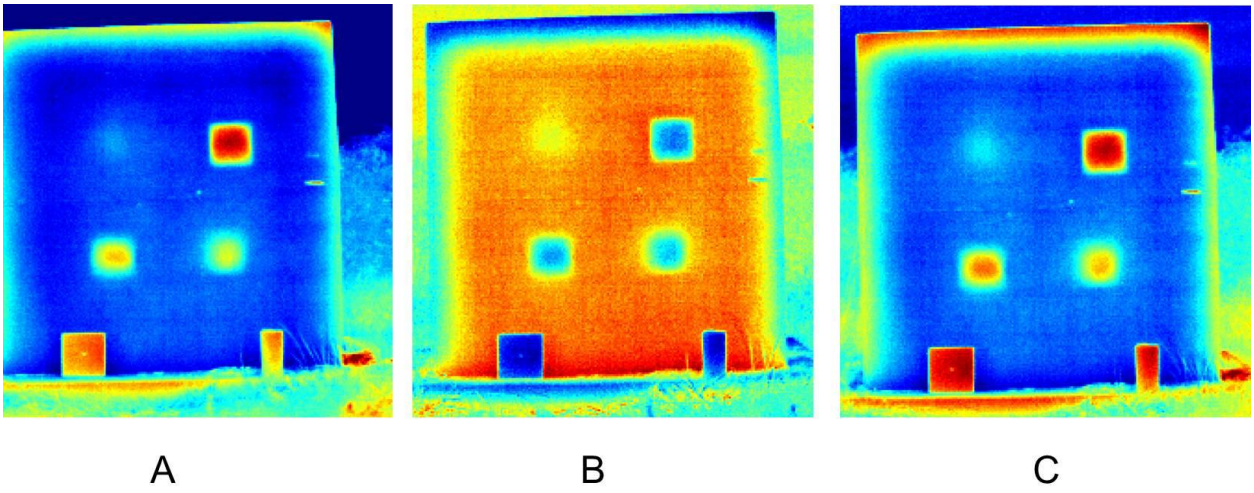

Figure 16. IR-UTD images showing the thermal inertia during the heating cycle (A), the cooling cycle (B), and the difference between heating and cooling (C).

These data were compared with images collected during phase I of the research, during which time an IR camera was used to collect individual images of the test block over a period of three months. Because the north side of the test block was not exposed to solar loading, the target at a depth of 5 in. was not typically detected in the thermal images collected during that portion of the research. Figure 17A shows a single IR image captured during phase I of the research, and figure 17B shows the IR-UTD data for that portion of the block. As this figure illustrates, the IR-UTD system has an improved ability to image the target at a depth of 5 in. relative to conventional IR imaging.

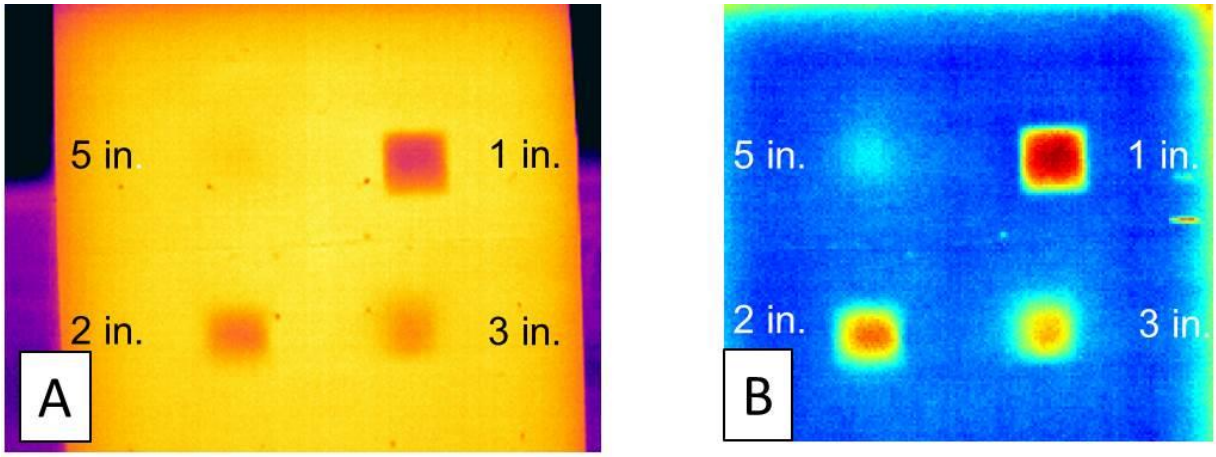

Figure 17. Comparison of conventional IR thermography (A) and IR-UTD imaging (B).

The results of these tests indicated that IR-UTD had an improved ability to image targets at a depth of 5 in. in the concrete, relative to conventional IR imaging. The results also confirmed that the results of the IR processing produced images in which the depth of the target corresponded with the magnitude of the thermal inertia.

2.3 Iowa Bridge

Testing was conducted on bridge 2706.9S069 in Lamoni, IA, that carries highway 69 over I-35. The bridge deck consisted of a reinforced concrete deck with a 1.75 in. overlay. This bridge was originally constructed in approximately 1970 and rehabilitation, which included deck repairs and installing the concrete overlay, occurred in 1992. Testing was performed over four days from September 8-11, 2014. The deck of the bridge was scheduled to be treated with epoxy injection during this time interval. Epoxy injection is a preservation / maintenance repair methodology in which epoxy is injected into the delamination to extend the service life of the bridge deck. The objectives of the test were as follows:

- Test the capability of the IR-UTD system to image delaminations in a bridge deck
- Evaluate the potential of the technology as a quality control tool for epoxy injection

To meet these objectives, the IR-UTD camera head was mounted on the mast extending above the bridge deck. From this position the IR-UTD was able to image approximately 100 lft of the 32 ft wide bridge deck, or about 3200 sq ft of the deck. An aerial view of the bridge is shown in Figure 18, showing the area of the bridge deck that was imaged by the IR-UTD system. This test area included both travel lanes and shoulders in the bridge end-span.

Figure 18. Aerial view of the Iowa Bridge deck showing area imaged by the IR-UTD.

During the course of the testing, hammer sounding was conducted by Iowa DOT personnel. The results of the sounding were used for comparison to the IR-UTD results. Drilling operations completed as part of the injection procedure also verified the IR-UTD results

and provided a means of evaluating the depth of the delaminations from the surface of the deck. Finally, hand-held thermographic images were captured using the FLIR 620 cameras and compared to the sounding and IR-UTD results.

2.3.1 Test Setup

The test set-up for this bridge consisted of mounting the IR-UTD camera on a 30 ft. pneumatic mast to provide a field of view extending over approximately 100 lft of the bridge deck. The mast was supported from a custom test frame constructed to support the mast and the IR-UTD DAQ module enclosure as shown in Figure 19. The main components of the steel structure included a strong-back (1.5 x 1.5 x ¼ in. tube) connected to the mast by ¼ in. plates. Perforated tubing attached to the strong-back were used to mount the IR-UTD DAQ such that DAQ could be accessed from the bridge deck. This test frame was then mounted to a ½ in. thick base plate (not shown). Four cast-in-place 1.25 in. threaded rods protruding from the light pole base were used to attach the baseplate.

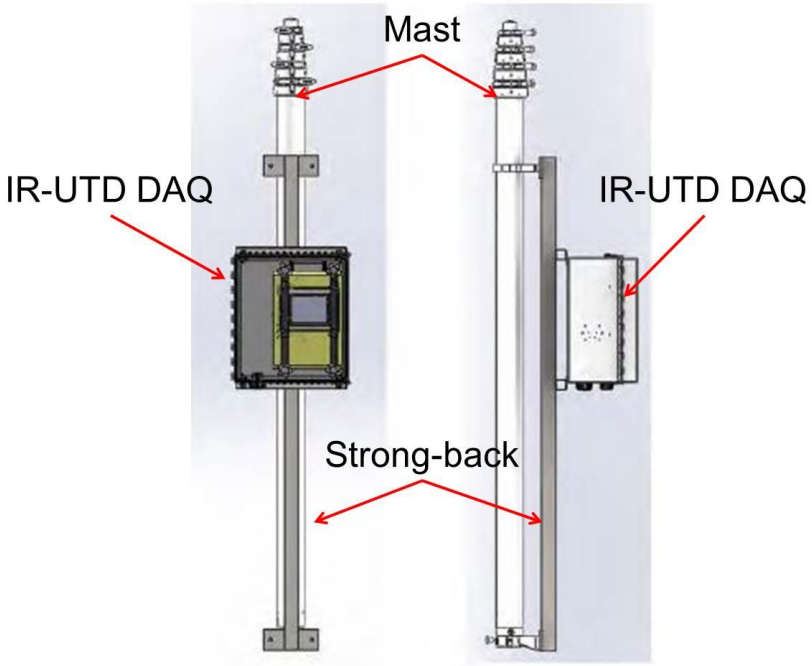

Figure 19. Diagram showing the test frame design for supporting a 30 ft. mast and the IR-UTD DAQ.

Figure 20 shows the IR-UTD mast and test frame mounted on the bridge. Figure 20A shows the mast extended to full height with the camera head mounted on the top of the mast. The concrete bolster that formed the light pole base on the bridge is also shown. Figure 20B shows the IR-UTD DAQ enclosure mounted on the test frame. The test frame attached to the

bridge through a base plate mounted on a light pole base is shown in Figure 20C. This light pole base was located outside the parapet and allowed the IR-UTD to operate without affecting traffic. The mast was raised with a foot pump in four sections using collar locks between each section.

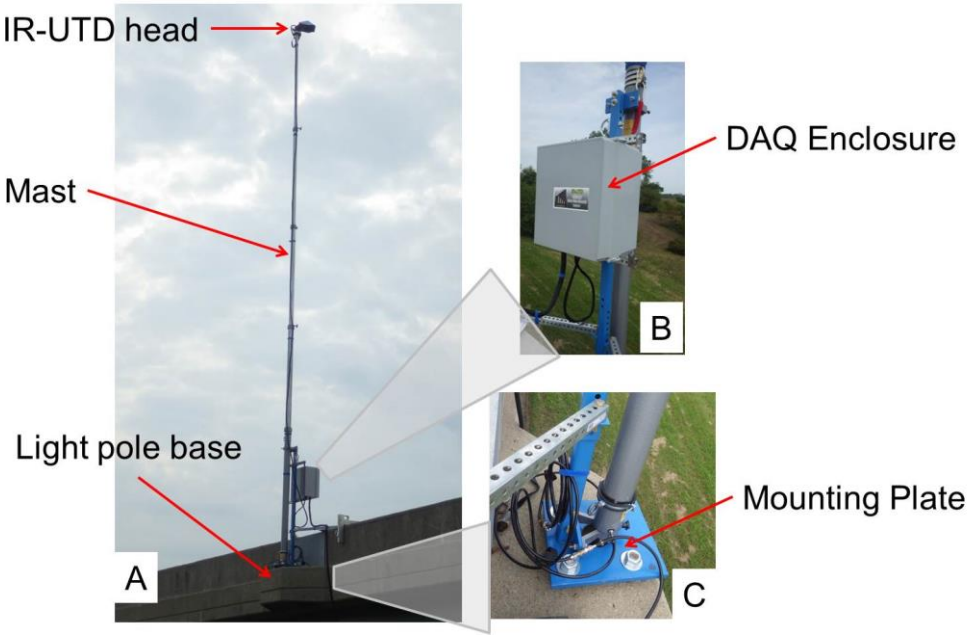

Figure 20. Photographs of the Iowa test set-up showing the mast mounted on a light pole base and the DAQ enclosure.

Figure 21 shows a photograph captured from the driving surface of the deck and illustrates that the IR-UTD support mast and enclosure were located behind the parapet, such that the roadway was clear during operation of the system. Power for the system was provided by a battery pack and generator that was placed on the ground below the bridge and connected via wire to the system. This power supply system provided DC power to the IR-UTD from the batteries, which could power the system for approximately 36 hours. The generator was used to recharge these batteries periodically during the course of the test.

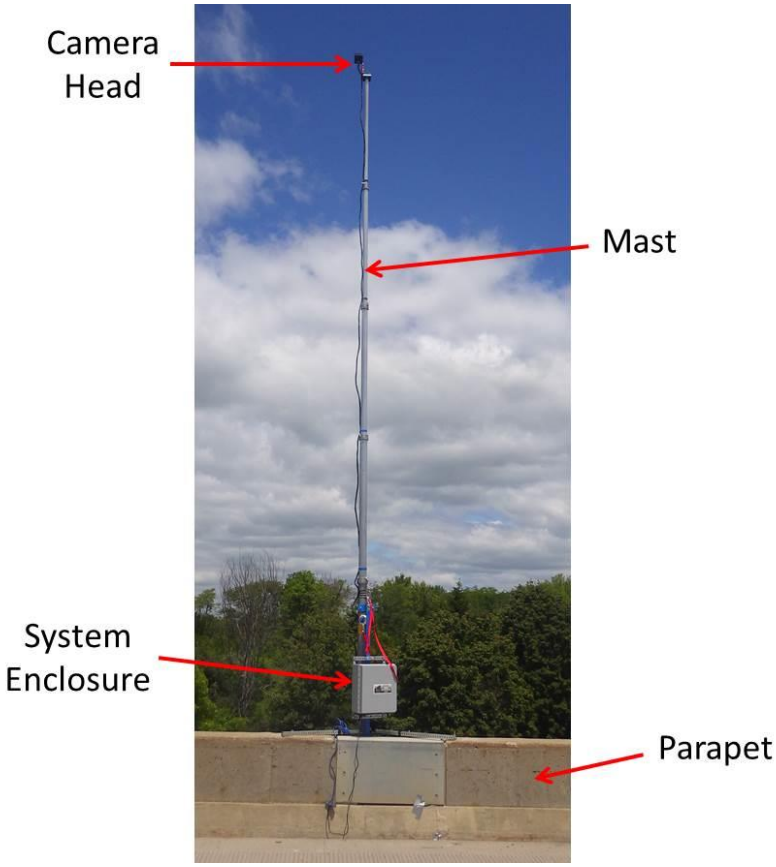

Figure 21. Photograph of the IR-UTD system mounted on the Iowa bridges.

2.3.2 Test Logistics

The testing of the IR-UTD system extended over a four day period from September 8 thru September 11, 2014. Setup of the steel test frame, mast, and IR-UTD system was completed with the assistance of IADOT personnel. The mast was extended and retracted several times to adjust the angle of the camera head. The angle of the camera head was adjusted to provide a suitable field of view for the camera showing the end span of the bridge from the first support to the joint at the end of the bridge.

Adhesive metal tape was placed on the surface of the deck to provide spatial markers that would be recorded in both visual images and the processed IR-UTD images. The metal tape was placed to form a 12 x 12 in. square, spaced 20 ft. apart on the bridge deck. A wireless thermocouple was also installed on the surface of the deck to monitor the deck temperatures during the testing.

Data collection was initiated on September 9, 2016 at approximately 10:30 a.m. Weather conditions for the first day included a maximum ambient temperature change of 24° F and an average wind speed of 9 mph [20]. During this day of testing, epoxy injection activities were focused on portions of the bridge that were not imaged by the IR-UTD.

Hammer sounding was conducted in the test area by Iowa DOT inspectors on the morning of September 9th. The area was prepared for epoxy injection by drilling holes in the deck where delaminations were located. At some locations, a borescope was used to inspect the holes in the deck in an effort to observe the delaminations and measure the depth of the delamination. Delaminations in the test area were filled with epoxy throughout the day. Weather for the day included an ambient temperature change of 6 degrees and an average wind speed of 9 mph [20]. The testing was suspended and the camera head was taken down in the 3 o'clock hour due to incoming storms, which were expected to include high winds. The test frame, mast, and DAQ enclosure were left in place, but the camera head was removed and the mast retracted as a precautionary measure.

The camera head was reinstalled and the test resumed on the morning of September 10th. Data was collected throughout the day and the following night. Data collection was stopped and the system removed from the bridge at 11:30 a.m., September 11, 2014.

Traffic control during the testing consisted of a single lane closure during the daytime hours to support the epoxy-injection activity. One lane of the bridge remained open to traffic with temporary traffic control lights installed at the ends of the bridge to provide single-direction traffic. During the overnight hours, there was no traffic control on the bridge.

2.3.2.1 Epoxy Injection Overview

The timing of the test allowed for the area of the bridge deck being imaged by the IR-UTD to be analyzed prior to the installation of epoxy into the delaminations in the deck and following the installation of epoxy. The process of epoxy injection is illustrated in Figure 22. Figure 22A shows hole-drilling into the deck in an area of delamination. The hole is drilled into the deck to the level of the delamination. An injection nozzle is then installed in the hole to allow epoxy to the injected into the delamination. Figure 22B shows the measurement of the depth of the delamination using a borescope. This allowed for the depth of the delamination to be determined by observing the delamination in the image of the borescope. Measuring the depth of the delamination was completed for research purposes to assess the capabilities of the IR-UTD. Figure 22C shows the injection device attached to an injection nozzle as epoxy is pumped into the delamination. After the injection of epoxy is completed, the nozzle is removed

from the hole. Frequently some epoxy material remains on the surface of the deck due to spillage, as shown in Figure 22D.

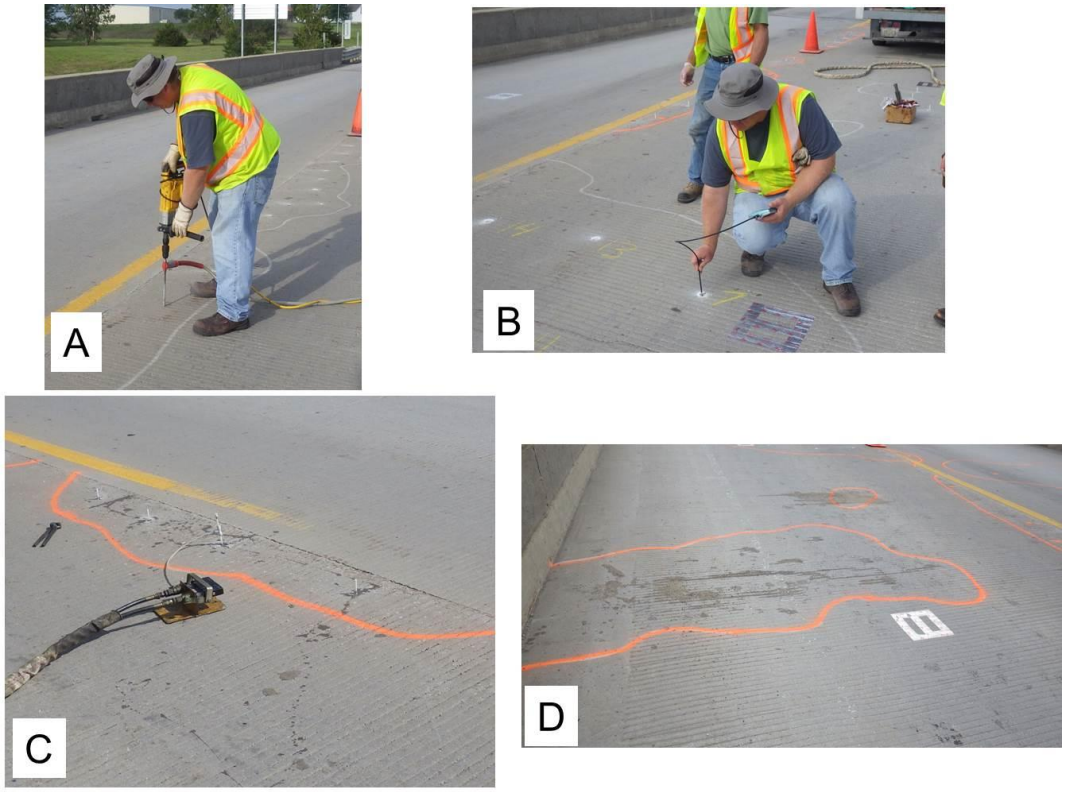

Figure 22. Photographs showing the process of epoxy injection on the Iowa Bridge deck showing (A) hole drilling, (B) measuring the delamination depth using a borescope, (C) injection of epoxy materials into a subsurface delamination, and (D) the deck surface after injection is complete.

The epoxy injection activity was ongoing during the IR-UTD testing as noted above. During the initial portions of the testing the epoxy injection activity was focused in other portions of the bridge, such that IR-UTD data could be collected on the test portion of the structure. The epoxy injection of the test area of the deck was completed on September 9, 2014. Data collected on September 10 and 11, 2014 consisted of imaging the deck after the delaminations were injected with epoxy.

2.3.2.2 Deck Temperatures During Testing

Figure 23 shows the deck temperatures from September 8, when the IR-UTD system was installed, through September 9 when the system was temporarily removed from the structure due to weather conditions. In this figure, a shaded area shows the period of time when epoxy injection was occurring in the test area of the deck. Time intervals for the heating

and cooling cycles are also shown in the figure. These data were processed to generate the IR-UTD images.

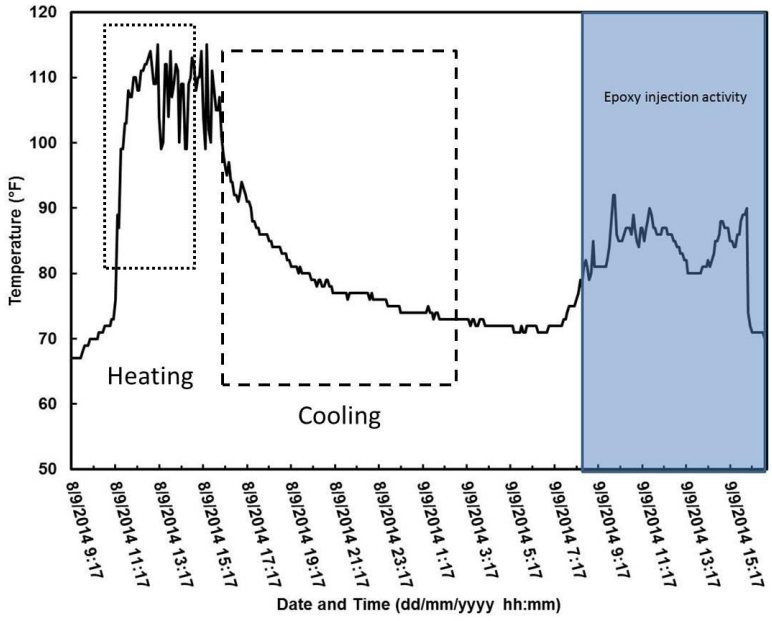

Figure 23. Deck temperature during the time interval of September 8 -9, 2014.

Figure 24 shows the deck temperature from the time the system was reinstalled on September 10 through the completion of the test on September 11, 2014. Heating and cooling cycle processed for IR-UTD imaging are also shown in the figure.

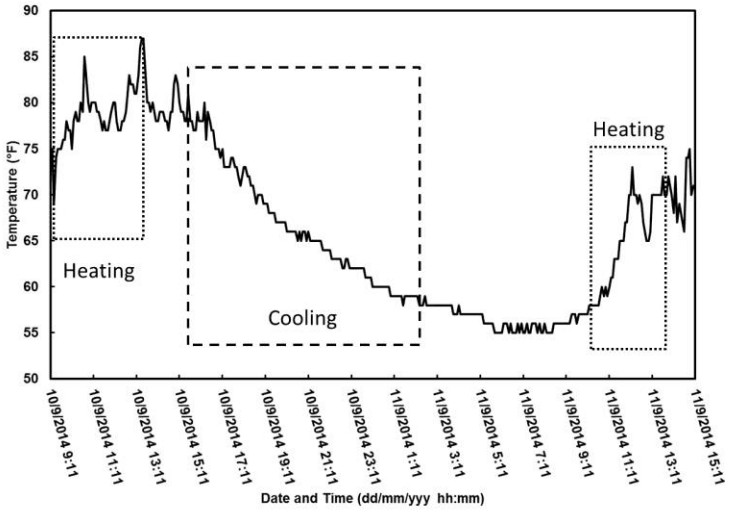

Figure 24. Deck temperature during the time interval of September 10-11, 2014.

2.3.3 Results

Figure 25 shows a visual photograph of the bridge deck captured by the IR-UTD. This image was captured near the completion of testing, after the delaminations in the bridge deck had each been outlined with orange paint to improve their visibility. Shown in the photograph are the IR markers placed on the deck to provide a spatial reference in the IR-UTD images. The photograph also shows dark areas on the deck that resulted from spillage of epoxy materials on the surface of the deck and traffic control cones placed on the deck during the daytime hours.

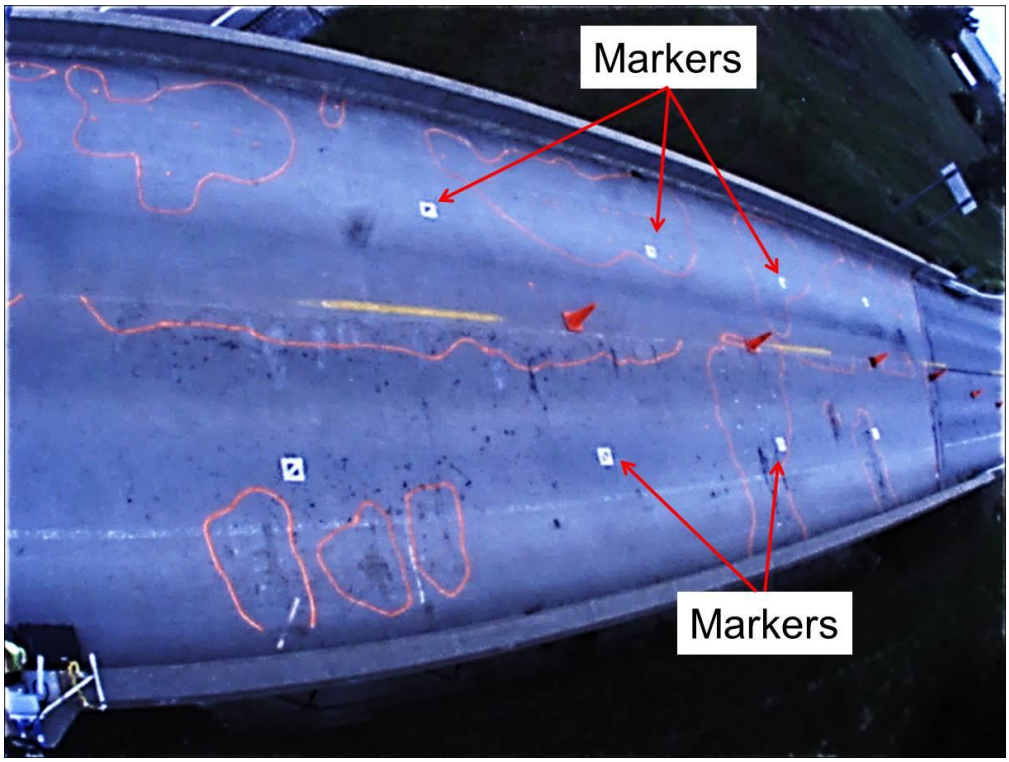

Figure 25. Image of the bridge deck captured by the IR-UTD visual camera.

IR-UTD data processed from the first 24 hr period of the test are shown in Figure 26. These data were processed based on the difference between the heating and cooling cycle during the time from the installation of the system on September 8 to the morning of September 9, 2014. The image captures approximately 3000 sq ft of bridge deck; a portion of the deck was obscured by a housing placed over the head of the IR-UTD to shield the camera head from rain. Although this shield was not directly in the line-of-sight of the camera, it was found that IR energy emitted by the shield, which was close to the camera lens, was contaminating a portion

of the IR data. Delaminations in the bridge deck are clearly observable in the image, with yellow to red colors indicating relatively deep delaminations and blue areas indicating areas of more shallow delamination. The IR markers placed on the deck at 20 ft intervals can also be seen, as well as traffic cones placed on the surface as part of the epoxy injection procedure.

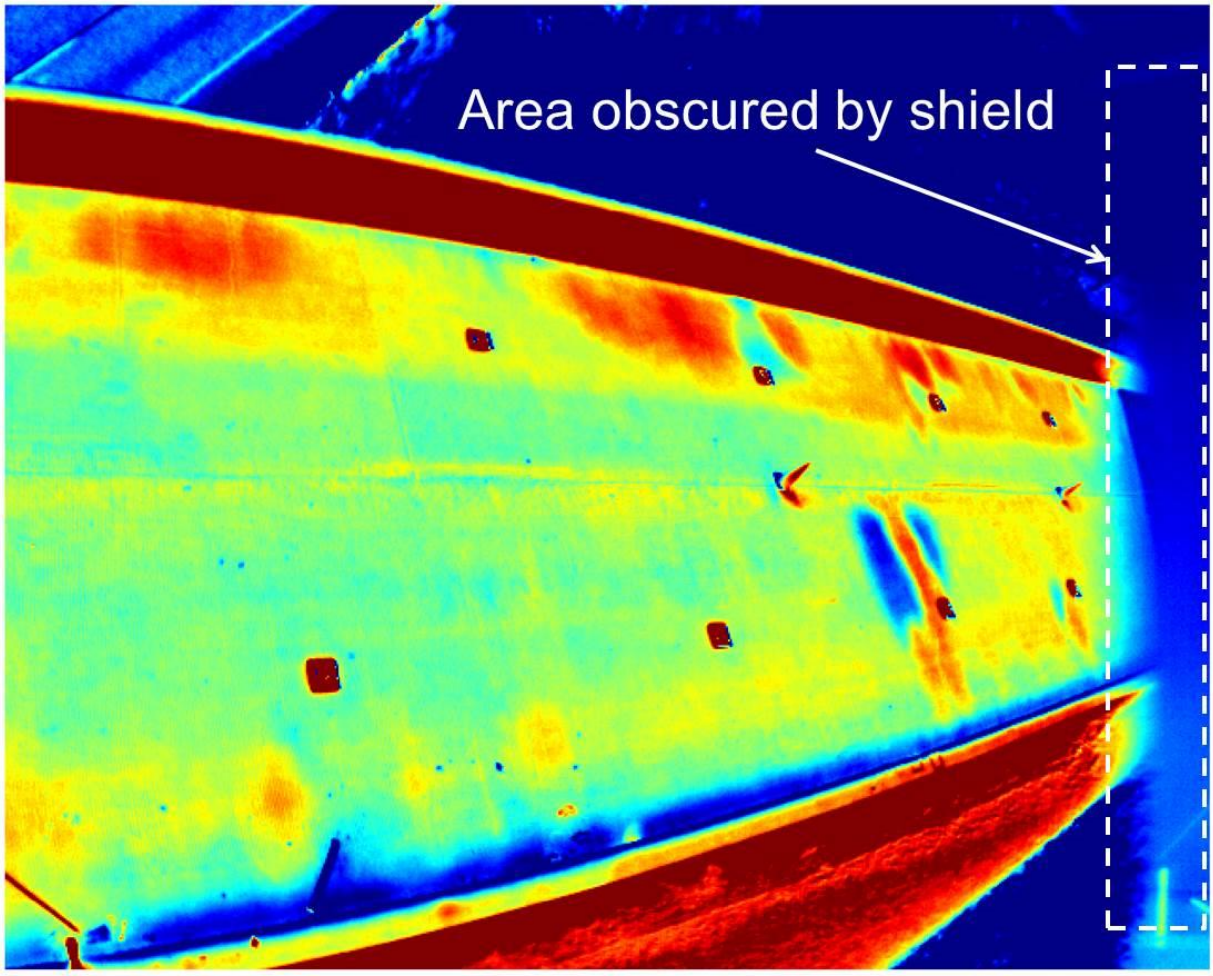

Figure 26. IR-UTD from the Iowa Bridge showing areas of delamination in the deck.

To verify the results shown in the IR-UTD image, an overlay of the IR-UTD data and the hammer sounding results was produced. This overlay consisted of placing the data shown in Figure 25, which shows the outline of delaminated areas determined using sounding, over the IR-UTD image shown in Figure 26. The overlay was trimmed slightly to remove the area of the deck obscured by the weather shield. Figure 27 shows the results of this overlay procedure. The overlay of these data provides a verification that the IR-UTD results match well with the sounding results. Both the location and spatial extent (i.e., size) of the delaminations correlate

with the location and extent identified through hammer-sounding. These data also demonstrate that the IR-UTD data contains information not included in the hammer sounding, namely the relative depth of the delamination.

Figure 27. Overlay of IR-UTD image and hammer sounding results, showing IR-UTD results (left), hammer sounding results (center), and an overlay showing IR-UTD data over hammer sounding results.

2.3.3.1 Spatial Resolution of the IR-UTD Image

Data from the Iowa Bridge deck was evaluated to demonstrate the spatial resolution of the image. Other bridge deck NDE technologies, such as Impact Echo (IE) or Ground Penetrating Radar (GPR), typically collect data on a test grid or on parallel lines along the length of deck. For example, IE data is typically collected on a 2 x 2 ft test grid, meaning a single test result is obtained every 4 sq ft. GPR data is typically collected along parallel lines every 2 ft across the bridge deck. For both technologies, data in between the test points or lines is inferred by interpolation of data from adjacent test points. These data are often plotted using contour lines or colored areas that make the data appear to be continuous across the deck, although the majority of area shown in the resulting image is not test data, but rather interpolations that assume data in-between test points. In contrast, the IR-UTD system collects data using a 640 x 512 pixel sensor array; this means that the image consists of 327,680 individual measurements covering the entire area being imaged. Consequently, the resolution of the image is much finer than any other deck evaluation technologies.

To illustrate this effect, Figure 28 shows a delamination that has deep portions shown in red to yellow on the image and shallow areas shown in blue. Figure 28A shows the overall view of the deck, Figure 28B shows a closer view, and Figure 28C shows an even closer view of these data. A marker that was placed on the deck is also shown in this image; this marker represents one sq ft. These data illustrate that IR-UTD data has very high spatial resolution for imaging delaminations in the bridge deck.

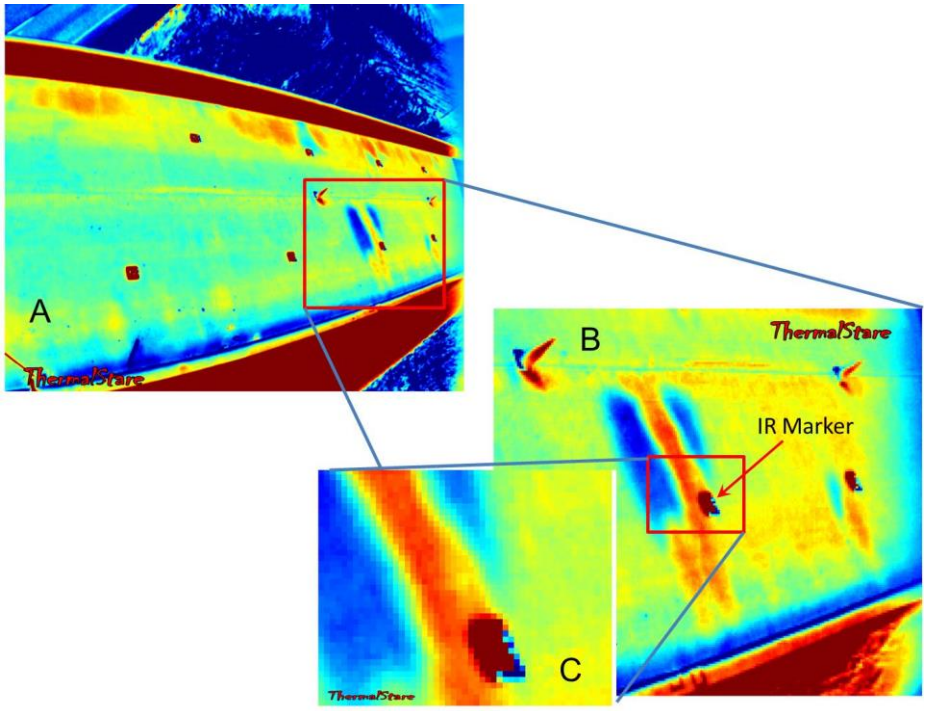

Figure 28. IR-UTD image demonstrating resolution of the image.

2.3.3.2 Depth Measurement

To better understand the depth measurements shown in the IR-UTD data, a borescope was used to measure the depth of several delaminations. Figure 29 shows the results of the depth measurements superimposed on a delaminated area of the bridge deck shown in the IR-UTD image. As shown in the figure, the different depths of the delamination are represented in IR-UTD by different colors, with red to yellow showing deeper portions of the delamination and blue areas representing shallow areas of the delamination. These data illustrate the contrast in thermal inertia between sound areas of the deck, where there are no delaminations, and damaged areas of the deck. Also, since delaminations at different depths will change temperature at different rates, as previously shown in the research, the different depths of the delamination areas are also differentiated in the IR-UTD data. The correlation between the exact depth of a delamination and the IR-UTD results is still a subject of research, due to the complexity of the interaction between the IR-UTD imaging technology and the environmental conditions surrounding a given test. However, these data provided empirical evidence that damage at different depths can be differentiated qualitatively by the IR-UTD technology.

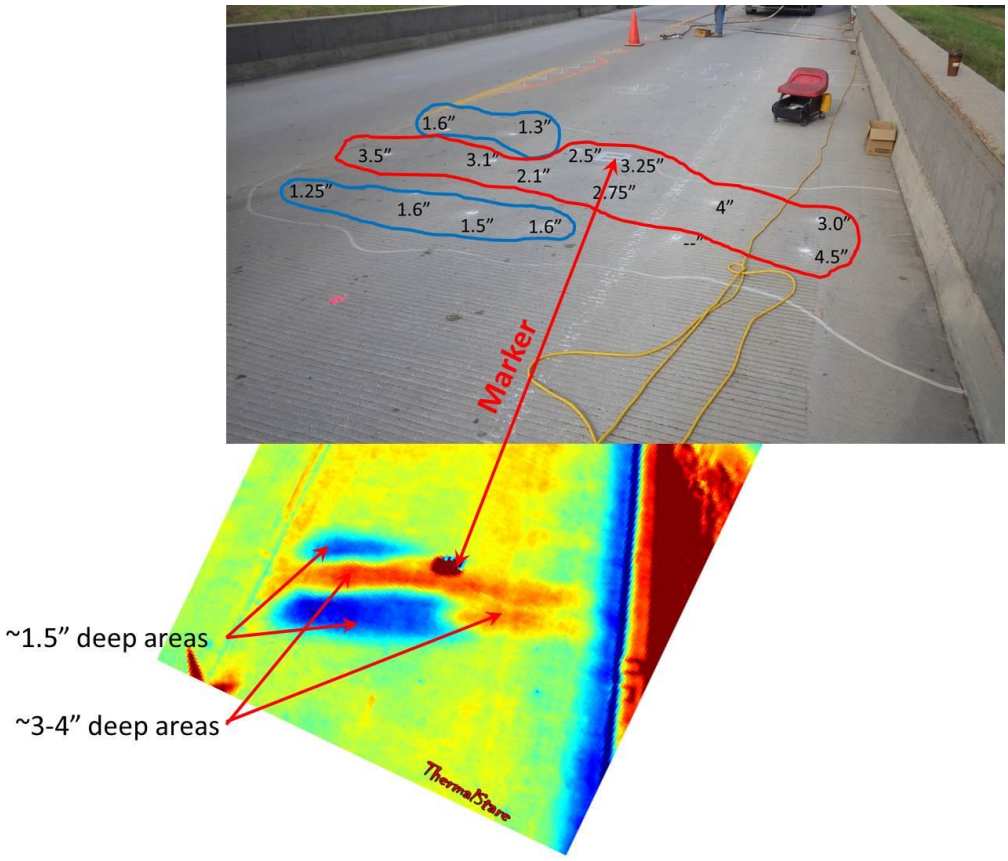

Figure 29. Visual image showing depth measurements and the IR-UTD image of a delamination with varying depths.

2.3.3.3 Comparison with Hand-held Thermography

Figure 30 compares the IR-UTD result for this delamination with data collected using a FLIR 620 hand-held thermal camera. The thermal image was captured near the optimum time for capturing subsurface delaminations, approximately 1 p.m. in the afternoon. The figure illustrates the challenge of hand-held thermal cameras when imaging a deep subsurface defect. The hand-held cameras collect only a single image at a particular point in time, which may or may not be the optimum time for inspection. In this case, the shallow areas of the delamination are captured in the IR data and appear as two separate defects because the deeper area of the delamination is not shown. In contrast, the IR-UTD data shows the entire area as a single defect, but with varying depth.

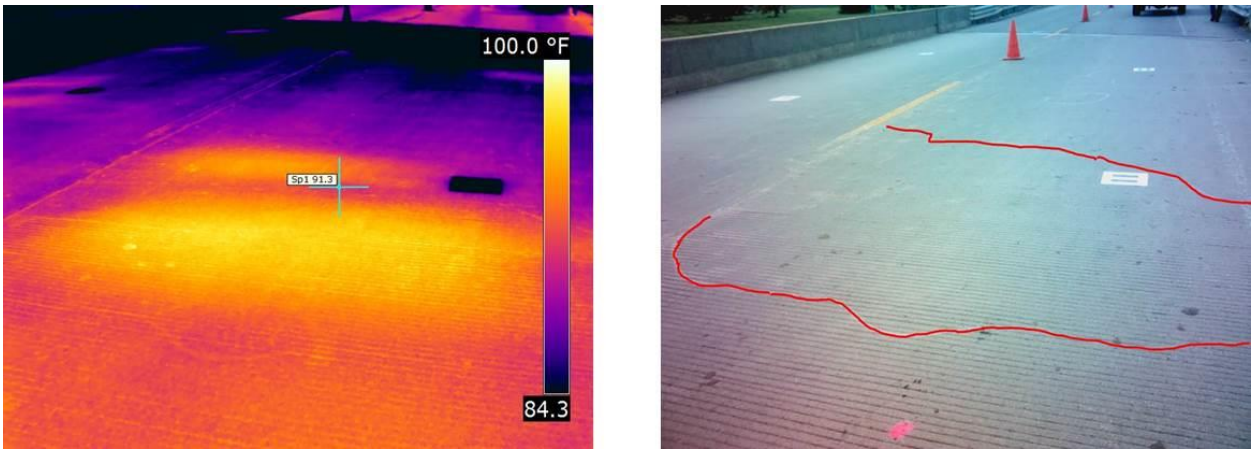

Figure 30. Thermal data from a hand-held FLIR 620 IR camera (left) and visual image of the area showing an outline of the delaminated area (right).

2.3.3.4 Post-injection data from the IR-UTD

Data from the IR-UTD was analyzed for the time period following epoxy injection in one lane of the test area of the deck. These data were analyzed to determine the effect of the epoxy injection on the IR-UTD results. Figure 31 (left) shows the IR-UTD image prior to epoxy injection in the deck; Figure 31 (right) shows data collected following the epoxy injection in one of the two travel lanes shown in the image. These figures indicate that epoxy injection diminishes the response of the delaminations in the bridge deck that had been treated with epoxy injection. Areas of delamination are shown in blue; however, the response of these areas is significantly reduced relative to the time period prior to the epoxy injection and relative to delaminations in the other travel lane, which had not yet been treated with epoxy injection. These data indicate that the IR-UTD system has potential as a tool for monitoring the epoxy-injection process, because delaminations that are missed or not properly injected would be revealed in IR-UTD images captured following the injection procedure.

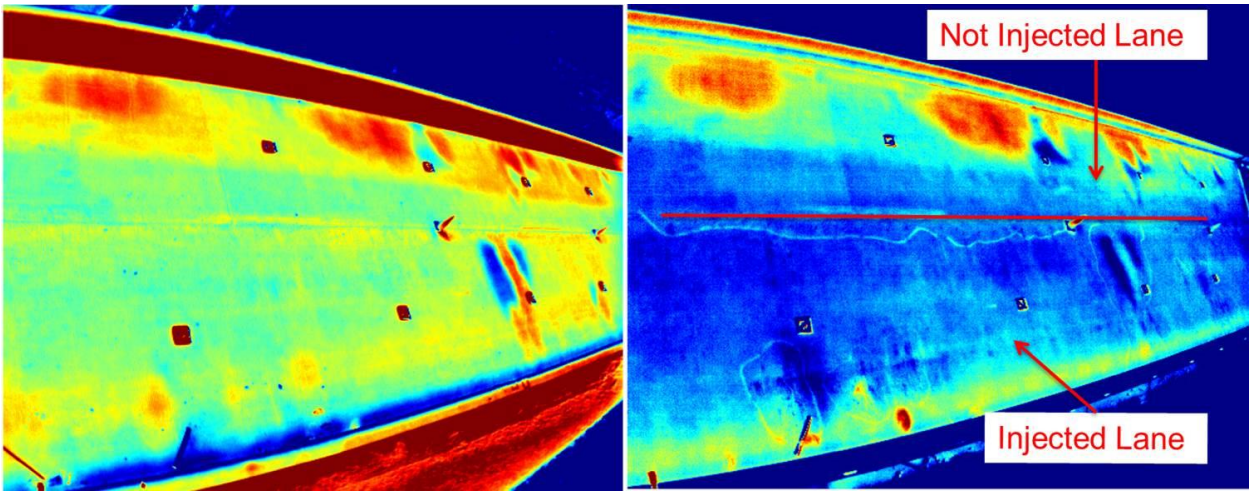

Figure 31. IR-UTD images showing delaminations prior to epoxy injection (left) and after epoxy injection (right).

2.3.4 Discussion

Testing of the Iowa Bridge demonstrated the deployment of the IR-UTD technology on a pneumatic mast to position its camera head at a height of 30 ft above the bridge deck. From this position, an area of approximately 3200 sq ft of bridge deck could be imaged. The testing provided the ability to evaluate several unique capabilities of the system. The IR-UTD was able to image subsurface delamination throughout the 3200 sq ft area, and these results correlated well with hammer sounding results both in terms of location and extent of delaminations. The ability of the IR-UTD data to differentiate the depth of a delamination was verified through physical measurements of delamination depth made using a borescope. This capability of the system is qualitative at this time; further research is needed to provide more quantitative data regarding the depth of a delamination.

The potential for the technology to serve as a quality control tool to monitor epoxy injection activities was also demonstrated. Areas of the deck where epoxy injection activities were completed showed a different response than prior to injection. These areas were also shown to have different response than nearby delaminations that had not yet been injected with epoxy.

The testing also indicated that the capabilities of the technology could be enhanced by implementing an automated pan and tilt function that would allow for the camera head to be repositioned during data collection.

2.4 Grindstone Bridge Testing

The Grindstone Bridge is located in Columbia, MO, over Highway 63. The roadway carries Grindstone Parkway. The bridge is a four-span voided slab. The deck carries five lanes of traffic. The surface of the deck has an asphalt chip seal overlay that has variations in thickness. The surface of the deck has a number of patch repairs, as can be seen in Figure 32.

Figure 32. Aerial view of the Grindstone Bridge.

The purposes of the Grindstone Bridge test were as follows:

1. Test the operation of the IR-UTD system with the automatic pan and tilt technology
2. Evaluate the capability of the IR-UTD to image a bridge deck that is open to traffic throughout the testing
3. Evaluate the capabilities of the system for imaging a concrete deck with an asphalt overlay and patches

Figure 33 shows the deck temperatures during the testing. These data were collected using a wireless thermocouple device placed on the shoulder of the bridge with the sensor taped to the surface of the deck. IR-UTD data was collected over a two day period. The first day had minimal temperature variation and conditions were overcast. The second day of testing provided a larger ambient temperature variation throughout the day, although a severe storm occurred in the afternoon. Lightning and high winds occurred during this time period and resulted in the IR-UTD system shutting down unexpectedly. Data stored prior to the storm was analyzed to evaluate delaminations in the bridge deck.

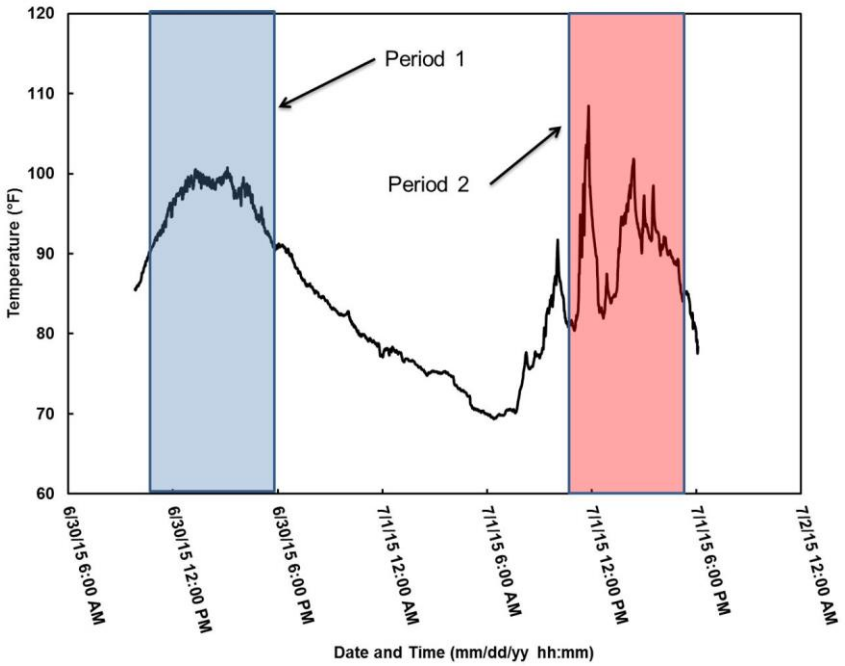

Figure 33. Deck temperature during the Grindstone Bridge test.

The test setup on the north-east side of the bridge is shown in Figure 34. From this position, a large portion of the deck could be captured in the images. The test setup was completed without any traffic control, as the portable mast was positioned behind the approach guardrail as shown in Figure 34. The bridge remained open to traffic throughout the testing.

Figure 34. – Photograph showing the position of the IR-UTD portable mast during data collection on the Grindstone Bridge.

Operational testing of the automated pan and tilt mount was completed during the testing of the Grindstone Bridge. The automated pan and tilt feature is intended for a test set-up on the bridge structure; for example, if the camera was installed mid-span on the bridge. From a camera position mid-span, the automated pan and tilt can be used reposition the camera to view areas on either side of its position. This type of application was demonstrated during the course of the Kansas City Bridge testing (Bridge A0295), described in section 2.5. For the Grindstone Bridge, the camera was positioned near the bridge abutment as shown in Figure 32. Consequently, the full advantage of the pan and tilt could not be evaluated.

To test the operation of the pan-and-tilt feature, two camera head positions were used to image slightly different portions of the bridge deck. During the testing, the camera captured an image at each of the two camera positions at each data collection interval, then returned to its original position. The testing was successful in demonstrating the operational use of the automated pan and tilt feature. However, because the two camera positions show essentially the same portions of the deck, albeit from slightly different angles, only images from one position are presented here.

Figure 35 shows two images of the bridge deck. Figure 35A is the visual image captured by the IR-UTD from its position on the mast. Figure 35B is a processed IR-UTD image based on the temperature variations during the heating and cooling cycle shown as shown as period 1 in Figure 33. Several features are identified in Figure 35A. First, the overlay on the bridge deck was distributed irregularly across the deck, which resulted in some areas having a thick overlay while other areas have little or no overlay; areas where the overlay appeared to be thickest are identified in the image. The thickness of the overlay was assessed qualitatively using sounding. Several patches are also shown in Figure 35A.

The locations of two delaminations are also shown in the image; these delaminations were confirmed with sounding. These variations in overlay thickness affected the IR-UTD images produced because these areas demonstrated a different thermal inertia than areas of the deck with thin or no overlay. This is due to the material properties and the color characteristics of the material (black), which absorbs radiant energy from the sun more efficiently than bare concrete.

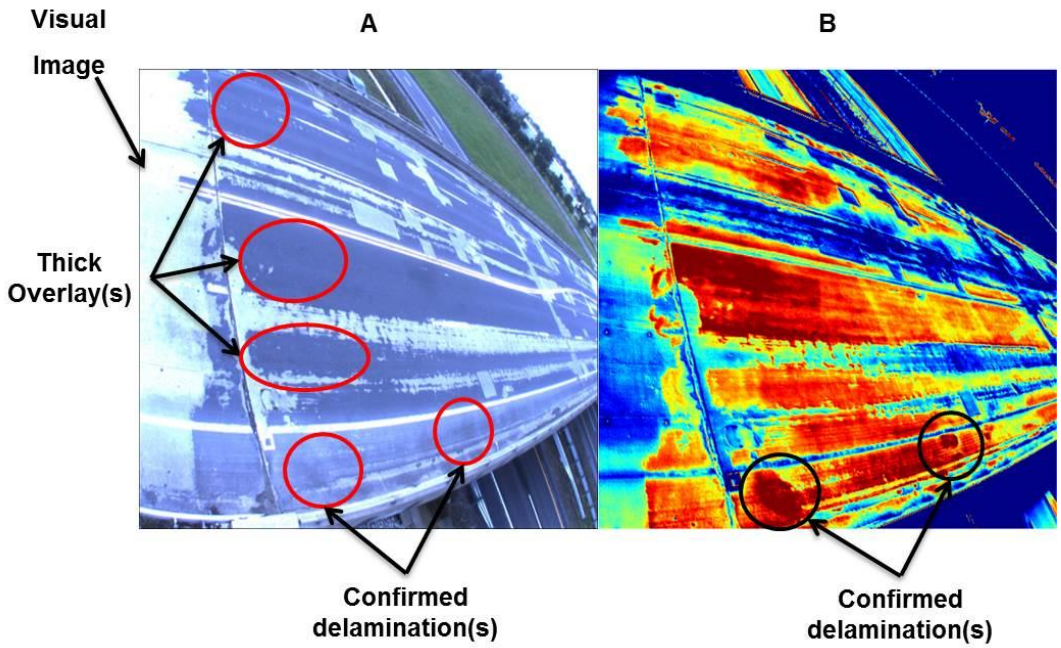

Figure 35. IR-UTD images of the Grindstone Bridge showing the visual image (A) and processed IR-UTD data (B).

Figure 35B shows the processed IR-UTD image. Delaminations in the shoulder area of the deck are identified in this image. However, generally these images are difficult to analyze to identify delaminations, because the variable nature of the overlay produced variations in the IR-UTD image produced from analyzing period 1.

To improve the quality of the data, the heating and cooling cycles were divided for processing of the data. Processing these data during separate time intervals produced results that were more easily interpreted. Generally, data was processed from two different intervals as shown in Figure 33. Period 1 consisted of the diurnal temperature variations from the first day of testing, which consisted of overcast skies and a relatively small change in ambient temperatures. Period 2 consisted of the second day of data collection, in which deck temperatures indicated several heating and cooling cycles due to the unsettled weather conditions associated with an oncoming storm. The temperature cycles of heating and cooling occurred over short intervals, which allowed analysis of the inertial effects for potential damage at different depths through the deck.

By processing these data through different time intervals, different IR-UTD images were produced that provided images that were more easily analyzed to identify damage in the deck. One of the outcomes of the processing can be seen in Figure 36, where the structural features and patches of the bridge are visible. This image was produced from period 1 to emphasize the

structural features of the bridge, rather than delaminations in the deck. It can be observed that the majority of the patches on the bridge deck are located above or near the bridge supports.

The location of these patches near the negative moment region above the support suggests that the negative moments may be creating tensile stresses in the concrete. These stresses may result in the concrete cracking which then provides a pathway for deicing chemicals to penetrate more rapidly to the level of the reinforcing. As a consequence, these areas have deteriorated more rapidly than other portions of the deck, causing delamination and spalling that have subsequently been repaired. These data illustrate the unique capability of imaging the structural features of the bridge using transient thermal data collected by the IR-UTD.

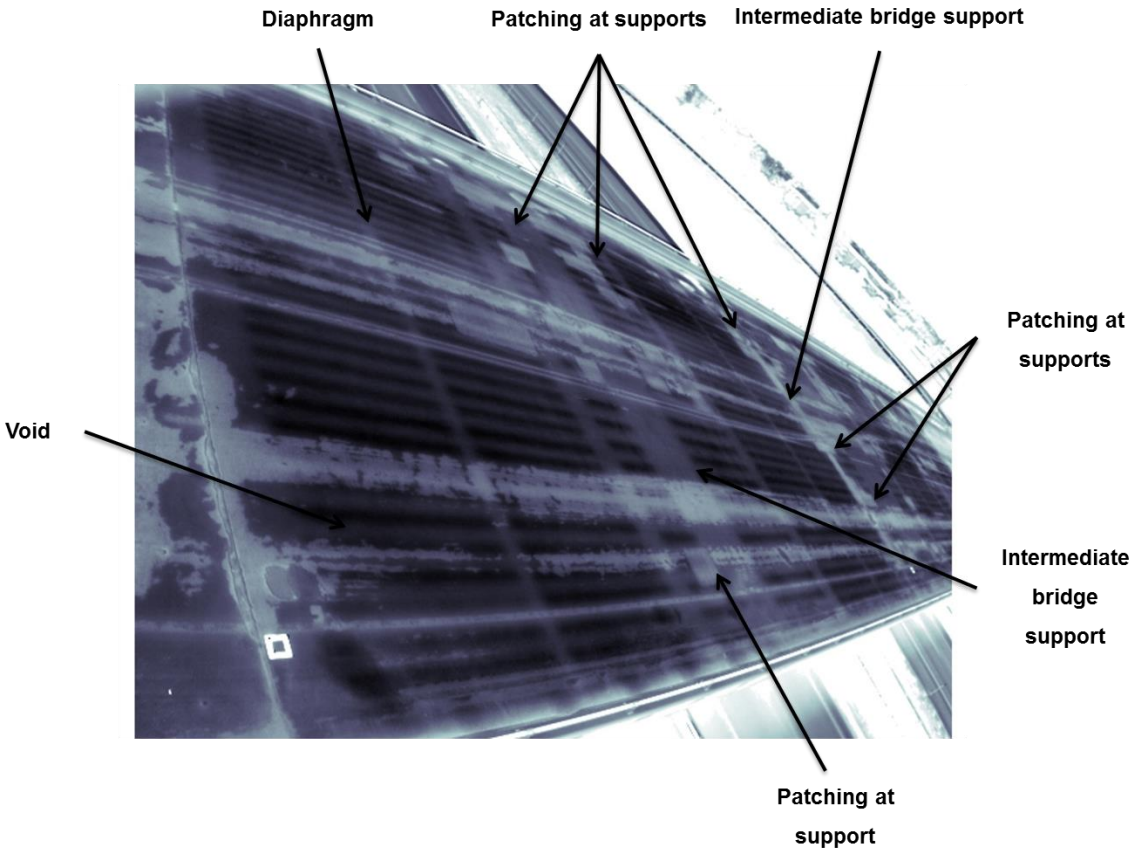

Figure 36. IR-UTD processed data showing structural features and patches above the support.

Figure 37 shows the location of damage in the bridge deck based on processing data from period 2, which consisted of several temperature cycles that occurred over a short time interval. Based on the processing of this time interval, two different types of defects were

identified as shown in the figure. Type 1 defects are potentially shallow defects located in areas of thin overlay or at shallow depths in the concrete. Type 2 defects are potentially deeper defects located where the overlay is thicker and/or the defect is deeper in the concrete. The depth of these two different types of damage was not verified in the field. The interpretation of these data was based on comparing processed data from both period 1 and period 2 as shown in Figure 33.

Traffic control was used to temporarily divert traffic from the center turning lanes on the bridge to verify results in this area. The Type 2 delaminations located along the centerline of the roadway and the Type 1 delaminations located on the shoulder were both verified using hammer sounding. Other Type 2 delaminations were not verified due to traffic.

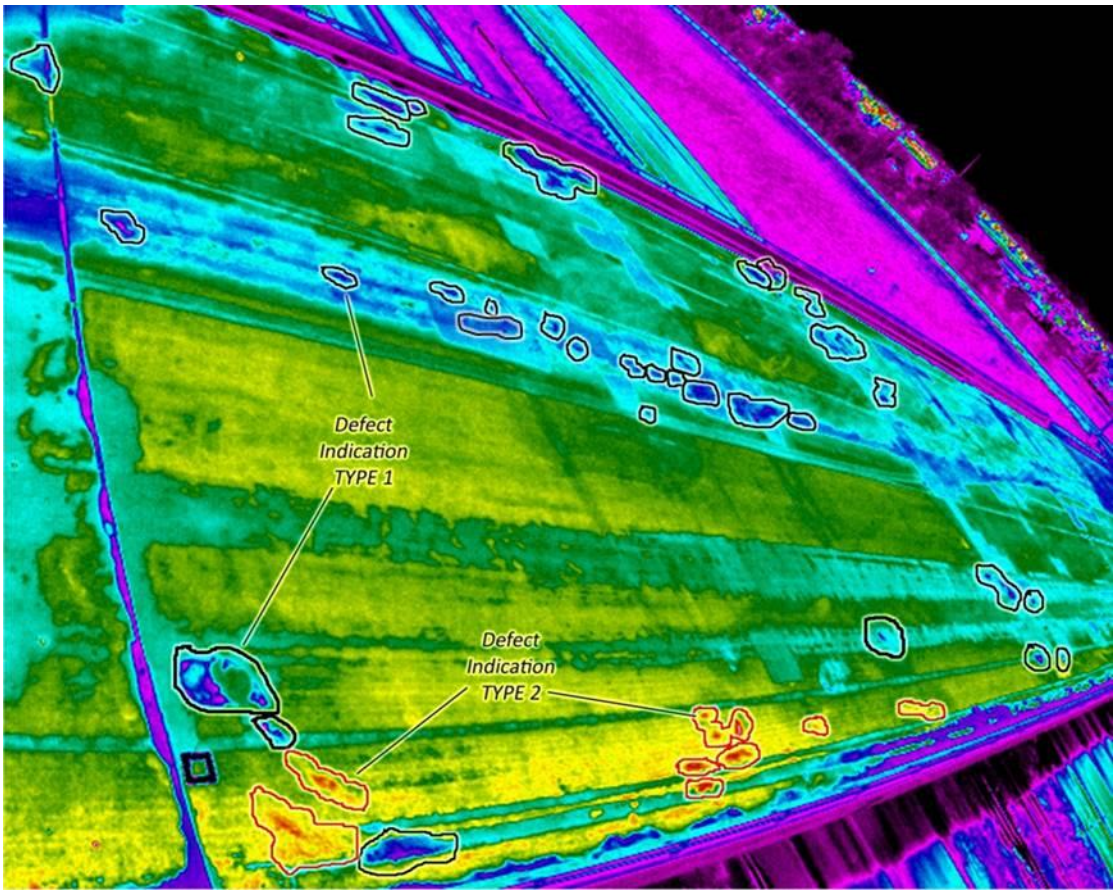

Figure 37. IR-UTD processed data from process period 2 showing defect indications with manual outlines.

Figure 38 shows an IR-UTD image processed to emphasize the type 2 defects overlaid onto a IR-UTD image processed to emphasize the structural features of the bridge. There are several expanded views of the data that show different defects observed in the deck. Superimposing the two sets of IR-UTD data in this way allows for visualization of structural

features of the bridge such as the location of patches and relative location of defects observed. For example, the defect marked A in the figure is a delamination located adjacent to a patched area of the deck. This delamination may be growing from the patched area. The expanded views marked B and C are delaminations located in the shoulder.

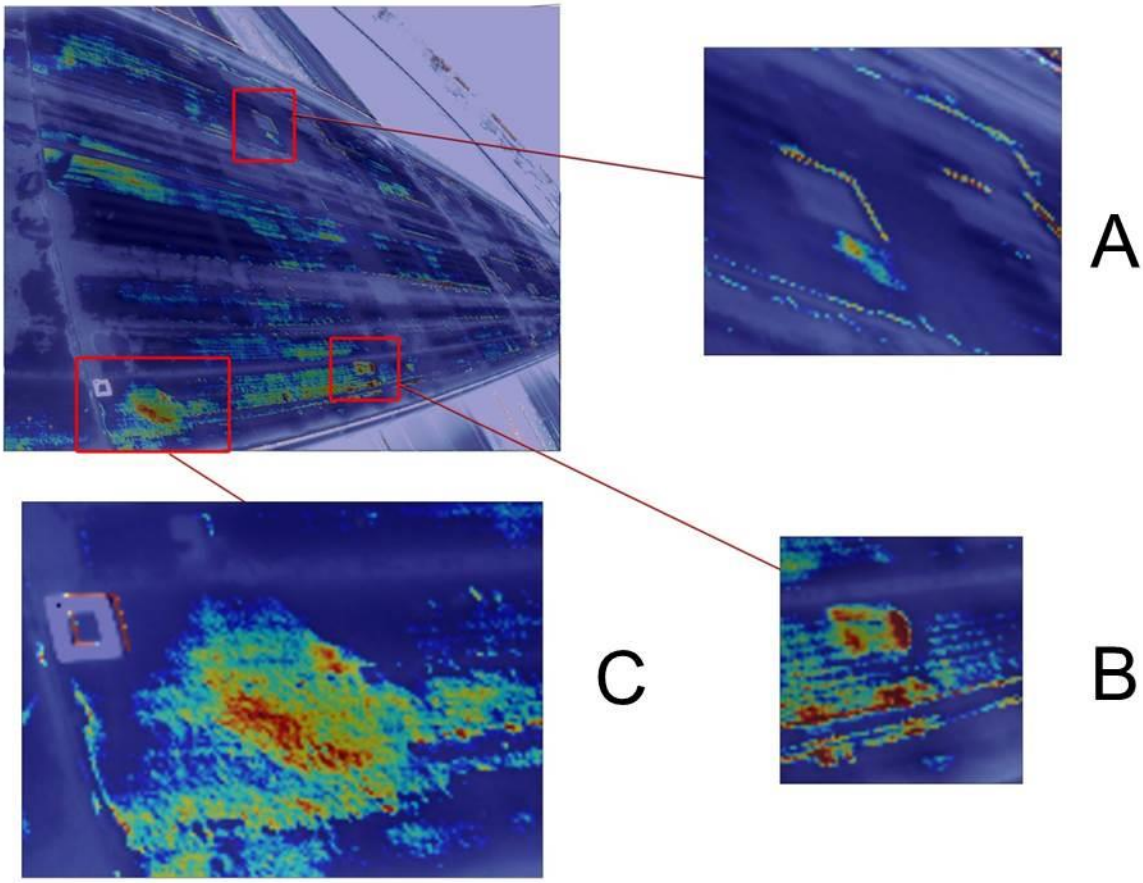

Figure 38. IR-UTD processed data from process period 1 showing entire image (top left) and three separate close-up images of defect indications (bottom left, top right, bottom right).

2.4.1 Discussion

The test at the Grindstone Bridge demonstrated the operation of the automated pan and tilt camera mount. Data was collected from two different camera head positions as an operational test; only one of the data sets was processed. The IR-UTD data was collected from a position adjacent to the roadway, such that no traffic control was required to implement the technology. Traffic on the bridge remained open throughout the test. Data from the test were processed from different time periods, and these data presented different types of defects. Based on the analysis, it is believed that these represent defects of different depths, although this has not been verified. Overall, the test demonstrated that the IR-UTD was capable of

imaging delaminations in a bridge deck that had a variable-thickness asphalt overlay and patches. Traffic remained open on the bridge throughout the testing without affecting the quality of the IR-UTD results. Delaminations were detected both in areas that had an overlay and areas where the overlay was not present.

2.5 Kansas City Bridge A0295

An out-of-service highway bridge located in Kansas City, MO (MoDOT bridge A0295) was utilized as a test specimen for evaluating the performance of both the IR-UTD system and the IR-DSS system. This bridge presents an unusual situation because it was built in 1958, but never used because approach roads to the bridge were never constructed. As a result, the bridge has never been exposed to vehicle loading and has never had deicing chemicals applied to the surface of the deck. The bridge is a three span, multi-cell cast-in-place box girder structure with a 7 in. thick deck forming the top flange of the box. The bridge is ~212 ft in length, and tapers from a width of 39 ft 3 in. at the north end of the bridge to a width of 21 ft 9 in. at the south end of the bridge. This bridge is located over Truman Road between Interstate 70 and Benton Boulevard in Kansas City, MO. An aerial view of this bridge is shown in Figure 39.

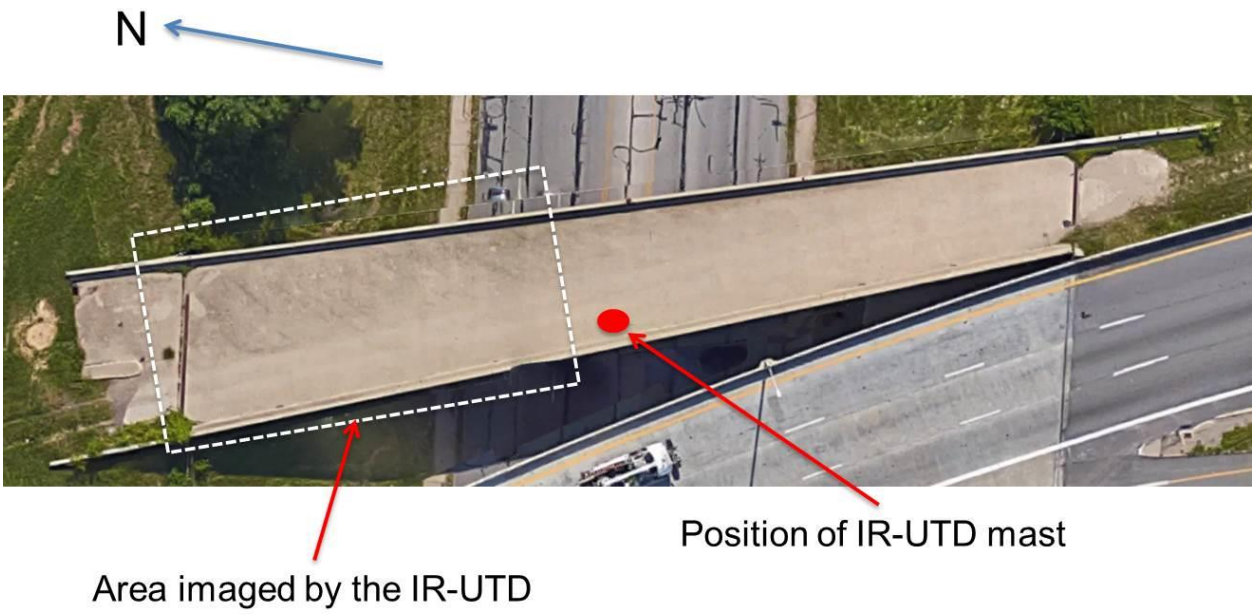

Figure 39. Aerial view of the bridge in Kansas City showing area imaged in Test 1 and Test 2 and the position of the IR-UTD mast.

Three separate tests were conducted on bridge A0295 as summarized in Table 1. Two tests were completed with the IR-UTD system with the camera in a fixed position imaging the north span of the bridge. A third test utilizing the automated pan and tilt features, added to the

system during the course of the research, was completed on September 3, 2015. Each of the tests had a different data collection interval, as shown in Table 2. Results of the three tests were compared to analyze the reproducibility of the IR-UTD technology.

Table 2. Date, data collection interval, and area imaged in three different tests of the KC Bridge.

Test No.	Date	Data collection interval	Area Imaged
1	June 5, 2014	12:30 pm to 6:30 pm	North end
2	August 20, 2014	7:30 am to 6:30 pm	North end
3	September 3, 2015	8:30 am to 8:00 pm	Entire deck

2.5.1.1 Test 1 June 5, 2014

Figure 40 shows the IR-UTD image from Test 1 compared with a chain drag completed independently by MODOT. There are several notable features in this image. First, the webs and diaphragms of the box girder are clearly visible in the IR-UTD data. Second, the delaminations in the bridge deck detected by the chain drag are also detected by the IR-UTD image. This image was produced based on only 6 hrs of data collected between 12:30 pm and 6:30 pm. Note that the color scale used in Figure 40 was intended to show both the structural features of the bridge and the delaminations in the deck.

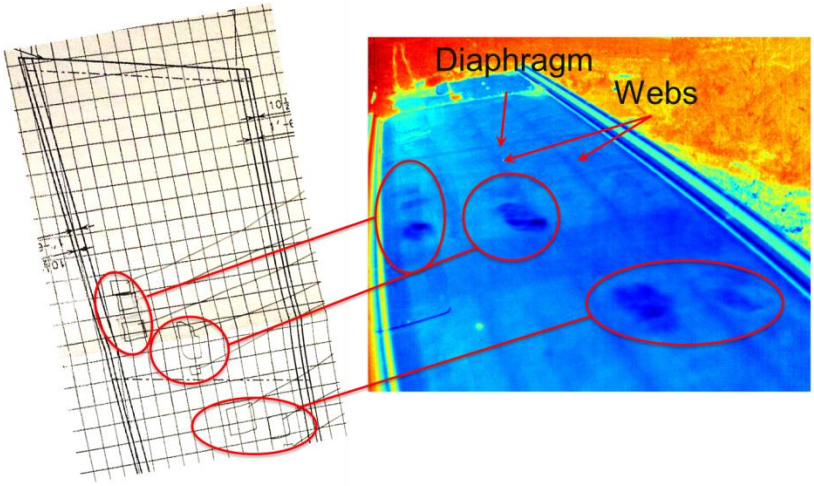

Figure 40. Image of chain drag results (left) and IR-UTD data from Test 1 (right).

2.5.1.2 Test 2 August 20, 2014

The delaminations shown in Figure 40 were subsequently imaged during Test 2. Data was collected over an 11 hr. period during Test 2. Figure 41 provides a comparison between the processed IR-UTD data and a typical, single-frame IR image. Figure 41A shows a single

frame of IR data collected by the IR-UTD system. This frame was selected because it was captured at a point in time when the thermal contrast of the delaminations on the deck was maximized. The delaminations can be observed in the image as well as the shadow of the mast. Since the IR-UTD system collects data periodically over time, individual images such as that shown in Figure 41A can be selected from the overall dataset; these data are essentially the same as IR data collected by a hand-held thermal camera. As shown in the figure, variations in the IR energy emitted from the surface of the deck create "noise" in the image, i.e., different areas of the deck appear as different colors. These variations in emitted energy may be caused by variations in exposure to solar loading, material properties, moisture content in the deck, or some combination of these factors.

Figure 41B shows the processed data from the IR-UTD system. The internal structure of the bridge (diaphragms and webs) can be seen in the image, as well as the delaminations in the bridge deck. In comparison with Figure 41A, the "noise" in the image of the deck is eliminated by the IR-UTD processing. This is because the processed IR-UTD data measures the thermal inertia, as represented by varying rates of change of IR energy emitted from the deck, which is much less sensitive to surface variations in solar loading, material properties, or moisture.

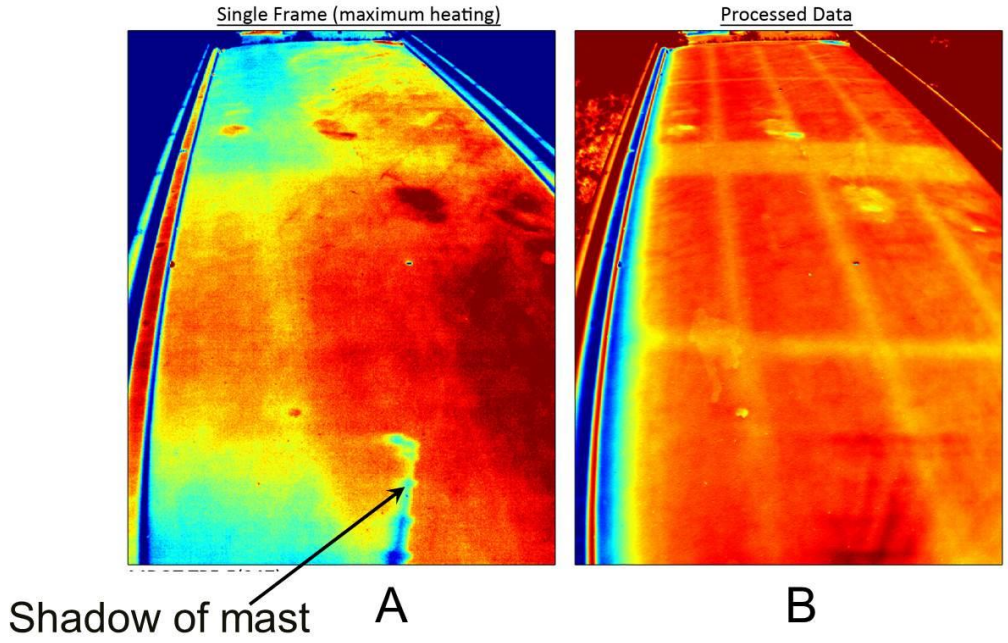

Figure 41. Data from test 2 showing single-frame IR image (A) and IR-UTD processed image (B).

2.5.1.3 Test 3 September 3, 2015

The third test of the bridge A0295 occurred in September, 2015. This test was intended to test the automated pan and tilt function that had been added to the system during the course of the research. The pan and tilt function allows the camera head to be repositioned during the data collection process such that a larger area of the bridge can be imaged from a single location. The IR-UTD system was programmed to collect data at three different camera positions to capture an image of the north span, center, and south span of the bridge. The data from each position are captured at each time interval. For example, if thermal images are captured every 10 minutes, the camera captures an image of south span, middle, and north span at each time interval, returning to first position during the time intervals between image capture times. Subsequent data processing is completed for each of the three camera positions separately.

Figure 42 shows data from the IR-UTD system captured from Bridge A0295. As shown in the figure, the entire bridge deck was imaged from a single location near the center of the bridge. The IR-UTD data shown in the figure (top) are optimized to show the structural features of the bridge, including the internal webs and diaphragms of the bridge. The visual images captured by the IR-UTD camera head are also shown in the figure (bottom). The mast trailer is shown in these images because the mast was positioned on the deck of the bridge.

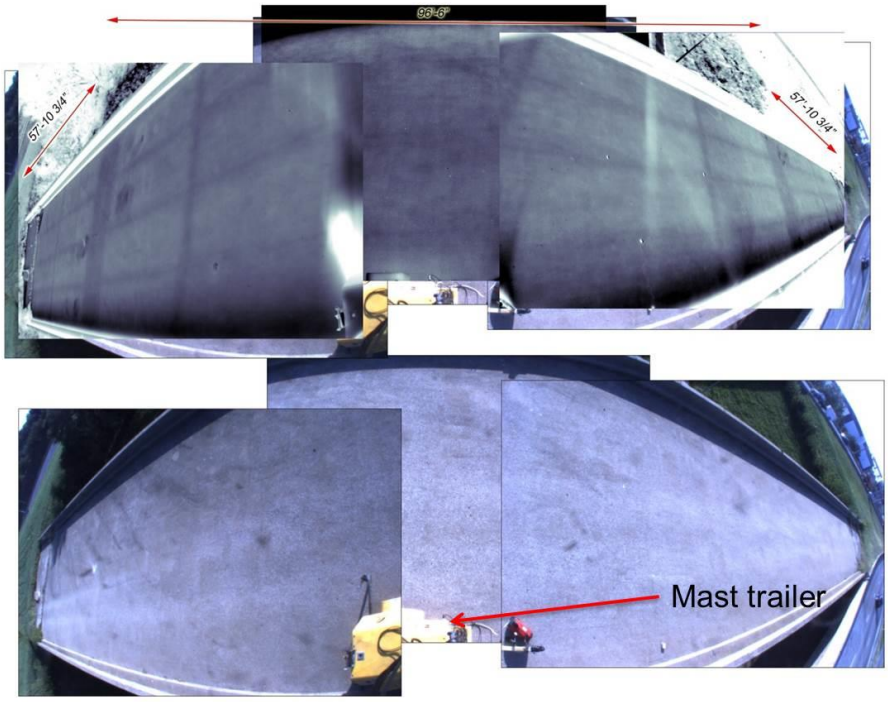

Figure 42. IR-UTD image showing structure features of the bridge (top) and visual images captured by the IR-UTD camera.

The delaminations imaged in the previous tests of bridge A0295 were also detected in Test 3. Figure 43 shows the IR-UTD data for each of the camera positions with the detected delaminations highlighted for clarity. As shown in this figure, each of the delaminations in the north span of the bridge that had been detected during previous testing was also detected in test 3. A single delamination was identified in the south span of the bridge. It should be noted that several delaminations identified in the chain drag data in the south span of the bridge were not detected in the IR-UTD data. There are several possible scenarios that could explain why these delamination were not imaged in the IR-UTD results. It may be that these delaminations were incorrectly identified in the original chain drag result. Another possibility is that angle of the camera from its position on the mast is too small to allow for quality data to be captured. Efforts to further verify the chain drag results and explore the cause of the false negative (i.e. delaminations not detected) results in this area are ongoing. Regardless, these data demonstrated that the IR-UTD could image the entire length (212 ft) of the bridge from a single position near mid-span, although the low angle with some portions of the deck may have had an effect on the quality of the data.

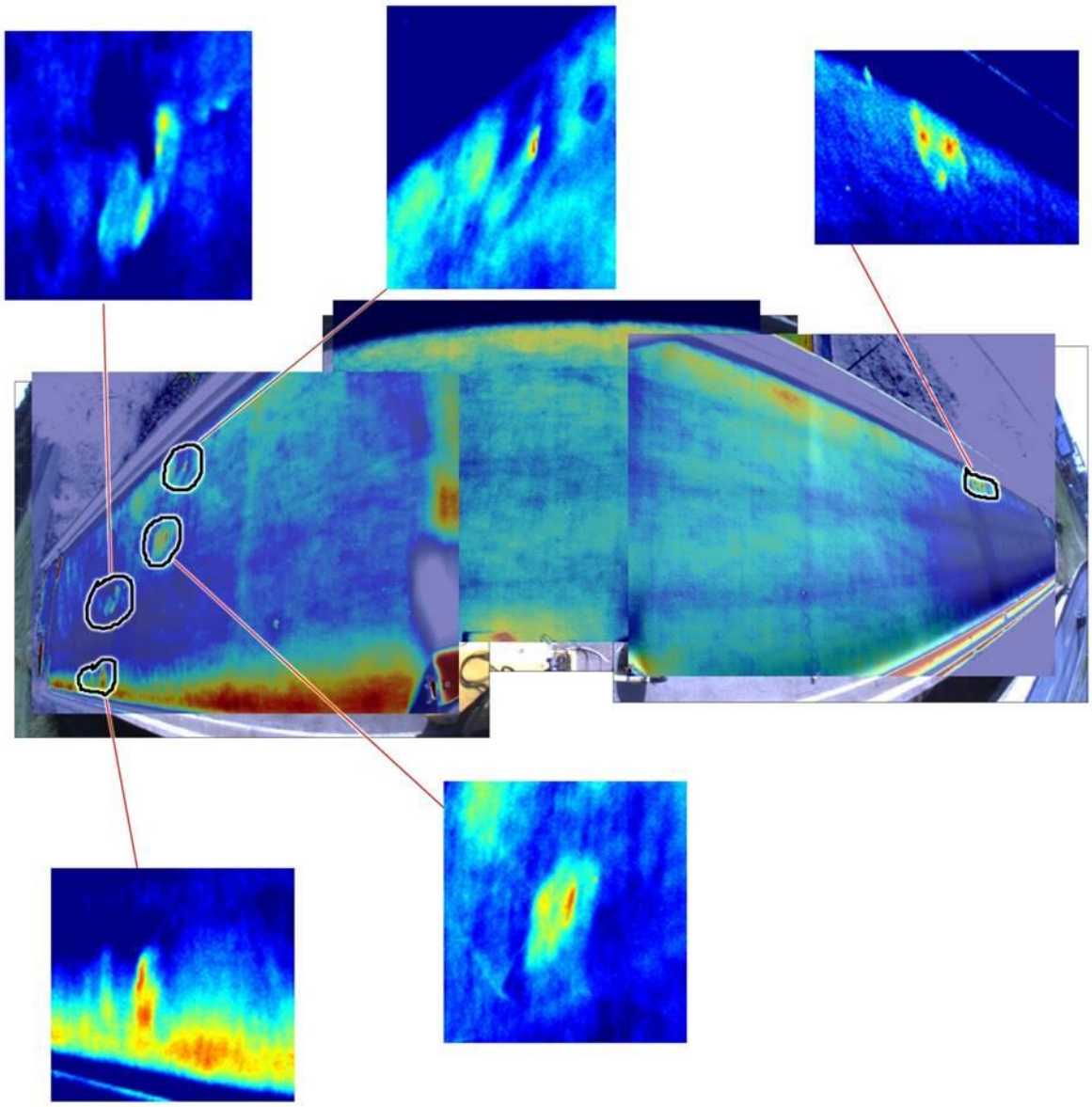

Figure 43. Measurement of three spans showing defect indications.

2.5.1.4 Reproducibility of the IR-UTD Data

The IR-UTD technology is new and has not been previously utilized for imaging of bridge components. As a result, the consistency of its performance (i.e., reproducibility) has not been previously analyzed. Traditional IR images captured at a single point in time are very difficult to reproduce due to the dependence of the results on the ambient weather conditions. Ambient weather conditions are constantly changing and differ from day-day, such that reproducing an image can be very challenging if not impossible. In contrast, the IR-UTD captures many images during the testing interval, and then processes those images to create an image based on the thermal inertia of the material under testing. In this way, the relative rates of change are

analyzed that may provide improved reproducibility. To evaluate the reproducibility of the images created by the IR-UTD system, images of the north span from each test of bridge A0295 were compared.

Figure 44 shows a comparison between the three different tests for the delaminations identified in the north span of the bridge. In this figure, call-outs show an expanded view of each of the defects such that these can be compared between each test. The position of the IR-UTD camera head was different for each of the three tests, such that the delaminations are shown from a slightly different perspective. The time interval over which data was collected was also different for each test, and obviously the weather was different for each of the tests. Regardless, these data indicate that the same delaminations were detected in each test and the size of the delaminations was consistent.

It should be noted that for one of the delaminations, a marker was inadvertently placed on the surface of the bridge during Test 3. This marker was placed on the surface of the deck as a fiducial mark for other testing that was occurring during the same time period. Because the delamination is not visible from the surface of the deck, the marker was inadvertently placed where the subsurface delamination was located. This affects the quality of this particular image. These data illustrated that the IR-UTD results were reproducible across three different tests involving different test set-ups, different data collection intervals, and different weather conditions.

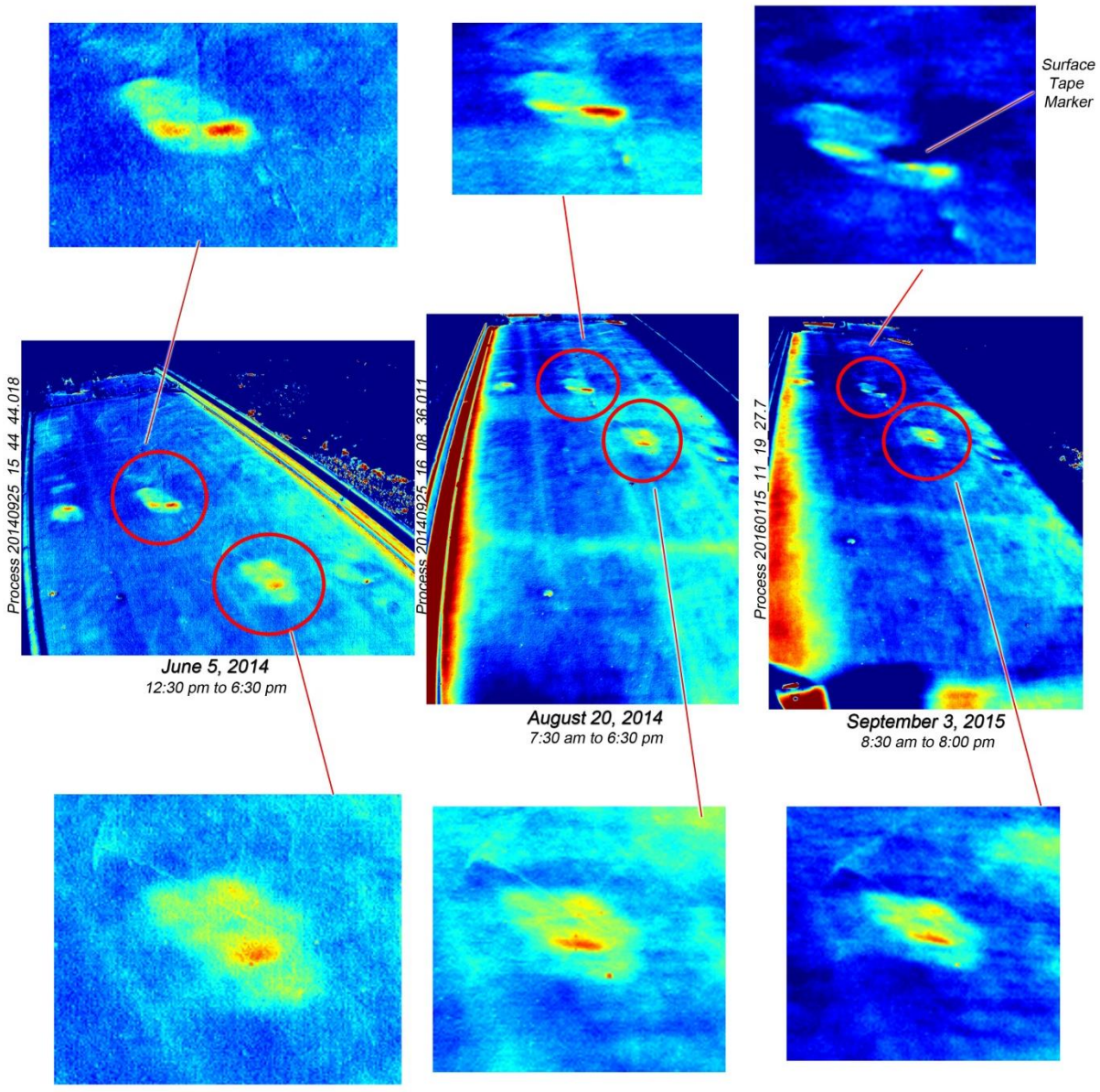

Figure 44. IR-UTD images of the north span of the Kansas City Bridge from three different tests

2.5.2 Discussion

This section of the report described three tests conducted on an out-of-service bridge located in Kansas City, MO. These three separate tests were used to evaluate the capabilities of the IR-UTD system and to evaluate the reproducibility of images created by the IR-UTD. The results of the testing demonstrated that the IR-UTD system was capable of imaging delaminations in the north span of the bridge. These images were consistent across three separate tests, demonstrating the reproducibility of the data. The results of the third test demonstrated the increased area of bridge deck that could be imaged using an automated pan

and tilt mount for the IR-UTD camera head. Using the pan and tilt mount, the entire 212 ft. length of the bridge could be imaged from a single position.

2.6 Soffit and Column Imaging

Tests were conducted to evaluate the capability of the IR-UTD system to analyze the soffit area of a bridge and vertical structures such as a pier. To evaluate the application of the IR-UTD to the soffit area of a structure, a voided-slab bridge in Columbia, MO, was tested. This voided slab has significant deterioration and is scheduled for replacement in 2016. To demonstrate the ability of the system to image a vertical structure such as a pier, the columns on the University of Missouri campus were evaluated. The following section describes the result of these tests.

2.6.1 West Blvd Bridge

The West Boulevard Bridge in Columbia, MO was tested in January of 2015. The West Boulevard Bridge carries Interstate-70 over Business Loop 70 in northwest Columbia, MO. The bridge is a three-span voided slab as shown in Figure 45. The objective of the West Boulevard Bridge test was to demonstrate application of the IR-UTD system for imaging the soffit area of a bridge.

The ambient temperatures for the day are shown in Figure 46. As shown in the figure, there was a large change in temperature during the course of the testing. Data was collected and analyzed during the heating cycle.

Figure 45. Photograph of the West Blvd Bridge illustrating the test set-up location.

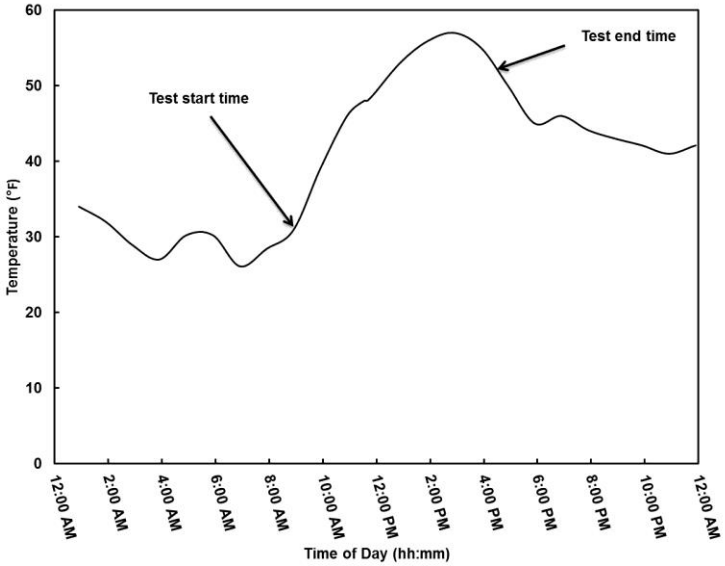

Figure 46. Ambient temperature conditions during data collection for the West Blvd Bridge.

Figure 47 shows the setup of the IR-UTD system under the bridge. The camera head was mounted on a common tripod designed for photographic and film applications. The DAQ enclosure was simply placed on the ground during the testing. The system was operated using its internal battery systems.

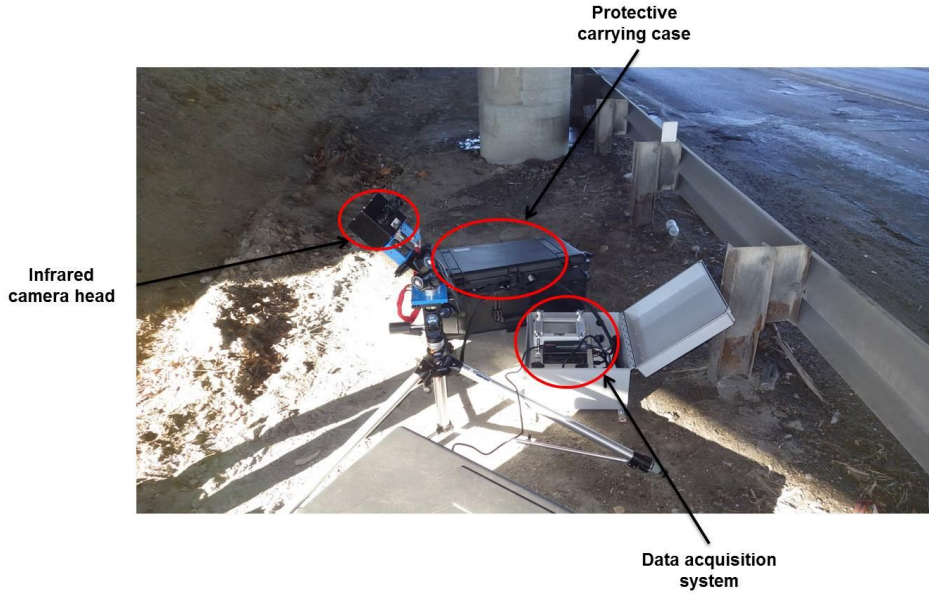

Figure 47. Photograph of the test setup for the West Blvd Bridge.

Figure 48 shows the view from the infrared camera of the soffit of the bridge. From this camera position and angle, an area of the bridge soffit that was located above the travel lanes passing under the bridge was imaged. No traffic control was necessary to conduct the test because the IR-UTD system was positioned behind the barrier.

Figure 48. Photograph showing the camera head and the area of the bridge soffit imaged during the test.

The results of processing the IR-UTD data indicate a large area of saturation as shown in Figure 49. As a result of the water saturation, there was very little temperature change in the saturated area, resulting in an anomaly in the IR-UTD data. The saturated areas of the concrete are enclosed in dashed lines in the figure. In other areas of the image, the signature of the voids is shown in the IR-UTD data, appearing as areas where the thermal inertia is reduced relative to area between the voids, where concrete is continuous through the thickness of the slab. The indication of the voids in the image indicates that heat transfer was occurring normally in these areas. In contrast, the voids are not apparent in the areas that are saturated, indicating that heat transfer was not occurring normally in these areas.

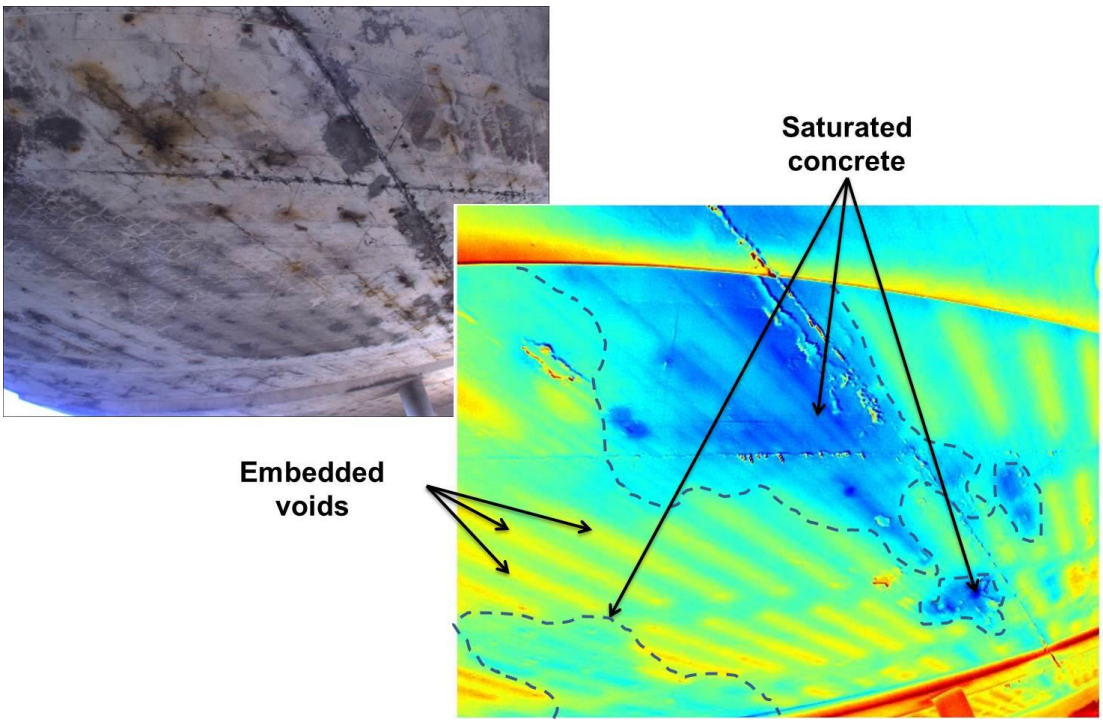

Figure 49. Image showing saturated portions of the soffit area of the bridge deck.

2.6.2 Columns at MU

To evaluate the capability of the technology to image a vertical surface, testing was conducted on the limestone columns on the University of Missouri campus. The iconic columns were originally part of Academic Hall, a building constructed in 1843. In 1892, a fire destroyed the building (Figure 50), but the columns remained standing and have been preserved as a campus landmark known as the “Mizzou Columns.” Testing was conducted on two opposite sides of the columns - the side of the column facing away from the fire and the side of the column closest to the building that faced the fire. This side of the column was known to have numerous delaminations of the limestone as a result of the fire.

Figure 50. Photograph of Academic Hall during the fire that destroyed the building in 1892.

The testing was completed in December, 2014. Ambient weather conditions were generally good throughout the testing. The testing was completed over a period of six hours during the daytime, and as such the heating cycle was analyzed to image subsurface damage in each side of the columns. The test setup for imaging the damaged side of the columns is shown in Figure 51. To image the other side of the columns this test setup was relocated to the opposite side of the columns. The IR-UTD camera head was mounted on a tripod approximately 75 ft. from the side of the column being imaged. The columns extend across a distance of approximately 75 ft. and are 46 ft. tall.

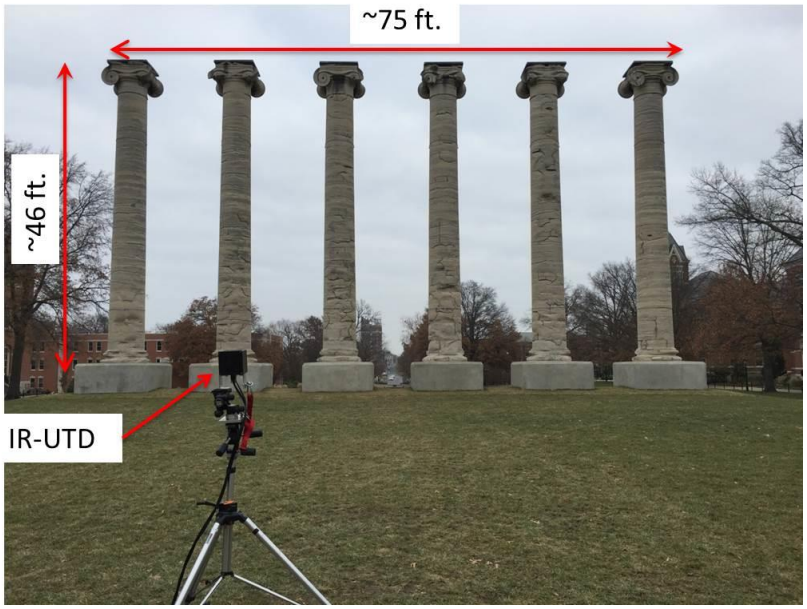

Figure 51. Photograph showing the location of the IR-UTD camera head during testing of the columns.

Figure 52 summarizes the results of the column imaging. These data were processed from the heating cycle of each day. Figure 52A shows the side of the columns facing away from the fire. As shown in this image, there is no damage on this side of the columns. Figure 52B shows the side of the column that faced the fire, and numerous delaminations are shown in the image. Figure 52C shows and expanded view of one of the columns. These data demonstrated the ability of the IR-UTD system to image a larger, vertical area from a distance. Delaminations in the limestone were detected by evaluating the heating cycle.

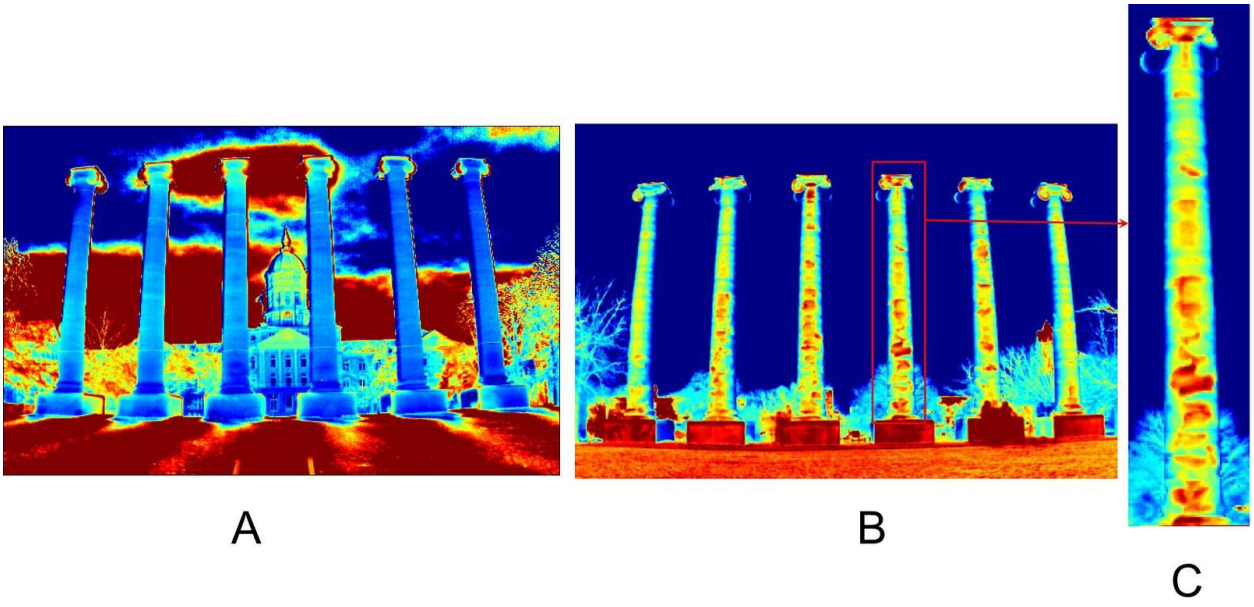

Figure 52. IR-UTD images of the columns on the MU campus showing (A) the undamaged side of the columns, (B) the damaged side of the columns, and (C) an expanded view of one of the columns.

3 IR-DSS TESTING

This portion of the report describes field testing of the IR-DSS system. This system is designed as a vehicle-mounted IR imaging system. This system was intended to provide a technology for creating a plan-view image of a bridge deck or other structure that showed the location and extent of delaminations. Two field tests were conducted. The first test was conducted on the deck of a highway bridge located in Fulton, MO. The second test was conducted on the out-of-service bridge A0295 located in Kansas City, MO.

3.1 Bridge A2111

Testing of the IR-DSS system was conducted on MoDOT Bridge A2111 in Fulton, MO. The objectives of this test were as follows:

- test and evaluate the newly developed IR-DSS system
- evaluate the quality and accuracy of data provided by the system
- compare the results provided by the IR-DSS with other deck scanning technologies

Bridge A2111 is three-span bridge 175 ft. in length, with a roadway width of 41 ft. The reinforced concrete deck is 7.5 in. thick and supported on steel stringers. A number of patch repairs have been made to the deck to address spalling damage. Some smaller areas of asphalt patching were present on the deck. An aerial view of the bridge is shown in Figure 53. This figure shows the direction of travel on the bridge as well as the position of the shoulder and driving lanes, which are numbered 1 through 4 in the figure to provide reference for test results reported in this section.

A Ground Penetrating Radar (GPR) technology was used to scan the bridge deck to provide data for comparison with the IR-DSS results. Sounding, hand-held thermal imaging, and Impact Echo were also applied at certain locations on the bridge deck to verify results. For example, a hand-held IR camera (FLIR 620) was used to identify locations on the deck that were delaminated. These areas were then verified with sounding and in some cases using Impact Echo.

Figure 53. Aerial view of Bridge A2111 in Fulton, MO.

Traffic control was provided by MoDOT during the testing. Traffic control consisted of a lane closure that allowed for sounding, GPR scanning, and testing of the IR-DSS system. Two separate lane closures were required to support the testing. A lane closure was established for the right driving lane and shoulder between the hours of 9:30 and 11:30 am for data collection in

lanes 1 and 2 (Figure 53). This lane closure was relocated to the left driving lane between the hours of 11:30 a.m. and 1:00 p.m. Data was collected from the left driving lane and shoulder between the hours of 1:00 and 2:30 pm (lanes 3 and 4 in Figure 53).

The weather conditions at the time of the testing included overcast sky. Three days prior to the testing, there had been 4.23 inches of rain, and weather patterns during the two days prior to the testing were overcast with a small amount of light rain or snow. The ambient temperature conditions at the time of the testing are shown in Figure 54. As shown in the figure, there was a temperature change of 16° F between sunrise and the time that data was collected in lanes 1 and 2. This temperature variation provided adequate conditions for thermal imaging during data collection from lanes 1 and 2. At 1:30 – 2:00 pm, rain moved into the area and light rain was occurring at the bridge deck. As a result of the diminishing ambient temperatures and light rain, the conditions were less favorable when the IR-DSS collected data from lanes 3 and 4 (Figure 53). Overall, weather conditions were not optimal for thermal imaging.

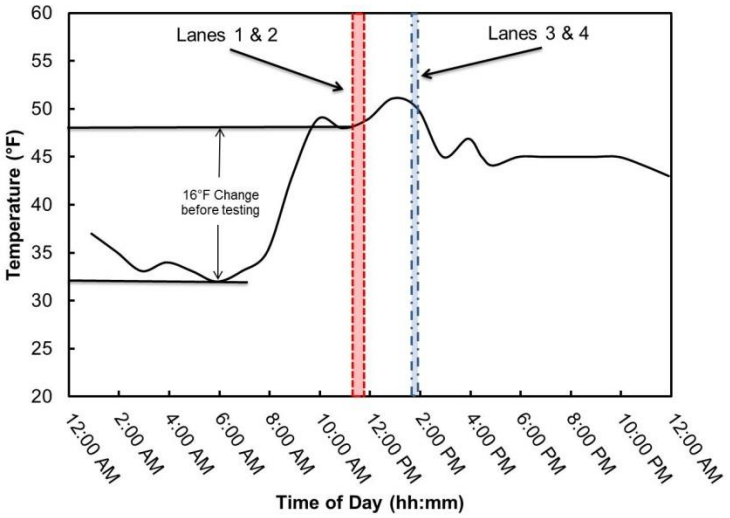

Figure 54. Ambient temperature conditions during testing.

3.1.1 IR-DSS Testing

The IR-DSS system was mounted to a typical pickup truck using the trailer hitch connection. The camera head of the IR-DSS system was positioned at a height of 10 ft during the testing as shown in Figure 10. From this position, the IR-DSS camera produced a thermal image that displays a portion of the deck approximately 8 ft x 10 ft in dimension. Data was collected as the vehicle drove slowly (<5 mph) across the bridge deck. Four individual scans across the bridge decks were used to provide coverage of the entire 41 ft width of the deck.

Data collection was initiated with the vehicle positioned on the approach slab at the west end of the bridge and data collection was stopped when the vehicle was positioned on the approach slab on the east side of the bridge. Data collection time for the IR-DSS scan of the four lanes was approximately six minutes. Repositioning was necessary between each scan to return the IR-DSS system to the initial position on the west approach slab. The total time required to complete four scans with the IR-DSS was approximately 15 minutes.

Data collected during the testing was post-processed to stitch together the individual frames of IR data such that a plan view of the bridge deck could be produced.

3.1.2 GPR and Thermal Imaging

A GPR system was used to scan the bridge deck to provide data for comparison between the GPR results and the IR-DSS results. This section provides a brief technical overview of GPR technology and its relationship with thermal imaging technologies.

GPR scanning provides data related to the likelihood of corrosion damage based on the attenuation (i.e., reduced signal amplitudes) of GPR signals reflected from reinforcing steel in the concrete. The attenuation of these signals is caused in large part by the presence of moisture and chlorides in the concrete between the reinforcing steel and the surface of the concrete deck, and to a lesser extent, scattering of the electromagnetic wave caused by cracking in the concrete [21-23]. The presence of moisture and chlorides affects the dielectric constant of the concrete, and these changes in dielectric properties manifest in attenuation and delay of the reflected GPR signal. Some theories postulate that corrosion products near the surface of the rebar contribute to the attenuation of the GPR signal [24]. Therefore, GPR does not detect delaminations in the bridge deck, but rather provides data on areas of the bridge deck where corrosion damage is likely based on the attenuation of electromagnetic waves [21, 25, 26].

In contrast, thermal imaging technologies detect delaminations and features that affect *heat transfer* in the concrete. Generally, the focus of thermal imaging technologies is delaminated or debonded materials that *interrupt heat flow* through the structure. Therefore, thermal imaging provides a more direct measurement of the damage (delamination or debonding) by interpreting variations in the IR energy emitted from the surface of the material.

Thermal imaging is also sensitive to water saturation of concrete, as shown in the soffit imaging section of this report. The reason that thermal imaging is sensitive to saturation is that water has a large specific heat, meaning that it requires a greater amount of energy to heat (or cool) water than it does to heat (or cool) concrete. Consequently, saturation creates anomalies

in the thermal behavior of materials that manifest in anomalies in thermal images. When a delamination is filled with water or saturated, it will not increase in temperature in a manner similar to a dry delamination. This effect was modeled using Finite Element Modeling (FEM) during this research, and those results are reported in Volume I of the report. When large areas of concrete are saturated, thermal changes due to diurnal temperature cycles in those areas lag behind thermal changes in areas that are not saturated. This effect was demonstrated in section 2.6.1 of this report.

GPR scanning of the bridge deck was conducted using a 1.6 GHz GSSI ground-coupled GPR system. Scans were conducted at 2 ft intervals across the width of the deck, with 24 scans per ft. recorded along the length of the bridge. The ground-coupled GPR system was operated at walking speed during scanning of the deck. The resulting GPR data were processed using the commercial software RADAN 7 provided by the manufacturer of the GPR system. Plotting of the GPR results was completed using OriginPro-2016 software.

3.1.3 IR-DSS Results

The results of the testing are summarized in Figures 55 thru 58 below. Figure 55 shows an overall plan view image of the bridge deck including the visual images (top) and the thermal images (bottom). The visual images are captured by the IR-DSS visual camera and show the deck patches on the bridge. The thermal images (bottom) show a number of delaminations in the bridge deck. Figures 56 and 57 provide the results for each lane of data captured separately, with expanded views of individual delaminations to demonstrate the resolution and spatial precision of the data captured by the IR DSS. Figure 56 shows delaminations in lane 1 as well as a spalling patch area with moisture on the surface. The moisture appears blue in the image. Lane 2 also shows delaminations in the deck including delamination developing around an area that has been patched. Figure 57 shows lanes 3 and 4, including a very large area of delamination in lane 4. Generally, the quality of data produced from lanes 3 and 4 was lower than data produced from lanes 1 and 2 due to the weather conditions, as previously mentioned.

Figure 58 shows an overall plan view of the deck with expanded views of patches on the deck. The data shows unsound patches and sound patches. Unsound patches appear in red in the image, indicating a positive thermal contrast with intact portions of the deck. Sound patches appear in green, indicating little or no thermal contrast with intact portion of the deck. These data are significant in terms of the ability of the IR-DSS system to provide information regarding the maintenance needs of a bridge, in this case the condition of previously applied patches.

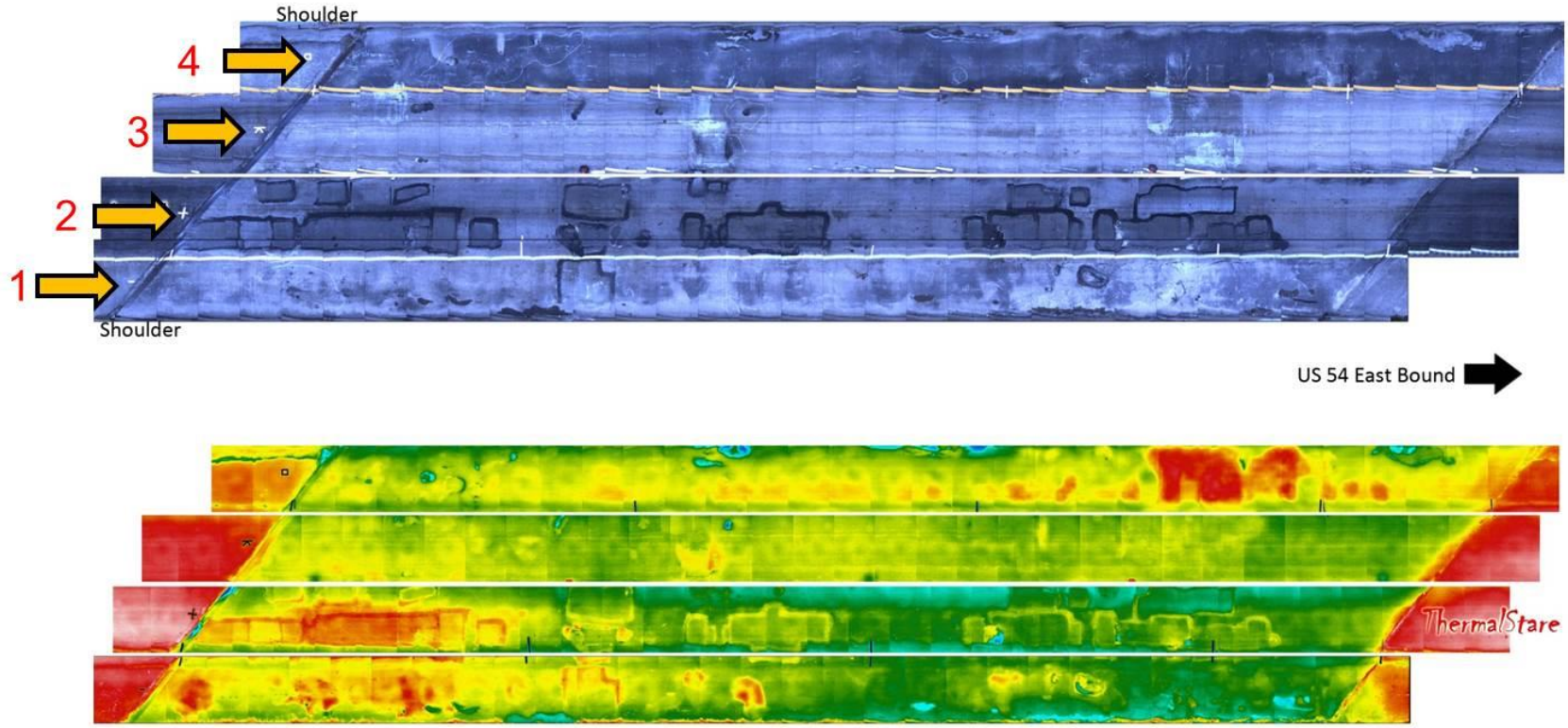

Figure 55. Plan view image of the bridge deck showing IR-DSS visual images (top) and thermal images (bottom).

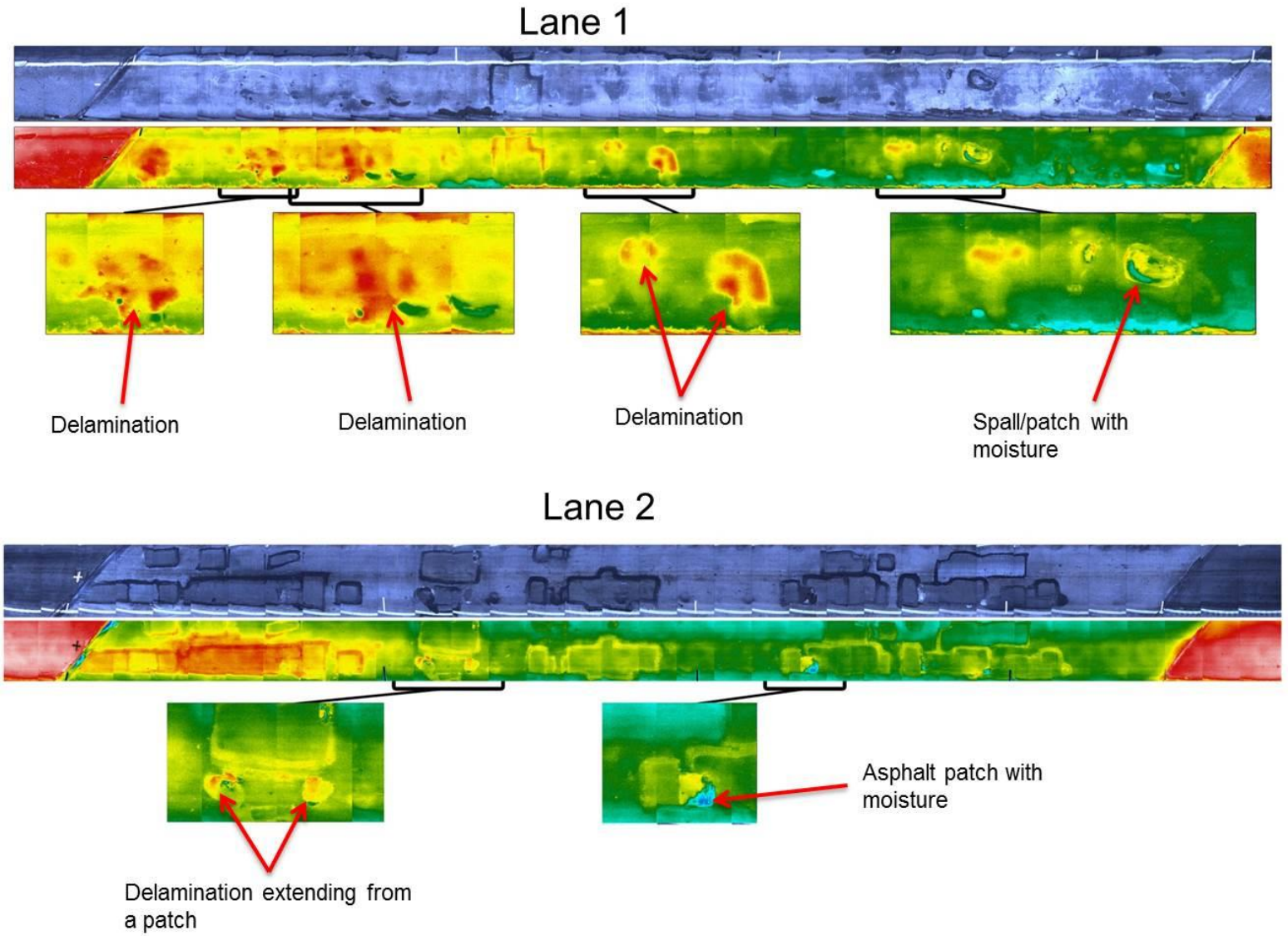

Figure 56. Plan view images of individual lanes 1 and 2 with expanded views of key portions of the deck.

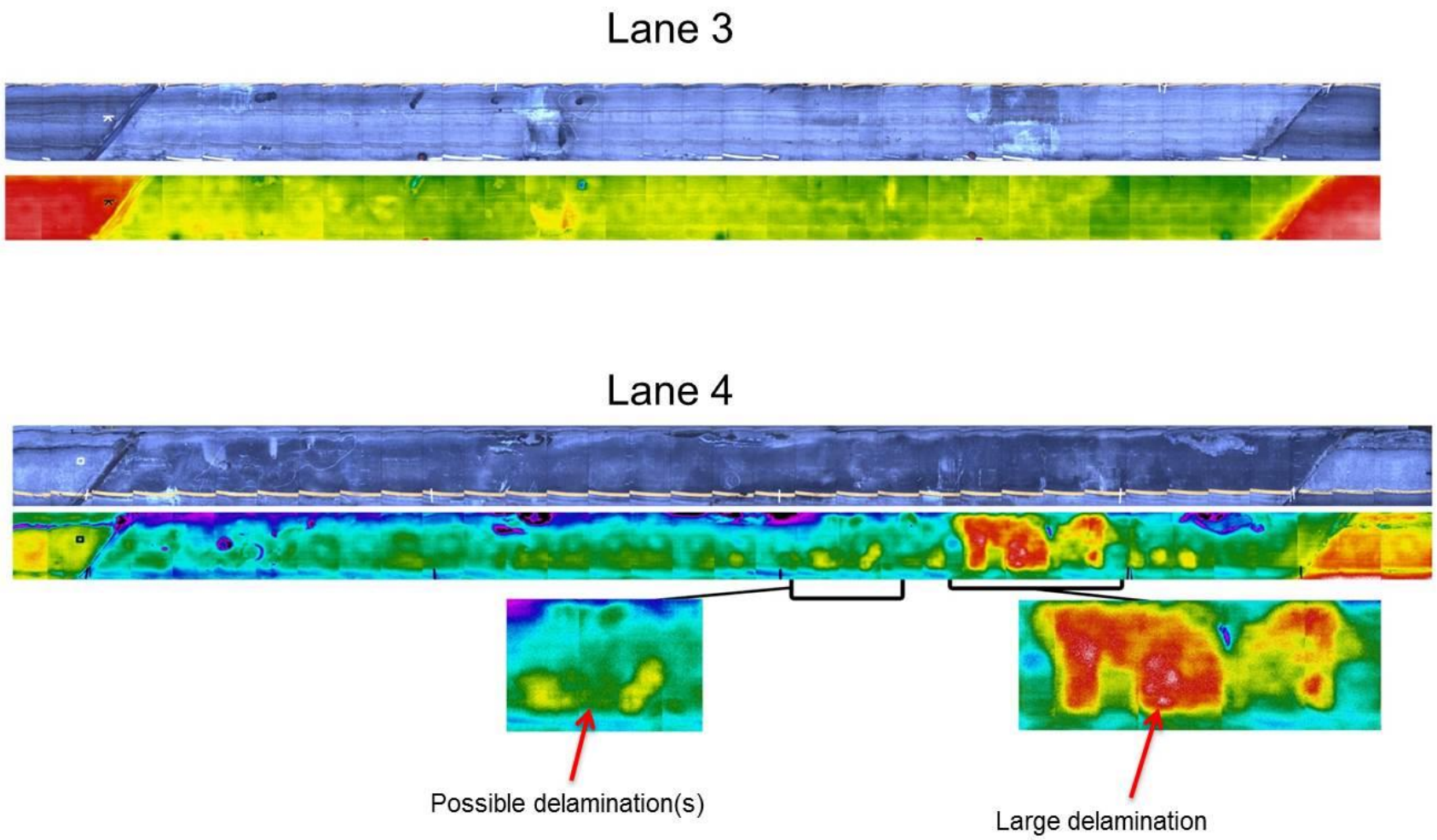

Figure 57. Plan view images of individual lanes 3 and 4 with expanded views of key portions of the deck.

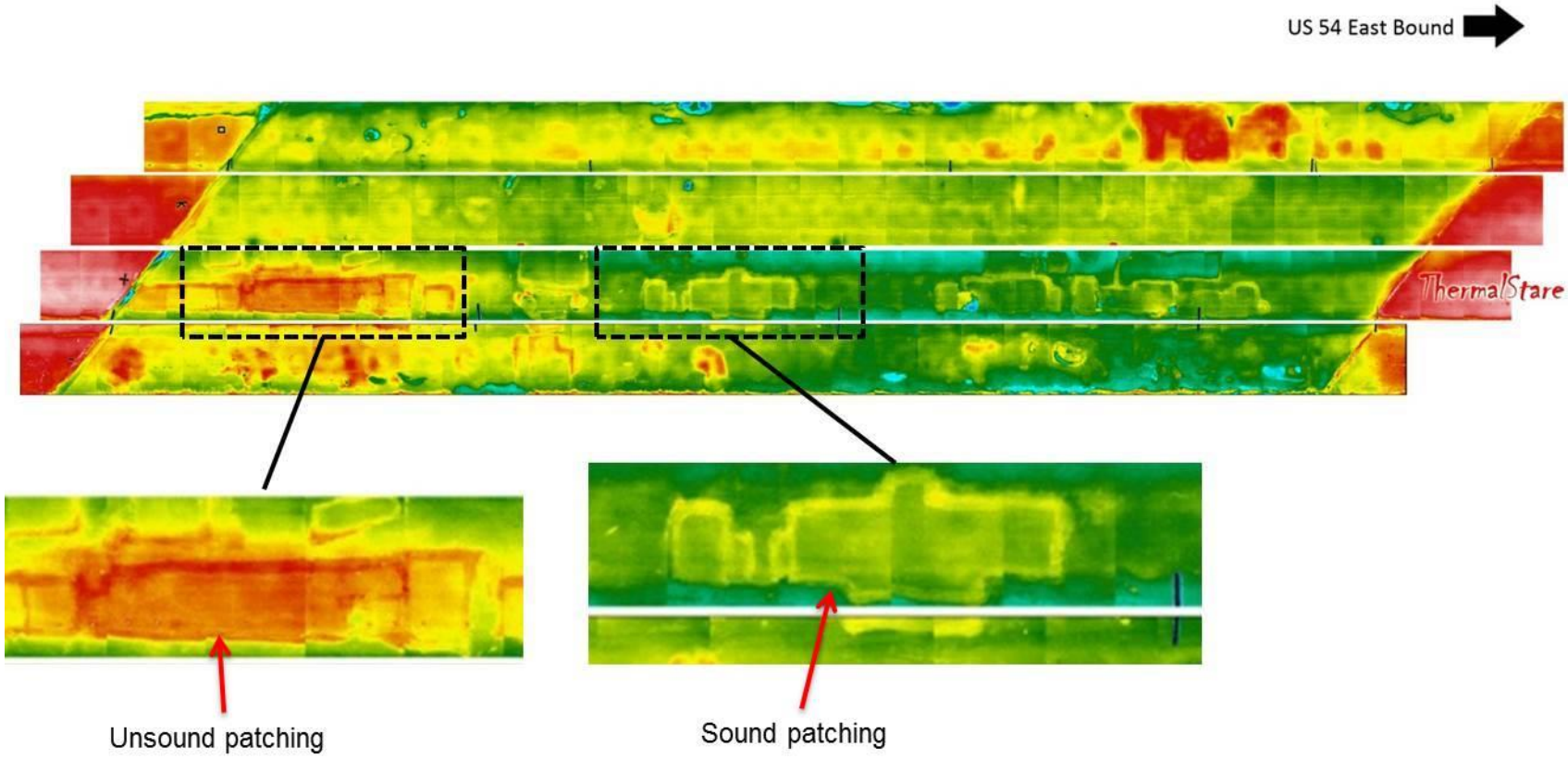

Figure 58. Plan view image showing sound and unsound patch areas.

3.1.4 Comparison of IR-DSS Results with GPR

The IR-DSS results were compared with GPR scans that were completed during the field test. The results of the GPR scanning are shown in Figure 59. In this figure, areas shown in blue have a low likelihood of corrosion damage, areas shown in green, red and yellow exhibit increased attenuation associated with increased likelihood of corrosion damage. To provide a comparison between the IR-DSS results and the GPR scan, a subjective threshold attenuation of -7 dB was applied to the GPR image. The threshold value of – 7 dB was determined from an analysis of the recommended values in the ASTM standard for applying GPR to bridge decks [27]. This standard indicates that a threshold value of signal amplitude loss of -6 to -8 dB (relative to the maximum signal amplitude measured for a given test) typically corresponds with deterioration [27]. These threshold values were analyzed to determine the area of bridge deck (in %) that would be determined to have a high likelihood of corrosion damage for each threshold value. Figure 60 shows results for threshold values of -6 (top) and -8 dB (bottom) threshold applied to the GPR data from bridge A2111. The areas of low likelihood are shown in black/grey in the figures.

Significantly different results in terms of deck area are found between these two different threshold values. For example, using a threshold attenuation of -6 dB results in approximately 43% of the deck area indicated as having a high likelihood of corrosion damage. Using a threshold value of -8 dB results in approximately 22% of the deck area indicated as having a high likelihood of corrosion. This means that the deck area measured by GPR as having a high likelihood of corrosion damage varies by a factor of almost 2 (1.96) between the recommended threshold values. A threshold value of -7 dB was selected as a nominal value that “split the difference;” using a threshold of -7 dB results in approximately 31% of deck area.

The color map for Figure 59 was modified to present the data in a two-color format. The areas of Figure 59 that did not have attenuation of at least -7dB were plotted with no color (clear); those areas with -7 dB or greater attenuation were plotted in gray. In other words, areas with little likelihood of corrosion are shown with no color and areas with high likelihood of corrosion damage are shown as gray areas. This allowed the GPR data to be overlaid with the IR-DSS results so that a comparison between the results could be made.

Figure 61 shows three plan-view images of the bridge deck. The top image is the GPR results with the –7 dB threshold and the modified color map applied. Areas shown as clear in this image have a low likelihood of corrosion damage based on the GPR results. The second

figure shows the IR-DSS results, and the third image shows an overlay of the GPR data with the IR-DSS data.

This comparison is useful for understanding the differences between the type of information provided by IR results and GPR results. The GPR results show general information on areas of the deck where corrosion damage is more likely, relative to other areas of the deck. This likelihood is based on the presence of moisture and chloride ions that affect the polarizability of concrete which manifest in signal attenuation and delay. GPR results do not by themselves provide information regarding the area of the deck that is delaminated, patched or has obvious spalls in the surface. In contrast, the IR results provides data on the specific areas that are damaged (delaminated), providing the location and extent of each individual area that is delaminated. Sound and unsound patches were detected and differentiated from the IR-DSS data. In addition, the visual image produced by the IR-DSS shows patches and spalling in the bridge deck.

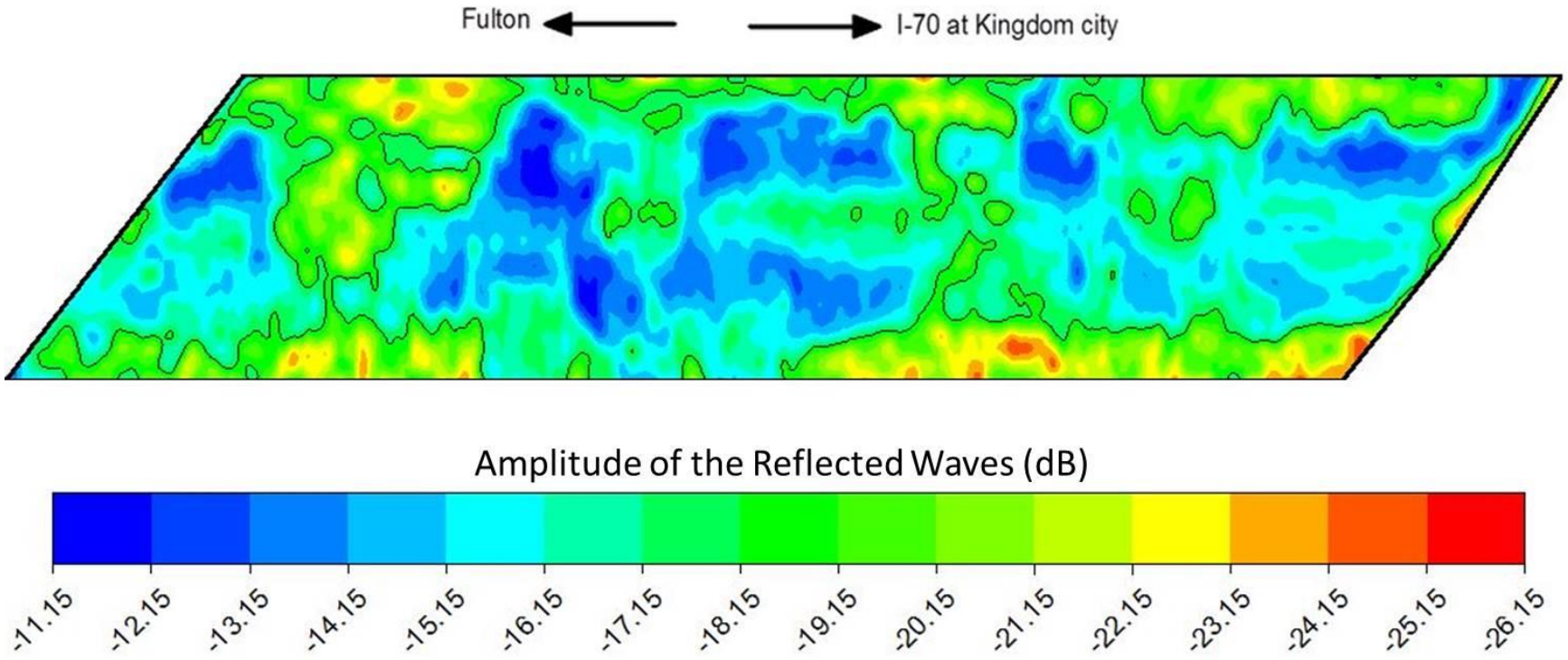

Figure 59. Image showing GPR scanning results of Bridge A2111.

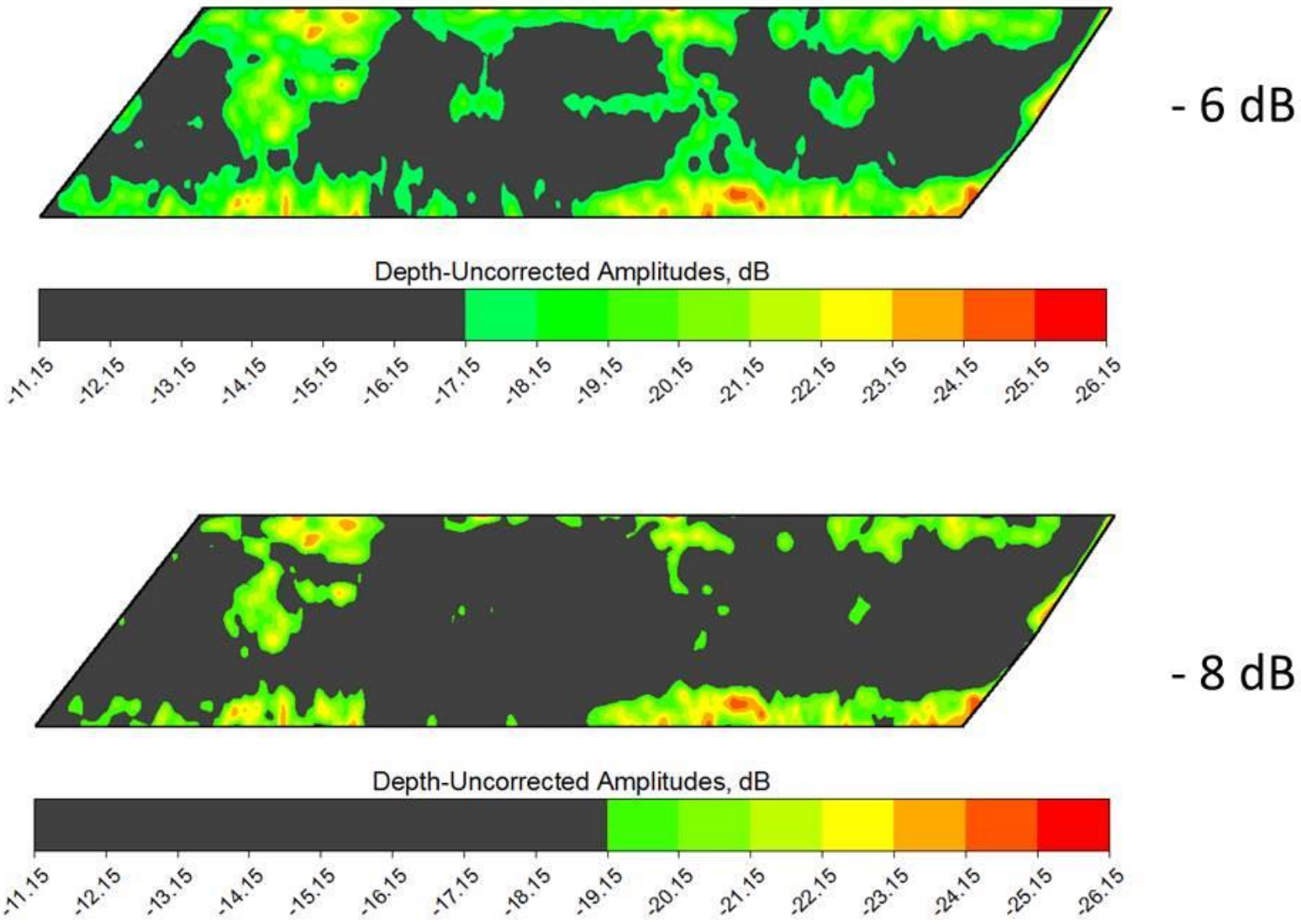

Figure 60. GPR scanning results showing threshold of -6 dB (top) and -8 dB (bottom).

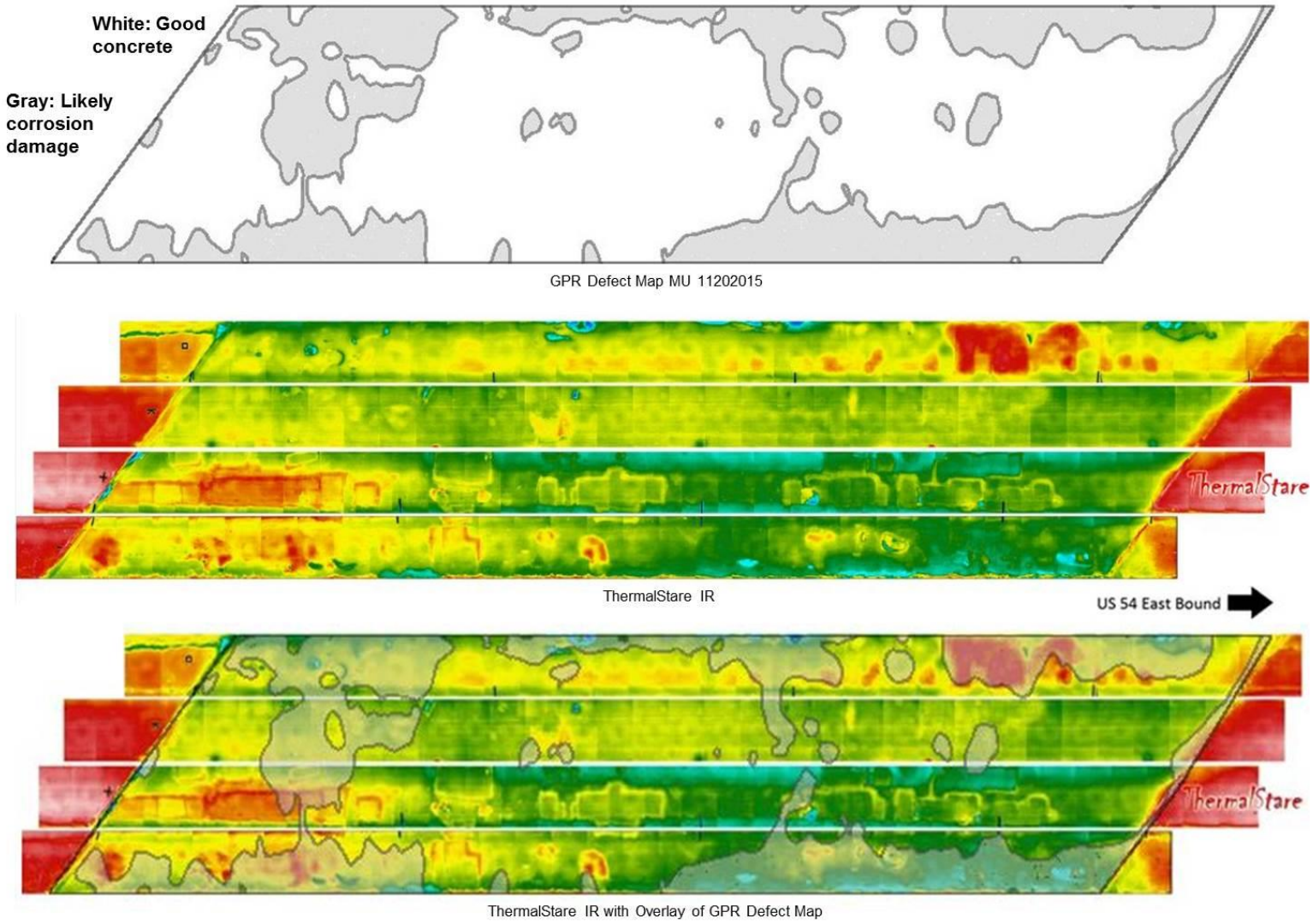

Figure 61. GPR data (top), IR-DSS data (middle) and the overlay showing the GPR data on the IR-DSS data (bottom).

Specific areas of the deck are highlighted in Figure 62 to further describe the differences between GPR results and IR-DSS results. Four areas have been highlighted in the figure and these areas have been labeled A, B, C, and D. The following paragraph provides analysis of each of the highlighted areas.

Area A illustrates an area of the deck where the GPR data indicated a high likelihood of corrosion damage, but the IR-DSS results did not show a delamination. A delamination in this area was confirmed with hammer sounding. This area of the deck was saturated, with water emerging from the delamination in the area of a pothole as shown in the photograph in the figure. This moist area of the deck is captured in the IR-DSS data as a blue area that is located where the moisture can be observed in the photograph. GPR is sensitive to moisture and chloride solutions and as such this area exhibits a large attenuation (see Figure 59). However, moisture in a delamination will cause the heating and cooling of the deck in the area to be slowed, such that a thermal contrast with the intact deck does not appear in the IR image, as previously discussed. Rain prior to the testing resulted in this saturated deck area. The saturation of the delamination was verified by drilling a ½ hole into the deck in this area. The material removed by the drill from the depth of the delamination was saturated.

Area B shows an area where the GPR scan indicated an area with low likelihood of corrosion damage, but in fact there are delaminations in this area as indicated by the IR-DSS scanning and verified with hammer sounding. Area C indicates an area where there are unsound patches detected by the IR-DSS, while the GPR scan indicates that this is an area with a low likelihood of corrosion damage. It may be that the damage in the partial-depth patch is not corrosion-related, but rather a debonding of the patch with the substrate. The GPR technology is sensitive to the presence of chloride ions and moisture; the technology is generally insensitive to dry delaminations. This may explain why the IR-DSS detected this unsound patch while the GPR did not indicate damage was likely in this area. Finally, area D illustrates delaminated areas of the deck where the GPR results indicate a low likelihood of corrosion damage, but the IR-DSS indicates a delamination. This delamination was confirmed with sounding and impact echo. It should also be noted that there are many areas of the bridge deck that GPR indicated a high likelihood of corrosion damage, but there are no delaminations detected in the IR-DSS data.

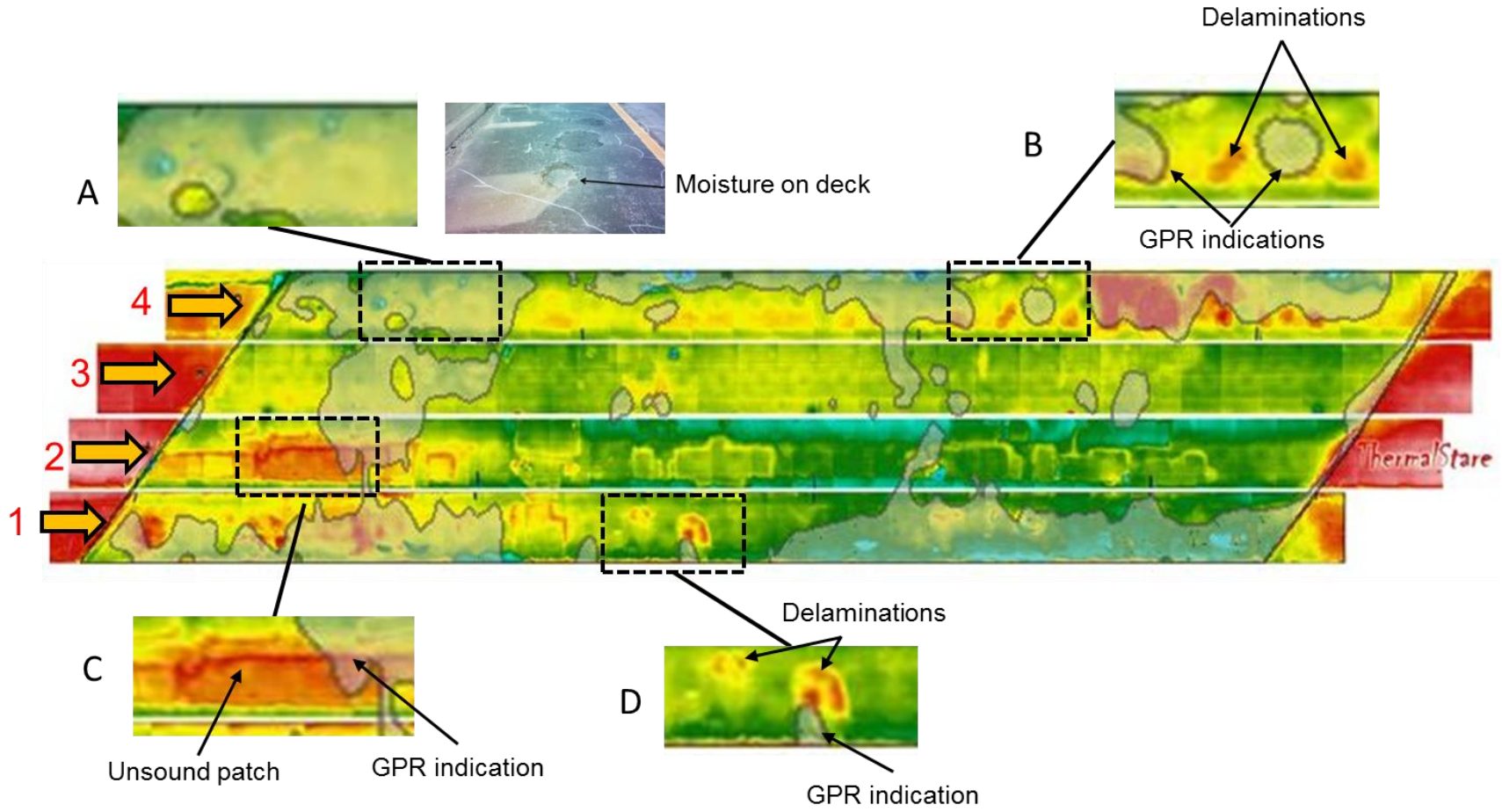

Figure 62. Overlay of GPR data and IR-DSS data showing plan view of bridge A2111 showing expanded view of several areas.

3.1.5 Discussion

The testing of the IR-DSS system illustrated the utility of the technology for imaging damage in a concrete bridge deck. It was demonstrated that the technology is capable of detecting delaminations and unsound patches in the surface of the deck. This was demonstrated for weather conditions that were less than optimal; the sky was overcast, and rain had occurred the day prior to the test resulting in saturation of some areas of the deck. In an area of the deck that was saturated, the IR-DSS did not detect a large delamination that was confirmed with hammer sounding. This area was observed to have moisture present that affected the IR results.

The comparison of the IR-DSS and GPR scans provided a good illustration of the differences between these two technologies. The GPR scans provide a general overview of the likelihood of corrosion damage in different areas of the bridge deck, based on the attenuation caused by moisture and chlorides in the concrete. The area of deck determined to have a high likelihood of corrosion damage varied by a factor of 2 depending on the threshold value selected. The IR-DSS is sensitive to thermal variations caused by subsurface damage interrupting heat flow in the deck. As a result, it was shown that there are areas of the deck where thermal imaging detected delaminations while GPR indicated a low likelihood of corrosion damage. There were also areas of unsound patches detected by thermal imaging that were not detected by GPR, possibly because the defect is not corrosion-related.

Data was collected at a speed of <5 mph during the testing of the IR-DSS system, and at walking speed for the GPR system. Practical implementation of the IR-DSS technology will require some form of traffic control. Moving traffic control, in which attenuators and signage are positioned in front of and behind the vehicle used for scanning is a suitable approach.

3.2 Testing of the IR-DSS System on the Kansas City Bridge A0295

Field testing was conducted on bridge A0295 on January 29, 2016. The objectives of the testing was to verify the IR-DSS capabilities for detecting delaminations and to compare the results with data produced from the IR-UTD system.

Weather conditions during testing consisted of clear skies and a significant temperature change between sunrise and the time of the test. Figure 63 shows the ambient weather condition on the day of the test, and these data indicate that the ambient temperature change between sunrise and the time of the IR-DSS scan was 21° F.

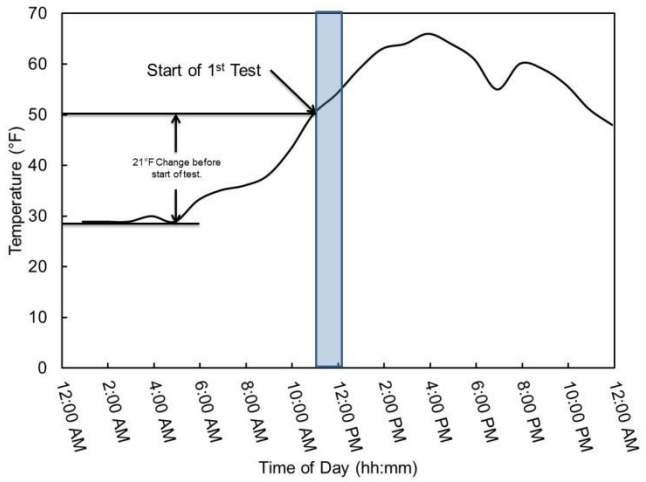

Figure 63. Ambient temperature variations during testing of the IR-DSS system on Bridge A0295.

The scanning pattern of the truck-mounted IR-DSS system on the bridge is shown schematically in Figure 64. Five scans were conducted on the bridge for each testing run performed, starting from the lane labeled "1" and finishing at the lane labeled "5." Several test runs were made to ensure sufficient data was collected and for analysis of repeatability. The results presented here were from the first scan completed. The scans were collected starting at the south end of the bridge and moving towards the north end of the bridge. Each test was conducted as straight as possible along the length of the bridge, with the 5th scan of each test skewed due to the bridge geometry shown in Figure 64. Since the bridge does not have approach spans, scans were initiated from a position on the south end of the bridge deck.

Data from the IR-DSS was processed to stitch together the individual images and provide a plan view of the bridge deck. This plan view was then compared with previous test results using the IR-UTD system. The results of the testing and analysis are presented in the following sections.

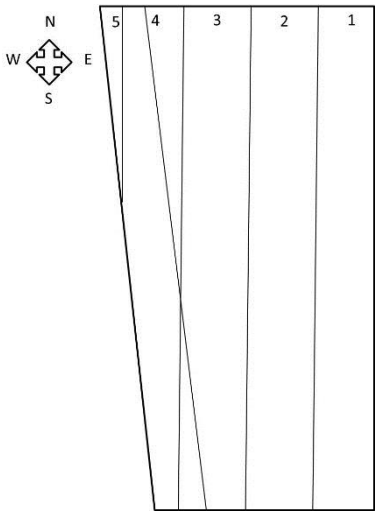

Figure 64. Schematic diagram of the scanning pattern used for bridge A0295.

3.2.1 Results

Figure 65 shows the results of scanning the Kansas City bridge deck with the IR-DSS system. There are several features identified in this image. First, metal tape markers were placed on the bridge to provide reference marks for research purposes, and these appear as dark lines in the IR-DSS data. Second, there is the shadow of a light pole on the bridge, and this appears in both the IR-DSS and visual image of the deck surface. Third, there is an area in the north east corner of the deck where the IR-DSS scan appears to show a delamination. This is possibly a false indication; a delamination in this area has not been confirmed with previous hammer sounding. A very faint indication in this area appears in the most recent IR-UTD image of this area of the deck; it is possible that a delamination in this area has developed since the chain drag was completed in 2013. Efforts are ongoing to verify this area. Generally, the north end of the bridge demonstrates “noisy” data such that there appears to be a greater thermal output from this area than other areas of the deck. This phenomena has also appeared in single-frame data collected when testing the IR-UTD system, as was shown in Figure 41. The cause of the increased noise on this portion of the bridge may be related to a variation in material properties or surface conditions. Fourth, on the south end of the bridge, the IR-DSS data is obscured by shadows that were created from a vehicle used during the test. The vehicle had to be positioned on the deck itself prior to the start of each test, creating an area of shadowing on the deck; this was a result of the bridge not having any approaches,

Individual delaminations in the bridge deck are also shown in the image, represented by red areas in the figure.

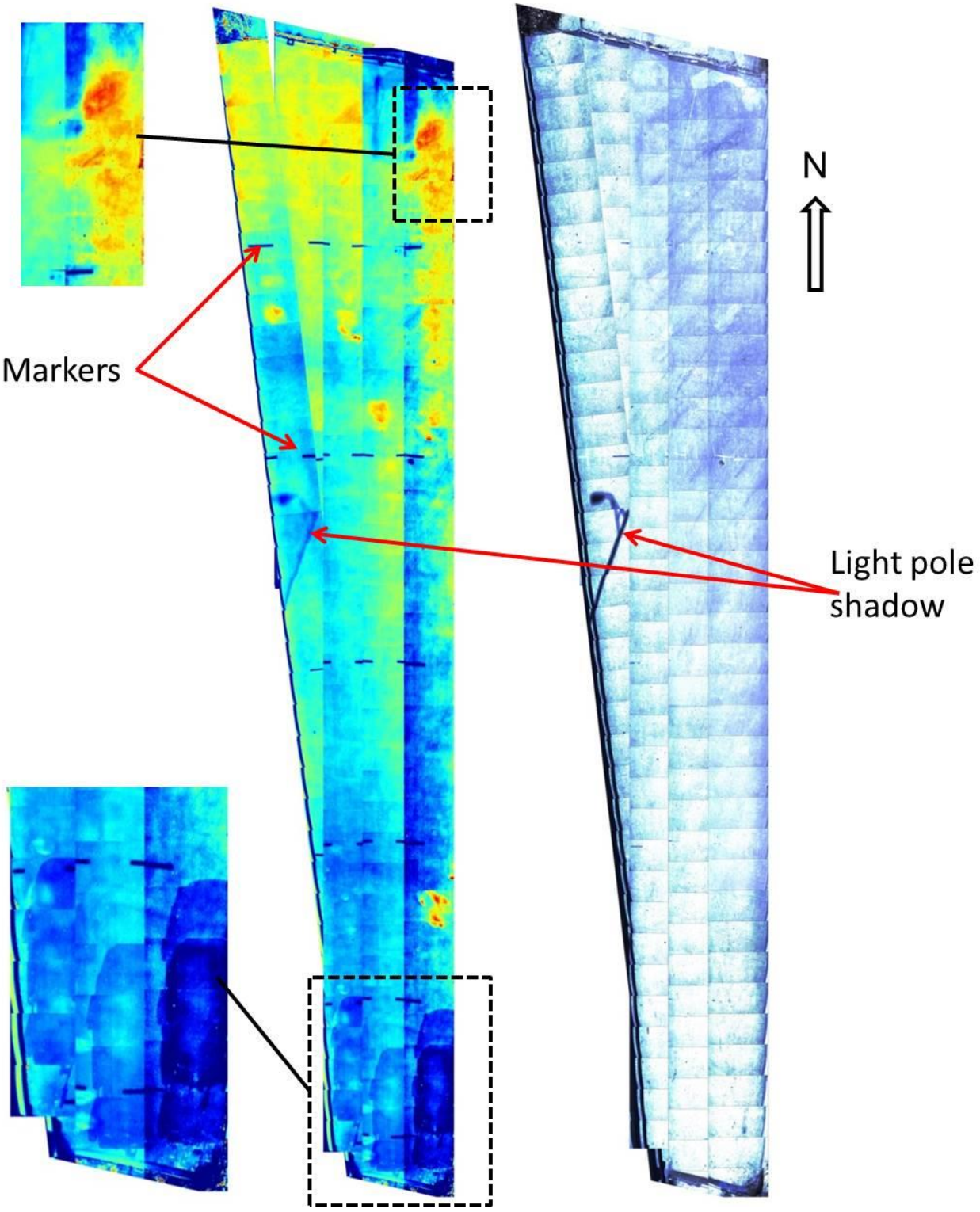

Figure 65. Plan view images of bridge A0295 showing visual image (right) and IR-DSS image (left).

3.2.2 Comparison with IR-UTD Data

The data from the IR-DSS scan of the bridge deck was compared with the IR-UTD images. Recall that the IR-DSS system captures singular thermal images as the system moves across the deck. These images represent the thermal energy emitted from the surface of the concrete at the time the data is captured. The IR-UTD collects many images of the thermal energy emitted from the surface of the concrete over time and from a fixed position, typically on a mast. The IR-UTD data are then processed to produce an image of the thermal inertia of the surface. The resulting images from the IR-DSS system and the IR-UTD system may look very similar in many respects, but the data from which the images are created is very different. A comparison of data from these two systems was completed to illustrate the different results.

Figure 66 shows a comparison between the IR-DSS system results and the IR-UTD system results for the north end of the bridge. Qualitatively it can be observed that the IR-UTD data has much less noise in the image such that the deck appears more uniform in color. As a result, the spatial extent of the delamination is unambiguous in the IR-UTD image. In the IR-DSS image, variations in the IR energy emitted from the surface create background noise that makes determining the spatial extent of a delamination difficult. Also, delaminations are detected by each of the systems, in the same area and sharing similar characteristics in terms of magnitude variations across the delamination (i.e., variations of red and yellow color). These variations result from variations in depth of the delamination from the surface. In other areas of the deck that are intact (no delamination), the IR-DSS shows thermal variations of a similar magnitude to areas that are known to be delaminated. These areas are false indications caused by the noise in the data.

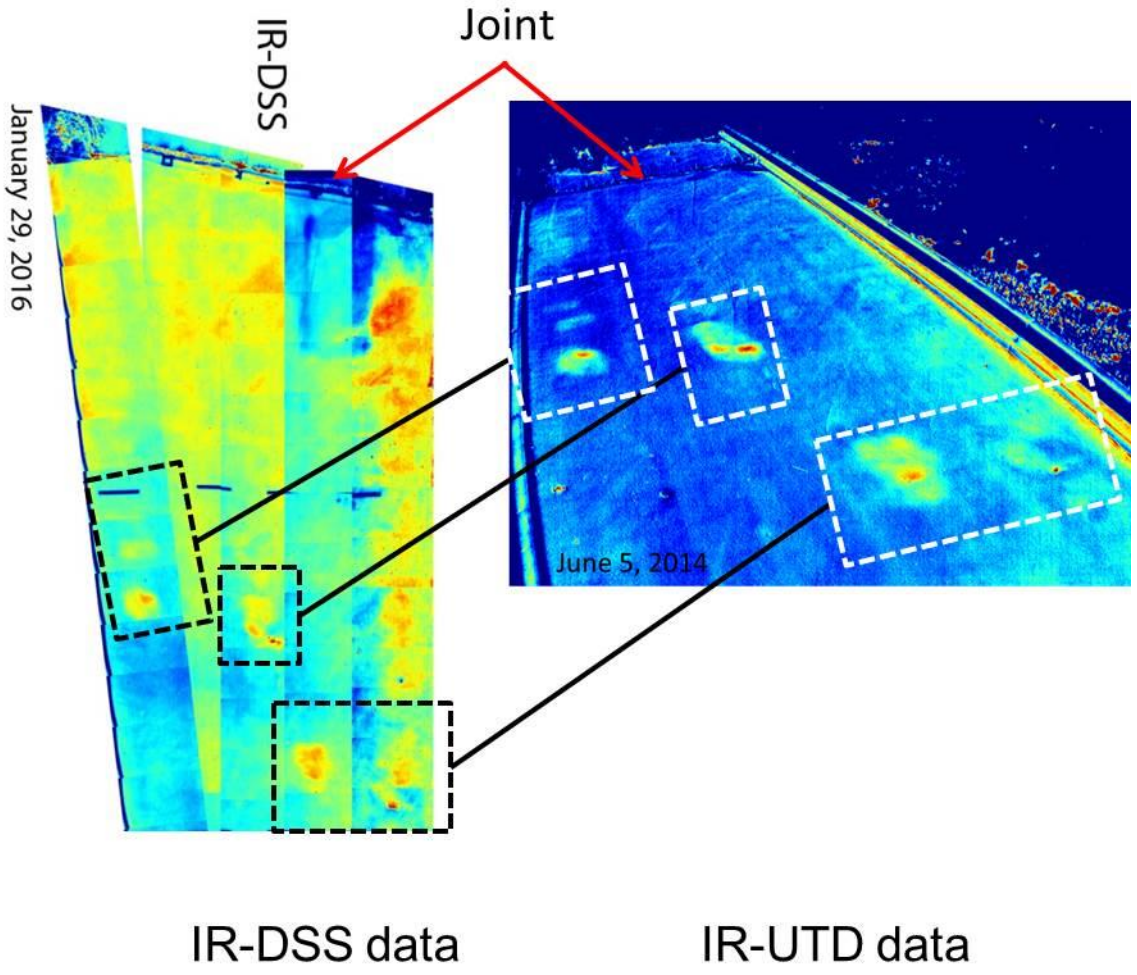

Figure 66. Images showing comparison between IR-UTD and IR-DSS images of bridge A0295.

Figure 67 shows a comparison of the IR-DSS results with the IR-UTD results for the entire length of the bridge. As shown in the figure, the correlation between the IR-DSS results and the IR-UTD results was very good. This is not surprising, since the ambient weather conditions were very favorable during the IR-DSS testing.

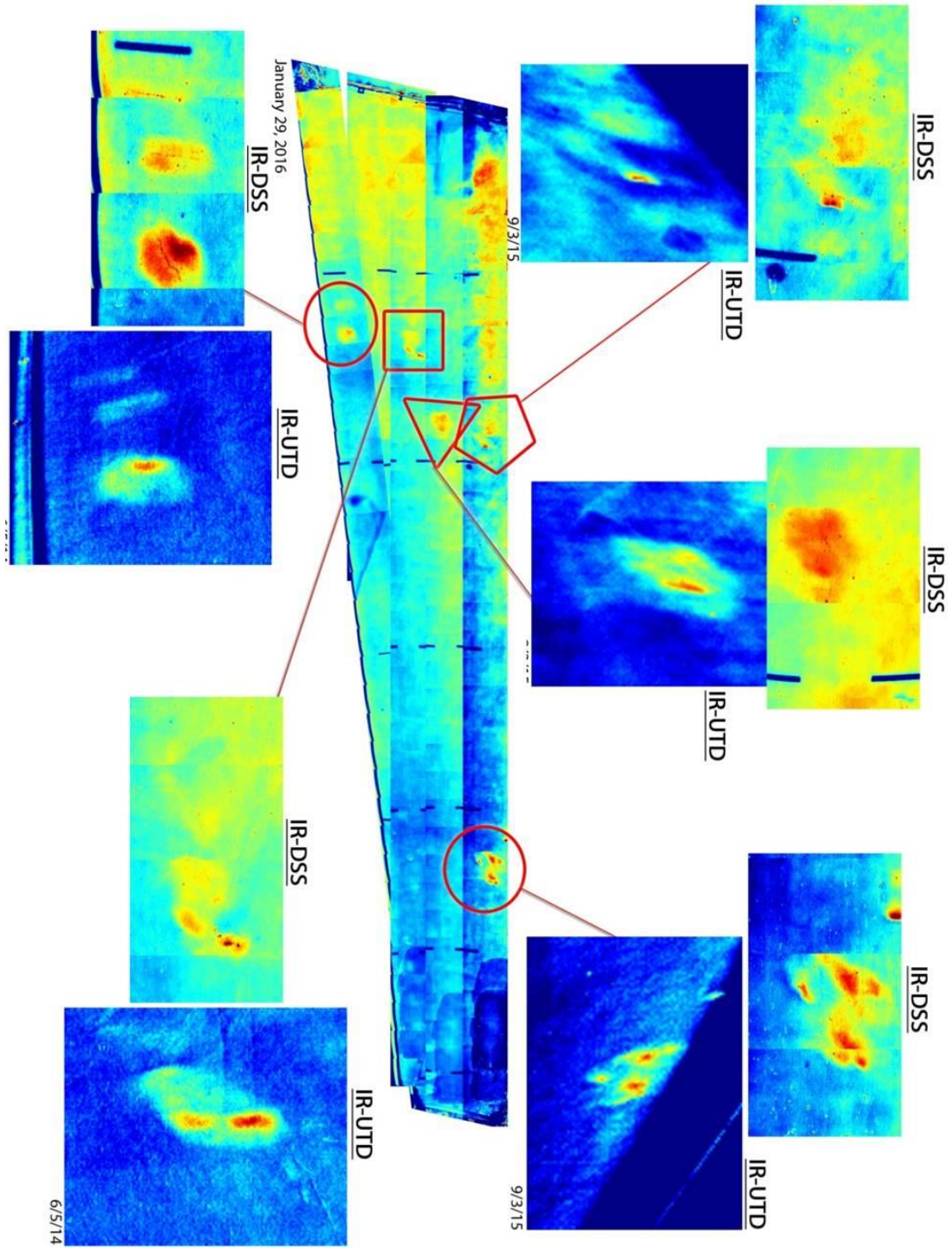

Figure 67. Image showing expanded view of delaminations imaged by the IR-UTD and the IR-DSS systems.

3.2.3 Discussion

The results of testing demonstrated the IR-DSS system was capable of producing images of delamination in the Kansas City Bridge deck. There was a good correlation between data collected with the IR-DSS and the IR-UTD system. Generally, data from the IR-DSS system was noisier than data from the IR-UTD system, resulting in a potential false indication and making determining the spatial extent of a delamination more difficult.

It was also shown through the testing that the IR-DSS produced spatially referenced data that accurately located the position of delaminations in the bridge deck. These data formed a plan view image of the bridge deck that was to scale.

4 CONCLUSIONS AND FUTURE RESEARCH

This report describes field testing conducted to evaluate the capabilities of two different technologies for detecting subsurface damage in concrete. The IR-UTD technology collects thermal images over a period of time; these data are processed to measure thermal inertia of a material. The IR-UTD technology is an entirely new approach for imaging damage in concrete structures. The IR-DSS technology automatically captures thermal images while the system is moved from one position to another. The IR-DSS technology produces images based on the radiant thermal energy from a material in the same manner as other typical thermal imaging systems. However, the IR-DSS has a unique design that allows the system to be implemented from different mobile platforms and uses a precision encoder to trigger data collection.

Field testing of each of these technologies was conducted for the purpose of evaluating the capabilities of the technologies. In general, it was found that the IR-UTD technologies had capabilities that exceeded the capabilities of conventional IR imaging. The technology provided highly accurate data that documented the size and shape of delaminations in bridge decks and other structures. The IR-UTD technology also provided data on the depth of damage and could image the structural features of a bridge. Traffic control was not required to implement the IR-UTD technology.

The IR-DSS capability was demonstrated to include the ability to produce spatially-referenced images that provided accurate depictions of subsurface damage, and these data were presented to-scale in a plan-view image of an entire deck. Traffic control was required to implement this technology, because the travel speed of the system is limited to < 10 mph. The specific conclusions reached from the study of each technology are described in the following sections.

4.1.1 Capabilities of the IR-UTD system

The results of the field testing of the IR-UTD system led to the following conclusions:

- *The IR-UTD technology is capable of making nonintrusive condition assessments of a concrete bridge deck*, i.e., the system can image damage in bridge decks without the use of any traffic control.
    - This conclusion was based on field testing of the Providence and Grindstone Bridge in Columbia, MO.
- *IR-UTD makes very accurate images of delaminations in concrete in terms of the location and extent (area) of the delamination.*
    - This conclusion was based on comparing IR-UTD results with chain drag and physical sampling of an out-of-service highway bridge (A0295), and hammer sounding and physical sampling of the Iowa Bridge (2706.9S069).
- *The IR-UTD is capable of qualitatively analyzing the depth of delaminations in concrete.*
    - This conclusion was based on measurements made on a test block, field experience, and physical sampling on highway bridge structures.
- *The IR-UTD has improved capability to measure deep delaminations relative to traditional IR imaging.*
    - This conclusion was based on measurements made on the test block and field measurements verified with physical sampling.
- *The IR-UTD is capable of imaging the structural features of a bridge.*
    - Features such as internal webs and diaphragms in concrete box girders, and voids and diaphragms in voided slabs, were imaged in the field using the IR-UTD technology.
- *The IR-UTD data has reduced noise levels in the images produced as compared with traditional IR imaging.*
    - This conclusion was based on qualitatively comparing processed IR-UTD images, which image the thermal inertia of a material, with traditional IR imaging which images the radiant IR energy emitted from a material.
- *Images created by the IR-UTD of subsurface delaminations in concrete are reproducible.*

- This conclusion was based on three different tests conducted on a bridge deck with delaminations identified by chain drag. Images produced from data collected:
  - at three different points in time (June 2014, Aug. 2014, Sept. 2015),
  - under three different weather conditions,
  - over three different time intervals,
  - from three different positions,

  produced nearly identical results in the processed IR-UTD images.

- *The IR-UTD is capable of imaging damage in bridge soffits and vertical structures.*
  - This conclusion was based on field testing of the soffit of a voided slab bridge and vertical columns with fire damage.

4.1.2 Capabilities of the IR-DSS system

Field testing of the IR-DSS system led to the following conclusions:

- *The IR-DSS is capable of accurately imaging the location and extent of delaminations in bridge decks.*
- *The IR-*DSS *provides spatially-referenced images that can be used to precisely locate the position of defects in the field.*

These conclusions were reached based on comparing the IR-DSS results with IR-UTD results and chain drag results from an out-of-service bridge (A0295). .

- *The IR-DSS can produce an accurate plan-view image of damage in a bridge deck that includes delaminations, sound patches, and unsound patches.*
- *The IR-DSS can provide spatially correlated infrared the visual images of a bridge deck.*

These conclusions were reached based on comparing the IR-DSS results with IR-UTD results and chain drag results from an out-of-service Bridge A0295 and results from field testing of Bridge A2111.

- *The implementation of the IR-DSS system requires some form of traffic control.*

This conclusion was based on the data collection speed for the system demonstrated in field testing on bridge A2111. Travel speeds of 10 mph or less were required when scanning

the bridge deck to ensure high-quality data. Moving traffic control is likely suitable to address this limitation.

4.2 Future Research

4.2.1 IR-UTD

The field testing of the IR-UTD system focused on the qualitative analysis of data produced by the IR-UTD, which was presented in color images. These images are formed from quantitative data that could be analyzed to improve the interpretation of results. For example, the depth of indications in an image can be analyzed quantitatively based on the calculated ROC (rate of change) data that are represented by colors in the image. This capability was largely unexplored during the course of the research. Future research focused on quantitative analysis of IR-UTD data is needed to fully realize the capability of this new technology for assessing damage in concrete.

The overall capabilities of the IR-UTD system are unique and significantly different than traditional IR imaging technologies. As a result, the range of potential applications for this technology needs to be explored. For example, the technology may have applications for pavement quality control, analyzing the thickness of overlays or concrete pavements, or detecting subsurface voids in concrete approaches or abutment aprons. The technology may also have application for imaging voids in post-tensioning ducts and large concrete structures such as piers and abutments. A myriad of other applications may be suitable for this technology; future research to explore these applications in needed.

4.2.2 IR-DSS

The IR-DSS technology is an implementable technology that improves the quality of IR results relative to currently available commercial systems. Several applications for this technology have not been explored. For example, this technology is suitable for condition assessment of tunnels and culverts. For the condition assessment of bridge soffits of overpass bridges, the IR-DSS camera head can simply be rotated to image the bottom of the deck. These applications have not yet been tested in the field. Other applications such as scanning retaining walls and mechanically stabilized earth (MSE) structures should be explored. Because the IR-DSS system provides data with highly accurate spatial resolution, images produced can document conditions over large areas such that future repairs can be made.

REFERENCES

1. C.F.R., *National Bridge Inspection Standards*, in *23 CFR part 650*. 2004: USA. p. 74419-74439.

2. Maser, K.R. and W.M.K. Roddis, *Principles of Thermography and Radar for Bridge Deck Assessment.* Journal of Transportation Engineering, 1990. **116**(5): p. 583-601.

3. Clemena, G.G., McKeel, W. T., *Detection of Delamination in Bridge Decks with Infrared Thermography.* 1978, Transportation Research Record 664. p. 180-182.

4. Manning, D.G., and Holt, F.B., *Detecting delamination in concrete bridge decks*. 1980, Concrete International. p. 34-41.

5. Washer, G., et al., *Guidelines for thermographic inspection of concrete bridge components in shaded conditions.* Transportation Research Record, 2013(2360): p. 13-20.

6. ASTM, *Standard Test Method for Detecting Delaminations in Bridge Decks Using Infrared Thermography. Standard ASTM D4788 - 03(2007)*. 2007, ASTM International: West Conshohocken, PA, United States.

7. Washer, G.A., Fenwick, R.G., and Bolleni, N. K., *Development of Hand-held Thermographic Inspection Technologies*, MoDOT, Editor. 2009, Missouri Department of Transportatoin Jefferson City, MO. p. 124.

8. Washer, G., et al., *Effects of Environmental Variables on Infrared Imaging of Subsurface Features of Concrete Bridges.* Transportation Research Record: Journal of the Transportation Research Board, 2009. **2108**: p. 107-114.

9. Khan, M.S., G.A. Washer, and S.B. Chase. *Evaluation of dual-band infrared thermography system for bridge deck delamination surveys*. in *Non-Destructive Evaluation Techniques for Aging Infrastructure & Manufacturing*. 1998. International Society for Optics and Photonics.

10. Maser, K.R., *Integration of Ground Penetrating Radar and Infrared Thermography for Bridge Deck Condition Evaluation*, in *7th International Symposium on Nondestructive Testing in Civil Engineering*. 2009: Nantes, France.

11. Maser, K., *Integration of Ground Penetrating Radar and Infrared Thermography for Bridge Deck Condition Testing.* Materials Evaluation 2008. **66**(11): p. 1130-1136.

12. http://bridgeguard.net/. 2016 [cited 2016 December 15]; Web site of a consultant marketing a vehicle-mounted IR system].

13. Maierhofer, C., R. Arndt, and M. Röllig, *Influence of concrete properties on the detection of voids with impulse-thermography.* Infrared Physics & Technology, 2007. **49**(3): p. 213-217.

14. Maierhofer, C., et al., *Application of impulse-thermography for non-destructive assessment of concrete structures.* Cement and Concrete Composites, 2006. **28**(4): p. 393-401.

15. Maierhofer, C., et al., *Quantitative impulse-thermography as non-destructive testing method in civil engineering – Experimental results and numerical simulations.* Construction and Building Materials, 2005. **19**(10): p. 731-737.

16. Starnes, M., N. Carino, and E. Kausel, *Preliminary Thermography Studies for Quality Control of Concrete Structures Strengthened with Fiber-Reinforced Polymer Composites.* Journal of Materials in Civil Engineering, 2003. **15**(3): p. 266-273.

17. Maierhofer, C., et al., *Transient thermography for structural investigation of concrete and composites in the near surface region.* Infrared Physics & Technology, 2002. **43**(3–5): p. 271-278.

18. Maser, K., *Active Heating Infrared Thermography for Detection of Subsurface Bridge Deck Deterioration*, in *IDEA Program*. 2004, TRB: Washington, D.C.

19. Fuchs, P.A., *Portable Active Thermographic Coating Inspection System*. 2014, United States Department of Transportation Washington, D.C. .

20. Wunderground, *Accessed multiple times for weather data corresponding to testing*. 2013-2015.

21. Barnes, C.L., J.-F. Trottier, and D. Forgeron, *Improved concrete bridge deck evaluation using GPR by accounting for signal depth–amplitude effects.* NDT & E International, 2008. **41**(6): p. 427-433.

22. Barnes, C. and J.-F. Trottier, *Phenomena and conditions in bridge decks that confound ground-penetrating radar data analysis.* Transportation Research Record: Journal of the Transportation Research Board, 2002(1795): p. 57-61.

23. Varnavina, A.V., et al., *Concrete bridge deck assessment: Relationship between GPR data and concrete removal depth measurements collected after hydrodemolition.* Construction and Building Materials, 2015. **99**: p. 26-38.

24. Tarussov, A., M. Vandry, and A. De La Haza, *Condition assessment of concrete structures using a new analysis method: Ground-penetrating radar computer-assisted visual interpretation.* Construction and Building Materials, 2013. **38**: p. 1246-1254.

25. Scott, M., A. Rezaizadeh, and M. Moore, *Phenomenology study of HERMES ground-penetrating radar technology for detection and identification of common bridge deck features*. 2001.

26. Popovics, J., *NDE techniques for concrete and masonry structures.* Progress in Structural Engineering and Materials, 2003. **5**(2): p. 49-59.

27. ASTM, *Standard Test Method for Evaluating Asphalt-Covered Concrete Bridge Decks Using Ground Penetrating Radar*. 2015: West Conshohocken, PA.